Ethylene Dibromide

CAS Registry Number: 106-93-4

Prepared by
Heather Reddick Schaefer, DrPH
Shannon Ethridge, MS, DABT
Jessica L Myers, PhD
Toxicology Division

Development Support Document

Final, November 29, 2017

TEXAS COMMISSION ON ENVIRONMENTAL QUALITY

DSD History

Effective Date	Reason
June, 2012	Public request for toxicity information
August 16, 2017	DSD proposed for public comment
November 29, 2017	DSD posted as final

TABLE OF CONTENTS

DSD HISTORY ..... **I**

TABLE OF CONTENTS ..... **II**

LIST OF TABLES ..... **IV**

LIST OF FIGURES ..... **VI**

ACRONYMS AND ABBREVIATIONS ..... **VIII**

CHAPTER 1 SUMMARY TABLES **1**

CHAPTER 2 MAJOR SOURCES AND USES **5**

CHAPTER 3 ACUTE EVALUATION **5**

3.1 HEALTH-BASED ACUTE REV AND ^{ACUTE}ESL 6
3.1.1 Key and Supporting Studies *6*
3.1.1.1 Human Studies 6
3.1.1.1.1 Letz et al. (1984) 6
3.1.1.2 Animal Studies 7
3.1.1.2.1 Rowe et al. (1952) 7
3.1.1.2.1.1 Single Exposure 7
3.1.1.2.1.1 Repeated Exposure 8
3.1.1.3 Developmental/Reproductive Studies 8
3.1.1.3.1 Human study - Schrader et al. (1988) 8
3.1.1.3.2 Animal study - Short et al. (1978) 9
3.1.1.3.2.1 Rats 9
3.1.1.3.2.2 Mice 9
3.1.2 Metabolism and Mode-of-Action (MOA) Analysis *10*
3.1.2.1 Metabolism 11
3.1.2.2 Absorption and Excretion 12
3.1.2.3 MOA and Dose Metric 12
3.1.3 Health-Based 23-h Acute 23-h ReV and ESL *13*
3.1.3.1 POD and Critical Effects and Dosimetric Adjustments 13
3.1.3.1.1 Default Exposure Duration Adjustments 13
3.1.3.1.2 Default Dosimetry Adjustments from Animal-to-Human Exposure 14
3.1.3.2 Adjustments of the POD_{HEC} 14
3.1.3.3 Health-Based 23-h Acute ReV and ESL 15
3.1.4 Health-Based 24-h Acute ReV *16*
3.2 WELFARE-BASED ACUTE ESLS 17
3.2.1 Odor Perception *17*
3.2.2 Vegetation Effects *17*
3.3 SHORT-TERM ESL AND VALUES FOR AIR MONITORING EVALUATION 17
3.4 SUBACUTE INHALATION OBSERVED ADVERSE EFFECT LEVEL (IOAEL) 17

CHAPTER 4 CHRONIC EVALUATION **18**

4.1 NONCARCINOGENIC POTENTIAL 18

4.1.1 Key and Supporting Studies *18*
4.1.1.2 Animal Studies 18
4.1.1.2.1 Key Animal Study – NTP (1982) 18
4.1.1.2.2 Supporting Animal Studies 21
4.1.1.3 Reproductive and Developmental Studies 23
4.1.2 MOA and Dose Metric *25*
4.1.3 POD for Key Study and Dosimetric Adjustments *26*
4.1.3.1 Benchmark Concentration (BMC) Modeling 26
4.1.3.2 Exposure Duration Adjustments 28
4.1.3.3 Default Dosimetry Adjustments from Animal-to-Human Exposure 28
4.2.3.3.1 POE effects – Category 1 gas 28
4.2.3.3.1.1 Male Rat Dosimetric Adjustments 29
4.2.3.3.1.2 Female Rat Dosimetric Adjustments 29
4.2.3.3.1.3 Female Mice Dosimetric Adjustments 29
4.2.3.3.2 Systemic effects – Category 3 gas 30
4.1.3.4 Selection of the Critical Effect and POD 31
4.1.4 Adjustments of the POD_{HEC} *33*
4.1.5 Health-Based Chronic ReV and $^{chronic}ESL_{threshold(nc)}$ *33*
4.1.6 Comparison of TCEQ's Chronic ReV to other Long-Term, Health Protective Comparison Levels from Other Agencies *34*
4.2 CARCINOGENIC POTENTIAL 35
4.2.1 Carcinogenic Weight of Evidence (WOE) *35*
4.2.2 Relevant Data *36*
4.2.2.1 Epidemiological Studies 36
4.2.2.2 Animal Studies 37
4.2.2.2.1 Key Study - NTP 1982 37
4.2.2.2.2 Supporting Studies 41
4.2.3 Carcinogenic MOA *41*
4.2.4 POD for Key Study and Critical Effect *42*
4.2.4.1 BMC Modeling 43
4.2.4.2 Default Exposure Duration Adjustments 43
4.2.4.3 Default Dosimetry Adjustments from Animal-to-Human Exposure 44
4.2.4.3.1 POE effects – Category 1 gas 44
4.2.4.3.2 Systemic effects – Category 3 gas 45
4.2.4.4 Selection of the Critical Effect and POD 45
4.2.5 Calculation of a Unit Risk Factor *46*
4.2.6 Calculation of an Air Concentration at 1 x 10^{-5} Excess Cancer Risk *46*
4.2.7 Comparison of Cancer Potency Factors *46*
4.2.8 Evaluating Susceptibility from Early-Life Exposures *47*
4.3 WELFARE-BASED CHRONIC ESL 48
4.4 LONG-TERM ESL AND VALUES FOR AIR MONITORING EVALUATION 48
4.5 CHRONIC IOAELS 48
4.5.1 Noncarcinogenic Chronic IOAEL *48*
4.5.2 Carcinogenic Chronic IOAEL *49*

CHAPTER 5 REFERENCES 50

APPENDIX 1 BENCHMARK CONCENTRATIONS (BMC) MODELING 52

1.1 NONCARCINOGENIC ENDPOINT MODELING 52
1.1.1 Dichotomous models using rat nonneoplastic data from NTP (1982) 52
1.1.1.1 BMDS Summary for suppurative inflammation in the nasal cavity of male rats 53
1.1.1.2 BMDS Summary for epithelial hyperplasia in the lung/bronchus of male rats 56
1.1.1.3 BMDS Summary for congestion in the lung of male rats 59
1.1.1.4 BMDS Summary for congestion in the liver of male rats 62
1.1.1.5 BMDS Summary of hepatic necrosis in male rats 65
1.1.1.6 BMDS Summary for mineralization in the kidney of male rats 68
1.1.1.7 BMDS Summary of toxic nephropathy in male rats 71
1.1.1.8 BMDS Summary of testicular degeneration in male rats 74
1.1.1.9 BMDS Summary of testicular atropy in male rats 77
1.1.1.10 BMDS Summary for suppurative inflammation in the nasal cavity of female rats 80
1.1.1.11 BMDS Summary for epithelial hyperplasia in the nasal cavity of female rats 83
1.1.1.12 BMDS Summary for congestion in the lung female rats 84
1.1.1.13 BMDS Summary of hepatic necrosis in female rats 87
1.1.1.14 BMDS Summary of degeneration of the adrenal cortex in female rats 90
1.1.1.15 BMDS Summary of thyroid C-cell hyperplasia in female rats 93
1.1.1.16 BMDS Summary of vaginal suppurative inflammation in female rats 96
1.1.2 Dichotomous models using mouse nonneoplastic data from NTP (1982) 99
1.1.2.1 BMDS Summary for suppurative inflammation in the nasal cavity of female mice 100
1.1.2.2 BMDS Summary of epithelial hyperplasia in the lung/bronchus of female mice 103
1.1.2.3 BMDS Summary of epithelial hyperplasia in the lung/bronchiole of female mice 106
1.1.2.4 BMDS Summary of alveolar epithelial hyperplasia in female mice 109
1.1.2.3 BMDS Summary of hematopoiesis in the spleen of female mice 112
1.1.2.4 BMDS Summary of hepatic necrosis in female mice 115
1.2 CARCINOGENIC ENDPOINT MODELING 118
1.2.1 Dichotomous and multistage cancer models using rat neoplastic data from NTP (1982) 118
1.2.1.1 BMDS Summary of Rat Male Nasal Cavity Adenocarcinoma 119
1.2.1.2 BMDS Summary of Rat Male Nasal cavity tumors 122
1.2.1.3 BMDS Summary of rat male tunica vaginalis 123
1.2.1.4 BMDS Summary of rats female nasal cavity adenocarcinoma () 126
1.2.1.5 BMDS Summary of Rat Female Nasal Cavity Tumors 129
1.2.1.6 BMDS Summary of Rat Female Mammary Gland Fibroadenoma 130
1.2.2 Dichotomous and multistage cancer models using mouse neoplastic data from NTP (1982) 131
1.2.2.1 BMDS Summary of Female Mice Respiratory Tumors 132
1.2.2.2 BMDS Summary of Mice Female circulatory system hemangiosarcoma 135
1.2.2.3 BMDS Summary of Female Mice Subcutaneous tissue or rib fibrosarcoma 139

LIST OF TABLES

Table 1. Acute Health and Welfare-Based Screening Values for EDB 2
Table 2. Chronic Health and Welfare-Based Screening Values for EDB 3
Table 3. Chemical and Physical Properties 4
Table 4. Summary of Acute Animal Reproductive/Developmental Key Study (Short et al. 1978) 10
Table 5. Derivation of the Acute ReV and acuteESL 16
Table 6. Summary of Results in Rats (NTP 1982) 20
Table 7. Summary of Results in Mice (NTP 1982) 21
Table 8. BMC Modeling Results for the Nonneoplastic Endpoints from NTP (1982) 27
Table 9. Endpoints and POD_{HEC} for the Nonneoplastic Endpoints from NTP (1982) 32

Table 10. Derivation of the Chronic ReV and chronicESL 34
Table 11. Long-Term, Health Protective Comparison Levels Developed by TCEQ and Other Agencies 35
Table 12. Carcinogenic Weight of Evidence 36
Table 13. Statistically Significant Tumor Incidence in Rats Exposed to EDB via Inhalation 39
Table 14. Statistically Significant Incidence of Tumors in Mice 40
Table 15. BMD Modeling for the Neoplastic Endpoints from NTP (1982) 43
Table 16. Endpoints and POD_{HEC} for the Neoplastic Endpoints from NTP (1982) 46
Table 17 Available Inhalation URFs and Chronic Toxicity Values 47
Table 19. Rat Nonneoplastic Data from NTP (1982) 52
Table 20. Summary of BMD Modeling Results for suppurative inflammation in the nasal cavity of male rats 53
Table 21. Summary of BMD Modeling Results for epithelial hyperplasia in the lung/bronchus of male rats 56
Table 22. Summary of BMD Modeling Results for congestion in the lung of male rats 59
Table 23. Summary of BMD Modeling Results for congestion in the liver of male rats 62
Table 24. Summary of BMD Modeling Results for hepatic necrosis in male rats 65
Table 25. Summary of BMD Modeling Results for mineralization in the kidney of male rats 68
Table 26. Summary of BMD Modeling Results for toxic nephropathy in male rats 71
Table 27. Summary of BMD Modeling Results of testicular degeneration in male rats 74
Table 28. Summary of BMD Modeling Results of testicular atropy in male rats 77
Table 29. Summary of BMD Modeling Results for suppurative inflammation in the nasal cavity of female rats 80
Table 30. Summary of BMD Modeling Results for epithelial hyperplasia in the nasal cavity of female rats 83
Table 31. Summary of BMD Modeling Results for congestion in the lung female rats 84
Table 32. Summary of BMD Modeling Results of hepatic necrosis in female rats 87
Table 33. Summary of BMD Modeling Results of degeneration of the adrenal cortex in female rats 90
Table 34. Summary of BMD Modeling Results of thyroid C-cell hyperplasia in female rats 93
Table 35. Summary of BMD Modeling Results of vaginal suppurative inflammation in female rats 96
Table 36. Mouse Nonneoplastic Data from NTP (1982) 99
Table 37. Summary of BMD Modeling Results for suppurative inflammation in the nasal cavity of female mice 100
Table 38. Summary of BMD Modeling Results of epithelial hyperplasia in the lung/bronchus of female mice 103
Table 39. Summary of BMD Modeling Results of epithelial hyperplasia in the lung/bronchiole of female mice 106
Table 40. Summary of BMD Modeling Results of alveolar epithelial hyperplasia in female mice 109
Table 41. Summary of BMD Modeling Results of hematopoiesis in the spleen of female mice 112
Table 42. Summary of BMD Modeling Results of hepatic necrosis in female mice 115
Table 43. Rat Neoplastic Data from NTP (1982) 118
Table 44. Summary of BMD Modeling Results for male rat nasal cavity adenocarcinomas 119
Table 45. Summary of BMD Modeling Results for Male Rat Nasal Cavity Tumors 122
Table 46. Summary of BMD Modeling Results for Male Rat Tunica Vaginalis Neoplasms 123

Table 47. Summary of BMD Modeling Results for female rat nasal cavity adenocarcinomas 126
Table 48. Summary of BMD Modeling Results for female rat nasal cavity tumors 129
Table 49. Summary of BMD Modeling Results for fmeal rat mammary gland fibroadenomas 130
Table 50. Mouse Neoplastic Data from NTP 1982 131
Table 51. Summary of BMD Modeling Results for female mice respiratory tumors 132
Table 52. Summary of BMD Modeling Results for female mice circulatory system hemangiosarcoma .. 135
Table 53. Summary of BMD Modeling Results for Female Mice Subcutaneous tissue or rib fibrosarcoma 139

LIST OF FIGURES

Figure 1. Metabolism of EDB by the oxidative route as cited in EPA (2004). 11
Figure 2. Metabolism of EDB by the conjugative route as cited in EPA (2004). 12
Figure 3. Plot of incidence rate by dose with fitted curve for LogLogistic model for suppurative inflammation in the nasal cavity of male rats; dose shown in ppm. 54
Figure 4. Plot of incidence rate by dose with fitted curve for LogLogistic model for epithelial hyperplasia in the lung/bronchus of male rats; dose shown in ppm. 57
Figure 5. Plot of incidence rate by dose with fitted curve for Gamma model for congestion in the lung of male rats; dose shown in ppm. 60
Figure 6. Plot of incidence rate by dose with fitted curve for LogLogistic model for congestion in the liver of male rats; dose shown in ppm. 63
Figure 7. Plot of incidence rate by dose with fitted curve for Quantal-Linear model for hepatic necrosis in male rats; dose shown in ppm. 66
Figure 8. Plot of incidence rate by dose with fitted curve for LogLogistic model for mineralization in the kidney of male rats; dose shown in ppm. 69
Figure 9. Plot of incidence rate by dose with fitted curve for Multistage 2° model for toxic nephropathy in male rats; dose shown in ppm. 72
Figure 10. Plot of incidence rate by dose with fitted curve for LogLogistic model of testicular degeneration in male rats; dose shown in ppm. 75
Figure 11. Plot of incidence rate by dose with fitted curve for Quantal-Linear model of testicular atrophy in male rats; dose shown in ppm. 78
Figure 12. Plot of incidence rate by dose with fitted curve for Multistage 2° model for suppurative inflammation in the nasal cavity of female rats; dose shown in ppm. 81
Figure 13. Plot of incidence rate by dose with fitted curve for Quantal-Linear model for congestion in the lung female rats; dose shown in ppm. 85
Figure 14. Plot of incidence rate by dose with fitted curve for Logistic model of hepatic necrosis in female rats; dose shown in ppm. 88
Figure 15. Plot of incidence rate by dose with fitted curve for LogLogistic model of degeneration of the adrenal cortex in female rats; dose shown in ppm. 91
Figure 16. Plot of incidence rate by dose with fitted curve for Quantal-Linear model of thyroid C-cell hyperplasia in female rats; dose shown in ppm. 94
Figure 17. Plot of incidence rate by dose with fitted curve for LogLogistic model of vaginal suppurative inflammation in female rats; dose shown in ppm. 97

Figure 18. Plot of incidence rate by dose with fitted curve for Quantal-Linear model for inflammation in the nasal cavity of female mice; dose shown in ppm. 101
Figure 19. Plot of incidence rate by dose with fitted curve for LogLogistic model of epithelial hyperplasia in the lung/bronchus of female mice; dose shown in ppm. 104
Figure 20. Plot of incidence rate by dose with fitted curve for Multistage 2° model of epithelial hyperplasia in the lung/bronchiole of female mice; dose shown in ppm. 107
Figure 21. Plot of incidence rate by dose with fitted curve for Multistage 2° model of alveolar epithelial hyperplasia in female mice; dose shown in ppm. 110
Figure 22. Plot of incidence rate by dose with fitted curve for LogLogistic model of hematopoiesis in the spleen of female mice; dose shown in ppm. 113
Figure 23. Plot of incidence rate by dose with fitted curve for LogLogistic model of hepatic necrosis in female mice; dose shown in ppm. 116
Figure 24. Plot of incidence rate by dose with fitted curve for LogLogistic model for male rat nasal cavity adenocarcinomas; dose shown in ppm. 120
Figure 25. Plot of incidence rate by dose with fitted curve for Quantal-Linear model; dose shown in ppm. 124
Figure 26. Plot of incidence rate by dose with fitted curve for LogLogistic model for female rat nasal cavity adenocarcinomas; dose shown in ppm. 127
Figure 27. Plot of incidence rate by dose with fitted curve for Probit model for ; dose shown in ppm. . 133
Figure 28. Plot of incidence rate by dose with fitted curve for Multistage-Cancer 2° model; dose shown in ppm. 136
Figure 29. Plot of incidence rate by dose with fitted curve for LogLogistic model; dose shown in ppm. 140

Acronyms and Abbreviations

Acronyms and Abbreviations	Definitions
AEGL	Acute Exposure Guideline Level
AMCV	Air Monitoring Comparison Value
BMC	benchmark concentration
BMCL	benchmark concentration 95% lower confidence limit
BMDS	Benchmark Dose Software
°C	degrees Celsius
d	day(s)
DAF	Dosimetric Adjustment Factor
DSD	development support document
ESL	Effects Screening Level
$^{acute}ESL$	acute health-based Effects Screening Level for chemicals meeting minimum database requirements
$^{acute}ESL_{generic}$	acute health-based Effects Screening Level for chemicals not meeting minimum database requirements
$^{acute}ESL_{odor}$	acute odor-based Effects Screening Level
$^{acute}ESL_{veg}$	acute vegetation-based Effects Screening Level
$^{chronic}ESL_{linear(c)}$	chronic health-based Effects Screening Level for linear dose response cancer effect
$^{chronic}ESL_{linear(nc)}$	chronic health-based Effects Screening Level for linear dose response noncancer effects
$^{chronic}ESL_{nonlinear(c)}$	chronic health-based Effects Screening Level for nonlinear dose response cancer effects
$^{chronic}ESL_{nonlinear(nc)}$	chronic health-based Effects Screening Level for nonlinear dose response noncancer effects
$^{chronic}ESL_{veg}$	chronic vegetation-based Effects Screening Level
GD	gestation day
h	hour(s)

H	humans
$H_{b/g}$	blood:gas partition coefficient
$(H_{b/g})_A$	blood:gas partition coefficient, animal
$(H_{b/g})_H$	blood:gas partition coefficient, human
HEC	human equivalent concentration
HQ	hazard quotient
IARC	International Agency for Research on Cancer
IOAEL	inhalation observed adverse effect level
^{acute}IOAEL	acute inhalation observed adverse effect level
^{subacute}IOAEL	subacute inhalation observed adverse effect level
$^{chronic}IOAEL_{(nc)}$	chronic inhalation observed adverse effect level (noncancer effects)
$^{chronic}IOAEL_{(c)}$	chronic inhalation observed adverse effect level (cancer effects)
kg	kilogram
LOAEL	lowest-observed-adverse-effect-level
MW	molecular weight
µg	microgram
µg/m^3	micrograms per cubic meter
mg	milligrams
mg/m^3	milligrams per cubic meter
min	minute(s)
MEK	methyl ethyl ketone
mm Hg	millimeters of mercury
MOA	mode of action
n	number
N/A	Not applicable
NAC	National Advisory Committee
n-BA	n-butyl acetate
NOAEL	no-observed-adverse-effect-level

NOEL	no-observed-effect-level
NOS	not otherwise specified
POD	point of departure
POD_{ADJ}	point of departure adjusted for exposure duration
POD_{HEC}	point of departure adjusted for human equivalent concentration
ppb	parts per billion
ppm	parts per million
ReV	reference value
Acute ReV	acute (e.g., 1-hour) health-based reference value for chemicals meeting minimum database requirements
Acute ReV-24hr	acute 24-hour health-based reference value for chemicals meeting minimum database requirements
Chronic $ReV_{threshold(nc)}$	chronic health-based reference value for threshold dose response noncancer effects
RGDR	regional gas dose ratio
RPF	relative potency factor
SA	surface area
SAR	structure-activity relationship
SD	Sprague-Dawley
TCEQ	Texas Commission on Environmental Quality
TD	Toxicology Division
UF	uncertainty factor
UF_H	interindividual or intraspecies human uncertainty factor
UF_A	animal to human uncertainty factor
UF_{Sub}	subchronic to chronic exposure uncertainty factor
UF_L	LOAEL to NOAEL uncertainty factor
UF_D	incomplete database uncertainty factor
URF	unit risk factor
USEPA	United States Environmental Protection Agency

V_E	minute volume
wk	week(s)
yr	year(s)

Chapter 1 Summary Tables

Table 1 and Table 2 provide a summary of health- and welfare-based values from an acute and chronic evaluation of ethylene dibromide (EDB), respectively, for use in air permitting and air monitoring. Please refer to Section 1.6.2 of the *TCEQ Guidelines to Develop Toxicity Factors* (TCEQ 2015a) for an explanation of air monitoring comparison values (AMCVs), reference values (ReVs) and effects screening levels (ESLs) used for review of ambient air monitoring data and air permitting. Table 3 provides summary information and the physical/chemical data of EDB.

Table 1. Acute Health and Welfare-Based Screening Values for EDB

Screening Level Type	Duration	Value 1 (µg/m³)	Value 2 (ppb)	Usage	Flags	Surrogated / RPF	Critical Effect(s)	Notes
Acute ReV	23 h	510	67	M	A	--	Reduced fetal body weight, increased incidence of fetal resorptions and skeletal anomalies. Maternal toxicity (decreased weight gain and feed consumption).	Reproductive/ developmental effects, duration not adjusted to 1-hour.
Acute ReV-24hr	24 h	510	67	M	A	--	Same as above.	--
^{acute}ESL [a]	**23 h**	**150**	**20**	**P**	**S,D**	**--**	**Same as above.**	**--**
^{acute}IOAEL	--	--	--	--	--	--	--	--
^{subacute}IOAEL	23 h	150	20	N	none	--	Same as above.	--
$^{acute}ESL_{odor}$	--	--	--	--	--	--	--	Sweet, chloroform-like odor.
$^{acute}ESL_{veg}$	--	--	--	--	--	--	--	No data found.

Bold values used for air permit reviews

[a] Based on the acute 23-h ReV of 510 µg/m3 (67 ppb) multiplied by 0.3 (i.e., HQ = 0.3) to account for cumulative and aggregate risk during the air permit review.

Usage:
P = Used in Air Permitting
M = Used to Evaluate Air Monitoring Data
R = Used to Calculate Remediation Cleanup Levels
N = Usage Not Defined

Flags:
A = AMCV report
S = ESL Summary Report
D = ESL Detail Report

Table 2. Chronic Health and Welfare-Based Screening Values for EDB

Screening Level Type	Duration	Value 1 (µg/m³)	Value 2 (ppb)	Usage	Flags	Surrogated/ RPF	Critical Effect(s)	Notes
Chronic $ReV_{threshold(nc)}$	70 yr	67	8.7	N	none	--	Suppurative inflammation in the nasal cavity in male rats.	--
$^{chronic}ESL_{threshold(nc)}$ [a]	70 yr	20	2.6	N	none	--	Same as above.	--
$^{chronic}IOAEL_{(nc)}$	103 wk	49,000	6400	N	none	--	Same as above.	--
$^{chronic}ESL_{threshold(c)}$	--	--	--	--	--	--	--	No data found
$^{chronic}ESL_{nonthreshold(c)}$ [b]	**70 yr**	**0.22**	**0.029**	**M,P**	**A,S,D**	**--**	**Increased incidence of nasal cavity adenocarcinomas in female rats.**	**--**
$^{chronic}IOAEL_{(c)}$	103 wk	18,000	2300	N	none	--	Same as above.	--
$^{chronic}ESL_{veg}$	--	--	--	--	--	--	--	No data found
$^{chronic}ESL_{animal}$	--	--	--	--	--	--	--	No data found

Bold values used for air permit reviews

[a] Based on the chronic ReV of 67 µg/m³ (8.7 ppb) multiplied by 0.3 (i.e., HQ = 0.3) to account for cumulative and aggregate risk during the air permit review.

[b] Based on the URF of 4.4E-05 $(µg/m^3)^{-1}$ or 3.4E-04 $(ppb)^{-1}$ and a no significant risk level of 1 in 100,000 excess cancer risk.

Usage:
P = Used in Air Permitting
M = Used to Evaluate Air Monitoring Data
R = Used to Calculate Remediation Cleanup Levels
N = Usage Not Defined

Flags:
A = AMCV report
S = ESL Summary Report
D = ESL Detail Report

Table 3. Chemical and Physical Properties

Parameter	Value	Reference
Molecular Formula	C2-H4-Br2	HSDB (2006)
Chemical Structure	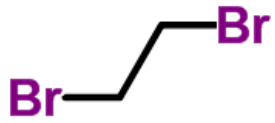	ChemSpider (2015)
CAS Registry Number	106-93-4	HSDB (2006)
Molecular Weight	187.9	HSDB (2006)
Physical State at 25°C	Liquid	HSDB (2006)
Color/Form	Colorless, heavy liquid	HSDB (2006)
Odor	Sweet, chloroform-like	Akron (2009)
Synonyms	EDB; 1,2 dibromoethane, α,β-dibromoethane; ethylene bromide	HSDB (2006)
Solubility in water	4,150 mg/L at 25°C	HSDB (2006)
Log K_{ow}	1.96	HSDB (2006)
Vapor Pressure	11.2 mm Hg at 25°C	HSDB (2006)
Relative Vapor Density (air = 1)	6.5	HSDB (2006)
Melting Point	9.97°C	HSDB (2006)
Boiling Point	131-132°C	HSDB (2006)
Conversion Factors	1 ppm = 7.7 mg/m^3	USEPA (2007)

Chapter 2 Major Sources and Uses

EDB is a heavy brominated hydrocarbon, which is manufactured by reacting ethylene and bromine (Ott et al. 1980). At room temperature, EDB is a colorless liquid with a sweet, chloroform-like odor with an odor threshold of 10 parts per million (ppm) (Ruth 1986). EDB is mainly a synthetic chemical; however, it is also formed naturally by microalgae growth found in small amounts in the ocean (EPA 2004). Until 1978, EDB was primarily used as a lead scavenger in antiknock mixtures added to gasoline. EDB was also used as a pesticide, chemical intermediate to the production of resins, gums, waxes and dyes, pharmaceuticals, and has also been used as a flame retardant. In the 1970s and early 1980s, EDB was sprayed directly onto fruits, vegetables, and grain crops to control insects. In 1984, the Environmental Protection Agency (EPA) eliminated most uses of EDB in the US (ATSDR 1992). The production of this chemical decreased in the US from 332 million pounds (lbs) in 1974 to 170 million lbs by 1982 (ATSDR 1992, HSDB 2009). Worldwide production of EDB as of 2009 consists of the US, Europe, China, and the Middle East (ATSDR 1992).

EDB is released into the environment from manufacturing use and emissions at waste sites. EDB is persistent in the environment, especially in groundwater, and breaks down slowly in air (over 4-5 months) and surface water (2 months) (ATSDR 1992). According to EPA's Toxics Release Inventory, total air emissions of EDB in the US and Texas have declined since 1988. Total air emissions in the US were approximately 63,000 lbs in 1988 and declined to approximately 836 lbs in 2015. In 1988, total air emissions of EDB in Texas were 2,900 lbs compared to 15 lbs in 2015. EDB is monitored for by the TCEQ's ambient air monitoring program and results are reviewed on a monthly basis. Since 2000, 99.99% of all validated 24-hour (h) canister measurements have been below the method detection limit of 0.50 parts per billion (ppb).

Chapter 3 Acute Evaluation

Acute exposure to high doses of EDB causes central nervous system effects in humans and animals. The available studies (occupational and experimental) indicate acute inhalation exposure to low to moderate concentrations of EDB (e.g., 75 ppm) can cause eye and respiratory tract irritation in humans (Ott et. al 1980). Gastrointestinal discomfort, vomiting, and respiratory tract irritation occurred after inhalation exposure to 100 – 200 ppm for 1 h or less or to 75 ppm for longer durations (ACGIH 1991). In general, the health effects reported in animals following short-term (acute and subacute) inhalation of EDB (50 – 100 ppm) include lung inflammation, increased liver weight, histopathological changes in the liver, and nervous system effects (Rowe et al. 1952).

3.1 Health-Based Acute ReV and ^{acute}ESL

A literature review was conducted regarding the acute inhalation toxicity of EDB. Information from both human and animal studies regarding the acute toxicity of EDB was reviewed in detail by ATSDR (1992), EPA (2004), OEHHA (1999), and AEGL (2008).

3.1.1 Key and Supporting Studies

3.1.1.1 Human Studies

Several studies have described the effects of acute or occupational exposure to high levels of EDB. Details about the exposure parameters are typically lacking, such as air concentrations, duration of exposure, and unknown but possibly significant dermal exposure, making these studies unsuitable for the derivation of an acute ReV. Some studies provide evidence that EDB may cause both reproductive and developmental effects in humans, although the significant limitations of the studies (i.e., poor exposure measurements, significantly high concentrations, lack of appropriate control groups, and concomitant exposure to other chemicals) prevent their use in the development of ReVs. Occupational studies suggest that short-term exposure to EDB may slow sperm velocity and decrease semen volume (EPA 2004 and Schrader et al. 1988). Reproductive endpoints are discussed in more detail in Section 3.1.2.3.

3.1.1.1.1 Letz et al. (1984)

Letz et al. (1984) discussed two case studies where workers accidentally exposed by inhalation and dermal contact to unknown concentrations of EDB experienced irritation to the eyes, throat, and respiratory tract; diarrhea and vomiting; and central nervous system effects including neurological effects such as restlessness, nervousness, combativeness, and lethargy. The first worker collapsed after five minutes (min) of entering a 28,500 liter nurse tank. After 45 min, fire crews rescued the man who was intermittently comatose, vomiting, and complained of burning of the eyes and throat. Twelve hours after exposure, the patient experienced cardiopulmonary arrest and resuscitative efforts were unsuccessful. Autopsy results exhibited metabolic acidosis, central nervous system depression, and liver damage. The second worker attempted to rescue his co-worker by climbing into the nurse tank and collapsed. He was in the tank for approximately 20-30 min before being rescued by the fire department. Once rescued, he was delirious, displayed combative behavior, vomited and complained of burning eyes. The patient died 64 h after exposure. Autopsy results revealed metabolic acidosis and hepatic and renal failure. Blood bromine levels were also raised to over 100 times the background level prior to death (Letz et al. 1984). In addition to inhalation exposure, dermal exposure may have played a role in the deaths of the two workers although dermal exposure rates were not quantified. Although a mean concentration of 28 ppm (with a range of 15 to 41 ppm) was measured in the tank approximately 20 h after the accident, the exposure concentration was

most likely significantly higher at the time of exposure, and likely significant but unquantifiable dermal exposure also occurred.

3.1.1.2 Animal Studies

Animal studies have revealed that EDB exposure results in a steep dose-response curve, with exposure duration playing an important role. For example, no effects were observed after a single 0.7-h exposure to 200 ppm, while death occurred after a 7-h exposure to 100 ppm (Rowe et al. 1952).

3.1.1.2.1 Rowe et al. (1952)

Rowe et al. (1952) exposed groups of rats, guinea pigs, rabbits, and monkeys to either a single or repeated EDB dosing regimen with exposure concentrations ranging from 0 -10,000 ppm and durations ranging from 0.02-16 h. Animals were exposed in whole-body chambers, and concentrations were measured repeatedly. The authors reported that the analytical results were within ± 10% of the theoretical values. Animals were examined for body weight, behavioral changes, undefined hematological parameters, organ weights and histological exams. The acute and subacute exposures are detailed below, while the subchronic results are described in Section 4.1.

3.1.1.2.1.1 Single Exposure

- Rats (male and female) were exposed by inhalation to 0, 100, 200, 400, 800, 3000, 5000, and 10,000 ppm EDB (4-20 animals per group) for single periods ranging from 0.02 h (1.2 min) to 16 h. Significant mortality occurred following exposure to concentrations greater than or equal to 400 ppm and for durations longer than 12 h. The authors reported that the majority of these deaths were the result of pneumonia and injury to the lungs. A group of rats (number not specified) euthanized 16-24 h after receiving a single exposure within the range of 100-1000 ppm at various durations [0.03 h (1.8 min) - 50 h] revealed an increase in weight of lungs, livers and kidneys and histopathological changes in these organs. According to Rowe et al. (1952), increased liver weight and slight histopathological changes in the liver were the most sensitive endpoints of EDB toxicity, although these endpoints are relatively serious considering they resulted from single exposure. The authors reported that rats exposed to 200 ppm for 0.7 h and 100 ppm for 1 h did not have detectable adverse effects (specifically changes in liver weight or histopathology), although the critical endpoints discovered in other studies, such as in the nasal passages, were not examined (NTP 1982). Therefore, 200 ppm for a 0.7 h and 100 ppm for 1 h were identified as the highest no observed adverse effect levels (NOAELs) for the liver effects examined in rats (Rowe et al. 1952).

- Guinea pigs (male and female, number not specified) were exposed by inhalation to EDB at concentrations of 0, 200 ppm for 7 h, and 400 ppm for 2 to 7 h. Fifty percent of guinea pigs died after exposure to 400 ppm for 3 h. The maximum nonfatal single exposures for guinea pigs were 2 h at 400 ppm and 7 h at 200 ppm; however, no details on clinical or pathological effects were presented in Rowe et al. (1952), and the guinea pig data could not be used for the identification of a critical effect.

3.1.1.2.1.1 Repeated Exposure

- Four unexposed controls were compared to ten female rats exposed to 100 ppm of EDB for 7 h/day (d) for up to 9 d. One rat died after a single 7-h exposure, one died after five 7-h exposures, and one died after seven 7-h exposures. Details on the cause of death were not specifically provided. The surviving rats, after receiving 7 exposures in 9 d, appeared thin and unkempt. At autopsy, lung, liver and kidney weights were increased significantly. In addition, microscopic examination revealed thickening of the alveolar walls, cloudy swelling of the liver and slight congestion and hemosiderosis of the spleen.
- Four female rabbits were exposed to 0 or 100 ppm of EDB for 7 h/d for up to 4 d. Two of the 4 rabbits died after two 7-h exposures and a third rabbit died after the third exposure. The surviving rabbit, after receiving 4 exposures in 4 d, was sacrificed for examination. Microscopic examination revealed central fatty degeneration of the liver with necrosis in some areas.

Multiple exposures, a lack of NOAELs, and relatively serious effects including high mortality following multiple exposures make this portion of the study unsuitable for the derivation of an acute ReV.

3.1.1.3 Developmental/Reproductive Studies

Some studies provide evidence that EDB may cause both reproductive and developmental effects in humans although limitations of the studies (i.e., poor exposure measurements, lack of appropriate control groups, and concomitant exposure to other chemicals) prevent their use in the development of ReVs. Animal studies provide evidence for EDB-induced developmental and reproductive toxicity and are reviewed extensively in USEPA (1994), ATSDR (1996), and NRC (2008).

3.1.1.3.1 Human study - Schrader et al. (1988)

Schrader et al. (1988) conducted a short-term longitudinal reproductive study on 12 male temporary forestry workers (20-32 years of age, average age = 25.1 years) exposed to EDB for approximately 6 weeks (wk). Semen analysis consisted of sperm velocity and motility analysis, semen pH and volume, sperm morphology and morphometry and viability assessments. Semen from 12 men (mean age 25.1) was collected 1 to 2 wk prior to exposure and during the last wk

of exposure to EDB. Due to missing data on abstinence and sample age, two individuals were eliminated from the analysis. The control group consisted of six forestry workers (mean age = 26.5 years) who had no known exposure to EDB. Air samples (n = 26) were collected in the breathing zone of the workers for 15 min to 1 h or for 8-h shifts. The concentration of EDB ranged from non-detectable (ND) to 2165 ppb (60 ppb time-weighted-average). Out of the 10 workers exposed to EDB, sperm velocity decreased in all men while semen volume decreased in 9 workers compared with 2/6 of the control workers. Sperm viability, sperm count, and semen pH did not change across the exposed and control groups (Schrader 1988). Confounding factors such as variable exposure concentrations and durations, multiple chemicals and routes of exposure, and overall length of exposure make this study unsuitable for derivation of the acute ReV.

3.1.1.3.2 Animal study - Short et al. (1978)

Pregnant rats and mice were exposed to EDB via inhalation at concentrations of 0, 20, 38, or 80 ppm, 23 h/d during gestation day (GD) 6-15 and sacrificed on GD 20 (rats) or 18 (mice). Fetuses were removed for evaluation of external, soft tissue, and skeletal anomalies. Two control groups exposed to room air were included in the study; one was provided food *ad libitum* and another was on a restricted diet. The animals were exposed in 3.5 m^3 Rochester-type stainless steel chamber, and chamber atmospheres were monitored by gas chromatography and flame ionization detection. As detailed below, the results indicated that EDB is more toxic to pregnant mice than pregnant rats (Short et al. 1978 and ATSDR 1992).

3.1.1.3.2.1 Rats

Groups of 15-17 pregnant Charles River CD rats were exposed to EDB at concentrations of 0, 20, 38, or 80 ppm, 23 h/d during GD 6-15 and sacrificed on GD 20. A statistically significant increase in mortality occurred in rats exposed to 38 and 80 ppm EDB. Weight loss was evident in dams exposed to 38 and 80 ppm and feed consumption was reduced at all exposures. Dams exposed to 80 ppm had evidence of embryo toxicity and reduced number of implants. The fetuses of dams exposed to 38 ppm weighed statistically significant less than the controls. Hematomas were the most common external anomaly in all exposure groups of fetuses. Umbilical hernia and clubbed foot in the group exposed to 38 ppm of EDB were 1/184 and 2/184 (fetuses affected/fetuses inspected). A statistically significant reduced percentage of fetuses with normally ossified centra occurred in the group exposed to 20 ppm and although the group exposed to 38 ppm also showed a decrease when compared to control, it was not statistically significant. Dams exposed to 20 ppm also experienced reduced food consumption (Short et al. 1978).

3.1.1.3.2.2 Mice

Groups of 18-22 pregnant CD-1 mice were exposed to EDB at concentrations of 0, 20, 38, or 80 ppm 23 h/d during (GD 6-15 and sacrificed on GD 18). Death occurred in all dams exposed to 80

ppm and seven dams exposed to 38 ppm. Dams exposed to 20 and 38 ppm experienced reduced body weights and feed consumption as well as an increased incidence of fetal resorptions. Fetal mortality was also increased in dams exposed to 38 ppm. Dose-dependent skeletal anomalies were statistically significant for the enlarged occipital fontanel and ossification problems with the supraoccipitals, incus, hyoid bone, sternebrae, and phalanges (Short et al. 1978).

Table 4. Summary of Acute Animal Reproductive/Developmental Key Study (Short et al. 1978)

Species	Exposure Concentration	Exposure Duration	NOAEL	LOAEL	Effects
Rats	0, 20, 38, 80 ppm	23 h/d on GD 6-15		20 ppm	Reduced percentage of fetuses with normally ossified centra, Maternal toxicity (decreased feed consumption).
Mice	0, 20, 38, 80 ppm	23 h/d on GD 6-15	--	20 ppm*	Reduced fetal body weight, increased incidence of fetal resorptions, and increased incidence of skeletal anomalies. Maternal toxicity (decreased weight gain and feed consumption).

* Point of Departure (POD) for derivation of the acute ReV

3.1.2 Metabolism and Mode-of-Action (MOA) Analysis

As cited in EPA (2004), the Hissink et al. (2000) physiologically based pharmacokinetic (PBPK) modeling indicated that uptake in rats exposed to EDB would be higher than humans, and rats produce more active metabolites from the cytochrome P450 pathway than humans. The PBPK model also predicted that rats would produce more glutathione-S-transferase (GST) metabolites than humans. Due primarily to the higher relative ventilation rate, cardiac output, and metabolic rate of rats, the Hissink et al. (2000) model predicts that blood concentrations of EDB and the metabolites of both pathways (P450 oxidative and GST conjugation) would be higher in rats than in humans. However, based on model limitations, according to the EPA, this model was not appropriate to use for quantitative (route-to-route or animal-to-human) extrapolations. Inhalation studies (National Toxicology Program [NTP] 1982; Stinson et al. 1981; Nitschke et al. 1981; Reznik et al. 1980; Short et al. 1978; Smith and Goldman 1983) showed that EDB is absorbed via the inhalation route of exposure and distributed systemically. Stott and McKenna (1984) showed that EDB is about 50% absorbed when presented to either the upper or lower respiratory tract of Fisher 344 rats at a flow rate equivalent to the animals' respiratory minute volume (53 mL/min) (EPA 2004).

3.1.2.1 Metabolism

As cited in EPA (2004) and ATSDR (1992),

> "1,2-Dibromoethane is metabolized by two major pathways, cytochrome-P450-monooxygenase and glutathione (GSH) conjugation via glutathione-S-transferase (GST) (Figure 1 and 2). Oxidative metabolism by cytochrome-P450 leads to the formation of the reactive metabolite 2-bromoacetaldehyde (Hill et al., 1978) via dehydrohalogenation of a gem-halohydrin. This route has been demonstrated to account for 80% of the metabolism of 1, 2-dibromoethane in the rat (van Bladeren et al., 1981)" (EPA 2004).

> "2-bromoacetaldehyde can produce histopathological changes such as liver damage, by binding to cellular proteins (Hill et al. 1978). 2-Bromoacetaldehyde can be metabolized further by aldehyde dehydrogenase in the presence of nicotinamide adenine dinucleotide dehydrogenase to 2-bromoethanol, which is highly toxic and causes genotoxicity. 2-Bromoacetaldehyde can also be metabolized by aldehyde dehydrogenase in the presence of nicotinamide adenine dinucleotide to bromoacetic acid, which is excreted in the urine" (ATSDR 1992).

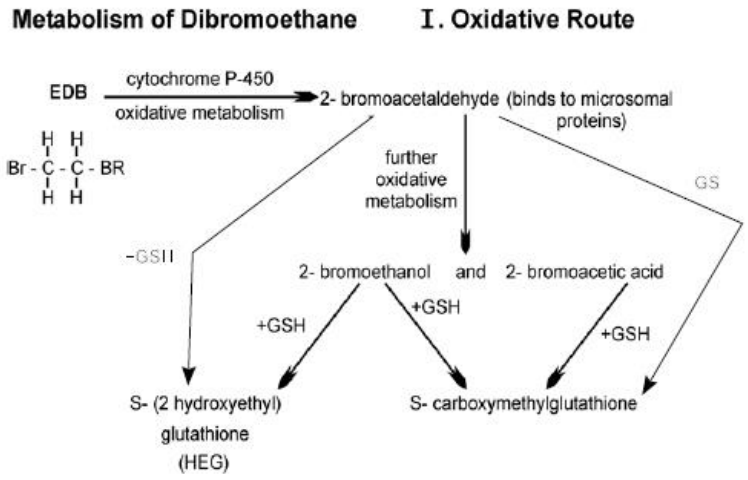

Figure 1. Metabolism of EDB by the oxidative route as cited in EPA (2004).

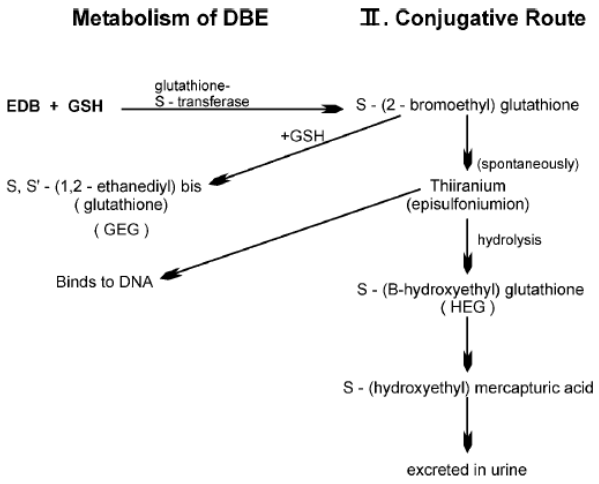

Figure 2. Metabolism of EDB by the conjugative route as cited in EPA (2004).

3.1.2.2 Absorption and Excretion

As mentioned previously and cited by the EPA (2004),

> "Inhalation studies (National Toxicology Program [NTP] 1982; Stinson et al. 1981; Nitschke et al. 1981; Reznik et al. 1980; Short et al.1978; Smith and Goldman 1983) show that EDB is absorbed via the inhalation route of exposure and distributed systemically. Stott and McKenna (1984) showed that EDB is about 50% absorbed when presented to either the upper or lower respiratory tract of Fisher 344 rats at a flow rate equivalent to their respiratory minute volume (53 mL/min) (EPA 2004). EDB is eliminated mainly in the urine. *In vivo* metabolic studies have identified a number of urinary metabolites, including S-(hydroxyethyl) mercapturic acid and S-(beta-hydroxyethyl) cysteine following oral administration of 100 mg/kg EDB in albino rats (Nachtomi et al. 1966). S-(hydroxyethyl) mercapturic acid, thiodiacetic acid, and thiodiacetic acid sulfoxide have been identified as major urinary metabolites following oral administration of EDB in Wistar rats (Wormhoudt et al. 1998). S-[2-(N7- guanyl) ethyl]-N-acetylcysteine, which is derived from the nucleic acid adduct S-[2-(N7-guanyl)ethyl] GSH, has also been identified as a urinary metabolite in rats following intraperitoneal injection (Kim and Guengerich 1989 and EPA 2004)."

3.1.2.3 MOA and Dose Metric

In Rowe et al. (1952), increased liver weights and slight histopathological changes in the liver were observed in female rats exposed to 100 ppm for 4 h and 200 ppm for 1 h. As described

above, metabolism of EDB results in metabolites, which are known to cause liver toxicity. In the Short et al. (1978) study, skeletal anomalies were observed in fetuses from mice exposed to EDB; however, morphological changes were observed at concentrations that also affected maternal welfare such as decreased feed consumption, reduced body weight gain, and increased incidence of fetal resorptions. EDB exposure was associated with alterations in maternal homeostasis, which may have produced fetal toxicity independently of a direct action of EDB on the fetus. Based on the available information, there is not a clear explanation as to why exposure to EDB causes reduced feed consumption. As cited in Short et al. (1979), studies have shown that reductions in food consumption may decrease the release of gonadotropins from the anterior pituitary and may produce a lengthening of the estrous cycle with a cessation of cyclic activity (Capmbell et al. 1977; Cooper and Haynes 1969; Piacsek and Meites 1967). Therefore, reduced feed consumption in dams, associated with EDB exposure, may contribute to the developmental changes observed in fetuses (Short et al. 1978, 1979). In both studies, data on the exposure concentration of the parent chemical were available, whereas data on more specific dose metrics were not available. Thus, exposure concentrations of the parent chemical were used as the dose metrics.

3.1.3 Health-Based 23-h Acute 23-h ReV and ESL

3.1.3.1 POD and Critical Effects and Dosimetric Adjustments

EDB induced developmental effects included anatomical and skeletal defects at 20 ppm in mice and rats. EDB also produced maternal toxicity in mice at 20 ppm and at 38 ppm in rats and mice as evidenced by decreases in food consumption, body weight gain, reduced fetal weight and survival. The LOAEL identified for this study was 20 ppm for fetal skeletal anomalies and maternal toxicity and was used as the POD in further calculations of the acute ReV.

The POD_{HEC} corresponding to an effect level was determined from the Short et al. (1978) study. The 20 ppm dose level from Short et al. (1978) was observed as a LOAEL in mice and rats for reduced fetal weights, skeletal anomalies and maternal toxicity (weight gain, feed consumption, and increased fetal resorptions) was used as the POD to derive a POD_{HEC} of 20 ppm.

3.1.3.1.1 Default Exposure Duration Adjustments

EDB produced adverse effects on fetal body weight, increased incidence of fetal resorptions and skeletal anomalies, maternal welfare, reduced body weight and feed consumption in mice at all doses tested. While reduced body weights were also observed in fetuses (e.g., mice exposed to 20 ppm) and may be related to maternal toxicity, other developmental effects observed in the study at ≥ 20 ppm (e.g., skeletal malformations, fetal resorptions and death) cannot necessarily be attributed to maternal toxicity. Since the POD is derived from developmental endpoints, the exposure duration was not adjusted to 1 h according to TCEQ Guidelines (TCEQ 2015a) due to potential sensitive windows of exposure. The guidelines also

state that the averaging time for ReV and ESL values based on reproductive or developmental effects is the number of hours of the single day of exposure, not a 1-h averaging time as is typical for 1-h ReVs. Therefore, the acute ReV and ^{acute}ESL derived using the Short et al. (1978) study will be a 23-h value. The POD_{ADJ} is equal to the POD of 20 ppm.

3.1.3.1.2 Default Dosimetry Adjustments from Animal-to-Human Exposure

The POD identified in Short et al. (1978) was based on effects observed in animals; therefore, an animal-to-human adjustment was necessary. Both rats and mice were included in the study; however, mice were more sensitive to EDB toxicity. EDB is considered a Category 2 gas because of insolubility in water and demonstration of systemic toxicity (EPA 2004). Because the critical adverse effects caused by EDB were systemic effects, EDB is treated as a Category 3 gas (TCEQ 2015a). For Category 3 gases, the default dosimetric adjustment from an animal concentration to a POD_{HEC} was conducted using the following equation:

$$POD_{HEC} = POD_{ADJ} \times [(H_{b/g})_A / (H_{b/g})_H]$$

where: $H_{b/g}$ = ratio of the blood:gas partition coefficient
A = animal
H = human

A blood:gas partition coeffcient for mice was not available. Gargas et al. (1989) reported blood:gas partition coefficient of 119 for rats, which is greater than the estimated human blood:gas partition coefficient of 24.8. According to TCEQ guidelines, if the animal/human ratio of the blood:gas partition coefficients is greater than 1, a default value of 1 is used (TCEQ 2015a). The resulting POD_{HEC} is equal to the POD_{ADJ} of 20 ppm.

3.1.3.2 Adjustments of the POD_{HEC}

The endpoint used for the POD was based on a LOAEL of 20 ppm in mice, the most sensitive species, increased fetal skeletal anomalies, reduced fetal body weight, increased incidence of fetal resorptions and for maternal toxicity (decreased weight gain and feed consumption). The MOA by which EDB may produce toxicity is assumed to have a threshold/nonlinear MOA. The following uncertainty factors (UFs) were considered appropriate for application to the POD_{HEC} of 20 ppm: 10 for intraspecies variability (UF_H), 3 for animals to humans (UF_A), 10 for LOAEL to NOAEL (UF_L), and 6 for database uncertainty (UF_D), for a total UF of 1800. According to TCEQ guidelines, if the cumulative UF exceeds 300, a maximum total UF of 300 will generally be used (TCEQ 2015a).

- A UF_H of 10 was used for intrahuman variability to account for variation in sensitivity among the members of the human population including possible child/adult differences, those with pre-existing medical conditions, etc.;

- A UF_A of 3 was used to account for potential pharmacodynamic differences between animals and humans (pharmacokinetic adjustment was already performed);
- A UF_L of 10 was used because the POD_{HEC} of 20 ppm from Short (1978) was considered a LOAEL based on anatomical and skeletal defects at 20 ppm in mice, reduced fetal body weight, increased incidence of fetal resorptions and maternal toxicity at 20 ppm, (decreased food consumption, body weight gain).
- A UF_D of 6 was used because although acute inhalation studies exist for both humans and multiple animal species as well as short-term reproductive/developmental animal studies, the database is somewhat deficient in studies that assess the types of mild effects most appropriate for use as critical effects (e.g., effects in the nasal/respiratory regions). Also, EDB shows a very steep dose-response curve, with no effects observed in rats after a single exposure to 200 ppm for 0.7 h, increased liver weight after a single exposure to 200 ppm for 1 h, and death in 1/10 rats exposed to 100 ppm for 7 h (Rowe et al. 1952). This steep duration-dependent, dose-response curve requisites due consideration when selecting the UF_D given the studies available. The overall database of acute toxicological studies with EDB is considered to be medium quality and the key study is considered to be medium to high quality (ATSDR 1996; AEGL 2008).

acute 23-h ReV = POD_{HEC} / (UF_H x UF_A x UF_L x UF_D)

= 20 ppm / (10 x 3 x 10 x 6)
= 20 ppm / 300 (maximum total UF)
= 0.0667 ppm
= 0.067 ppm or 67 ppb (rounded to two significant figures)

3.1.3.3 Health-Based 23-h Acute ReV and ESL

The acute 23-h ReV of 67 ppb (510 µg/m^3) derived based on the Short et al. (1978) study was multiplied by 0.3 to calculate the ^{acute}ESL. At the target hazard quotient of 0.3, the ^{acute}ESL is 20 ppb (150 µg/m^3) (Table 5. Derivation of the Acute ReV and acuteESL). Values were rounded to two significant figures at the end of all calculations.

Table 5. Derivation of the Acute ReV and acuteESL

Parameter	Values and Descriptions
Study	Short et al. (1978)
Study Population	4 Groups of 18-22 pregnant CD-1 mice
Study Quality	Medium to High
Exposure Methods	Exposure via inhalation of 0, 20, 38, or 80 ppm EDB
POD (LOAEL)	20 ppm
Critical Effects	Reduced fetal body weight, increased incidence of fetal resorptions and skeletal anomalies. Maternal toxicity (decreased weight gain and feed consumption).
Exposure Duration	23 h/d during GD 6-15, sacrificed on GD 18
Extrapolation to 1 h	N/A
POD_{HEC} (23 h)	20 ppm
Total UFs	3000
Maximum UFs (TCEQ 2015a)	300
Intraspecies UF	10
Interspecies UF	3
LOAEL UF	10
Incomplete Database UF *Database Quality*	10 Medium
acute ReV [23 h] (HQ = 1)	**67 ppb (510 µg/m^3)**
^{acute}ESL [23 h] (HQ = 0.3)	**20 ppb (150 µg/m^3)**

3.1.4 Health-Based 24-h Acute ReV

Since the LOAEL identified for the acute ReV was 20 ppm for reduced fetal body weight, increased incidence of fetal resorptions and skeletal anomalies and maternal toxicity (decreased weight gain and feed consumption) following a 23-h exposure, the resulting 23-h ReV will also be used for the acute 24-h ReV.

3.2 Welfare-Based Acute ESLs

3.2.1 Odor Perception

EDB has a sweet, chloroform – like odor with an odor threshold of 10 ppm (Ruth 1986). Because the odor value is significantly higher than the determined acute ESL, and the odor of EDB is described as sweet, an $^{acute}ESL_{odor}$ will not be derived (TCEQ 2015b).

3.2.2 Vegetation Effects

No studies were found regarding acute effects of EDB on vegetation.

3.3 Short-Term ESL and Values for Air Monitoring Evaluation

The acute evaluation resulted in the derivation of the following values:

- Acute 23-h ReV = 67 ppb (510 µg/m^3)
- ^{acute}ESL [23 h] = 20 ppb (150 µg/m^3)
- Acute 24-h ReV = 67 ppb (510 µg/m^3)

For the evaluation of ambient air monitoring data, the acute 24-h ReV of 67 ppb (510 µg/m^3) will be used to evaluate 1-h and 24-h monitoring data. The health-based 23-h ^{acute}ESL of 20 ppb (150 µg/m^3) will be conservatively used as the 1-h ESL for air permitting.

The ^{acute}ESL (HQ = 0.3) is not used to evaluate ambient air monitoring data and will be used in air permitting applications.

3.4 Subacute Inhalation Observed Adverse Effect Level (IOAEL)

Risk assessors, and the general public, often ask to have information on the levels in air where health effects would be expected to occur. So, when possible, the TCEQ provides chemical-specific observed adverse effects levels in DSDs (TCEQ 2015a). As the basis for development of inhalation observed adverse effect levels is limited to available data, future studies could possibly identify a lower POD for this purpose. Regarding critical effects due to acute EDB exposure, the animal study by Short et al. (1978) found a 23-h, multiple-day LOAEL of 20 ppm for maternal toxicity (decreased weight gain and feed consumption), reduced fetal body weight, and increased incidence of fetal resorptions. This animal LOAEL was used as the animal acute inhalation observed adverse effect level (IOAEL) for extrapolation to humans. No duration adjustment was made (TCEQ 2015a). As discussed in Section 3.1.5.2, for these effects the animal-to-human dosimetric adjustment results in a $LOAEL_{HEC}$ equal to the animal exposure concentration (e.g., a DAF of 1 is used). Thus, the subacute $LOAEL_{HEC}$ based on this animal study is estimated to be 20 ppm.

The $LOAEL_{HEC}$ determined from an animal study represents a concentration at which similar effects could occur in some individuals exposed to this level over the same duration as used in the study or longer. Importantly, effects are not a certainty due to potential interspecies and intraspecies differences in sensitivity. The subacute IOAEL of 20 ppm (150 mg/m^3) is provided for informational purposes only (TCEQ 2015a).

The margin of exposure between the estimated subacute IOAEL of 20 ppm and the acute 24-h ReV of 67 ppb is a factor nearly 300.

Chapter 4 Chronic Evaluation

4.1 Noncarcinogenic Potential

A comprehensive literature search was conducted regarding the chronic inhalation toxicity of EDB through July 2016. Information from both human and animal studies regarding the chronic toxicity of EDB was reviewed in detail by ATSDR (1992), EPA (2004), OEHHA (1999), and NRC (2008).

4.1.1 Key and Supporting Studies

Reproductive endpoints have been the primary focus of EDB epidemiology studies. Several human studies suggest that EDB is a male reproductive toxicant. However, limitations such as inadequate exposure data, confounding factors, possible exposure to other chemicals and lack of dermal exposure quantification limits the use of these studies in developing the chronic ReV. Animal studies have also demonstrated noncancer effects such as early mortality, depression of body weight gain, and non-neoplastic lesions of the respiratory system, liver, kidney, testis, eye, and adrenal cortex in rats and mice after chronic exposure to EDB and are summarized in 4.1.2.2.

4.1.1.2 Animal Studies

As cited in EPA (2004), chronic inhalation animal studies have determined that weight gain depression, hepatic necrosis, nephropathy, testicular atrophy, and degeneration of the adrenal cortex have been reported in rats and mice (EPA 2004). The results of subchronic inhalation studies revealed weight gain depression, swelling of adrenocortical cells, decreases in thyroid follicle size, and formation of megalocytic cells of the lining of bronchioles in rats and mice (NTP 1982; Nitschke et al. 1981; Reznik et al. 1980). In rats, relative liver and kidney weights, focal epithelial hyperplasia of the nares, and diffuse respiratory hyperplasia have also been reported (EPA 2004).

4.1.1.2.1 Key Animal Study – NTP (1982)

The NTP (1982) performed a chronic inhalation bioassay in rats and mice designed to assess potential adverse effects of EDB after 78-103 wk of exposure (both noncarcinogenic and carcinogenic effects). Male and female Fischer 344 rats and B6C3F1 mice (n = 50 per sex, species, and exposure group) were exposed to 0, 10, or 40 ppm EDB for 6 h/d, 5 d/wk for 78-103 wk. Untreated controls consisted of 50 rats and mice (n = 50 per species and sex). High mortality in both species prompted early termination in some of the exposure groups. In male mice, the principal cause of death was suppurative urinary tract infections that were unrelated to exposure of EDB and were not considered relevant for derivation of the ReV. The carcinogenic effects observed in the NTP bioassay will be summarized in detail in the Carcinogenic Potential Section 4.2. While statistics were only performed for histopathologic findings on neoplasms, all non-neoplastic endpoints that showed an increasing response across doses (i.e., a dose-response) were considered in identifying the critical effect and are summarized in Table 6 and Table 7. Effects observed in male mice were not considered due to unrelated high mortality rates.

Table 6. Summary of Results in Rats (NTP 1982)

Endpoint in Rat	0 ppm	10 ppm	40 ppm
Males			
Suppurative inflammation in the nasal cavity	0/50	8/50	20/50
Epithelial hyperplasia in the lung/bronchus	0/50	7/50	13/50
Congestion in the lung	0/50	4/50	14/50
Congestion in the liver	0/50	4/50	9/50
Hepatic necrosis [a]	2/50	6/50	19/50
Mineralization in the kidney	0/50	4/50	5/50
Toxic nephropathy	0/50	4/50	28/50
Testicular degeneration	1/50	10/50	18/49
Testicular atrophy	1/50	2/50	5/49
Degeneration of the adrenal cortex	0/49	1/49	1/48
Females			
Suppurative inflammation in the nasal cavity	0/50	1/50	15/50
Epithelial hyperplasia in the nasal cavity	0/50	27/50	31/50
Congestion in the lung	0/50	1/48	8/47
Hepatic necrosis [a]	2/50	3/49	13/48
Degeneration of the adrenal cortex	4/50	7/49	13/47
Thyroid C-cell hyperplasia	0/49	1/48	4/45
Vaginal suppurative inflammation	0/50	2/50	5/50

Highlighted/shaded endpoints were further analyzed by the TCEQ for use as a POD

[a] Includes focal and centrilobular necrosis

Table 7. Summary of Results in Mice (NTP 1982)

Endpoint in Mouse	0 ppm	10 ppm	40 ppm
Males			
Serous inflammation of the nasal cavity	0/45	15/50	22/50
Suppurative inflammation of the nasal cavity	0/45	3/50	9/50
Epithelial hyperplasia in the lung/bronchiole	0/41	3/48	29/46
Alveolar epithelial hyperplasia	0/41	2/48	31/46
Preputial gland abscess	1/45	4/50	6/50
Females			
Suppurative inflammation of the nasal cavity	0/50	4/50	20/50
Epithelial hyperplasia in the lung/bronchus	0/49	10/49	18/50
Epithelial hyperplasia in the lung/bronchiole	0/49	13/49	44/50
Alveolar epithelial hyperplasia	0/49	11/49	44/50
Hematopoiesis in the spleen	0/50	8/49	16/49
Hepatic necrosis [a]	0/50	3/50	7/50

Highlighted/shaded endpoints were further analyzed by the TCEQ for use as a POD
[a] Includes focal and centrilobular necrosis

The NTP (1982) study results demonstrated that inhalation of the lowest concentration of EDB tested (10 ppm) caused non-neoplastic lesions including hepatic necrosis and toxic nephropathy in rats of both sex, testicular degeneration and atrophy in males, retinal degeneration in female rats, splenic hematopoiesis in female mice, and inflammation of the nasal cavity and hyperplasia of the respiratory system in female mice.

4.1.1.2.2 Supporting Animal Studies

Several animal studies have examined noncancer effects in rats and mice in both subchronic and chronic inhalation studies.

- Stinson et al. (1981) examined groups of 50 male and 50 female B6C3F1 mice that were exposed by inhalation to 10 ppm for 103 wk, 40 ppm for 90 wk or filtered air 6h/d, 5 d/wk. Dose-dependent hyperplastic lesions were found in 1 (low dose group) and 10 (high dose group) males and 3 (low dose group) and 11 (high dose group) females.
- NTP (1982) conducted subchronic inhalation studies in male and female Fischer 344 rats (n = 4 to 6 per sex and exposure group) and B6C3F1 mice (n = 10 per sex and

exposure group). Each group was exposed to 0, 3, 15, or 75 ppm EDB 6 h/d, 5 d/wk for 13 wks. No deaths occurred for rats at any exposure group. Dose-related depression in weight gain occurred in male rats at all concentrations and female rats at 75 ppm. Rats of both sexes exposed to high doses of EDB (75 ppm) experienced swelling and/or vacuolation of adrenal cortical cells and decreases in thyroid follicular size. Four out of 10 male mice in the 3 ppm exposure group and 1 female in the 75 ppm exposure group died prior to the termination of the study. Although the cause of death was not mentioned, an increase in mortality of male mice was also observed in the chronic study and attributed to suppurative urinary tract infections that were unrelated to exposure of EDB. A dose-related decrease in body weight was observed for both sexes. At wk 12 and 13, eye irritation was observed in both sexes in the 75 ppm exposure group. Megalocytic cells in the lining of the bronchioles were found in 3/10 male mice and 9/10 female mice exposed to 75 ppm. Based on the effects observed at 75 ppm, exposure concentrations of 10 and 40 ppm EDB were chosen for chronic toxicity and cancer study.

- Rowe et al. (1952) determined that exposure to 25 ppm for approximately 7 h/d, 5 d/wk for 3 months duration represented the most severe repeated exposures without detectable adverse effects in rabbits and monkeys and probably in rats and guinea pigs. Signs of toxicity were observed in subchronic exposure of rats (20/sex/group) to 50 ppm EDB for as many as 63 seven-h exposures in 91 d resulted in death and increased liver and kidney weights (Rowe et al. 1952). Testes weights decreased in males while lung weights in males were elevated and spleen weights in females were decreased. Histopathological examination revealed no changes. Guinea pigs (8/sex/group) were subjected to 57 seven-h exposures of 50 ppm EDB in 80 d and exhibited reduced body weights, central fatty liver degeneration and slight internal congestion and edema of the kidney tubular epithelium. Four rabbits exposed to 59 seven-h sessions at 50 ppm in 84 d showed no signs of adverse effects. Clinical signs of monkeys exposed to 50 ppm EDB (49 seven-h exposures in 70 d) included ill unkempt appearance and nervousness, and exhibited fatty degeneration of the liver and increased relative kidney weight (Rowe et al. 1952). As in previous sub-chronic studies, nasal tissue was not examined by Rowe et al. (1952) and the study is considered limited based on the sample sizes of species used (EPA 2004) and the study was not considered during the development of the ReV.
- In a 13-wk inhalation study, Nitschke et al. (1981) examined 40 male and 20 female CDF (F 344) rats that were exposed to 0, 3, 10 or 40 ppm EDB for 6 h/d, 5 d/wk for 13 wk for a total of 67-68 exposures in 95-96 d (Nitschke et al. 1981). Necropsies of 10 males per exposure group were conducted at 1, 6, and 13 wk; 10 females per exposure group were sacrificed at 13 wk. The remaining male and female animals were sacrificed 88–89 d post exposure. Rats exposed to 3 ppm EDB showed no consistent adverse effects. At 10 ppm, EDB caused slight epithelial hyperplasia of the

nasal turbinates after 1, 6 or 13 wk of exposure; however, 88 d after the last exposure to EDB, nasal turbinate changes were not observed. The most sensitive response associated with repeated subchronic exposure of rats to 10 or 40 ppm EDB involves pathologic changes in the respiratory epithelium of the nasal turbinates. Exposure to 3 ppm EDB elicited no discernible response in any of the tissues examined; 3 ppm was defined as the NOAEL and 10 ppm the LOAEL for slight epithelial hyperplasia of the nasal turbinates. Male rats in the 40 ppm group exhibited decreased weight gain throughout most of the 13-wk exposure period; however, reduced weight gain was never more than 6-8% below control levels and returned to normal after the exposure period. With the exception of decreased specific gravity of urine in females of the 40 ppm group, no treatment-related changes were observed in any rat group with respect to urinalysis, hematology, and clinical chemistry. At the end of 13 wk, relative liver and kidney weights of males exposed to 40 ppm EDB were significantly elevated and absolute liver weight of females was also significantly elevated. Organ weights returned to control levels post exposure. Histopathological examination revealed lesions primarily confined to the anterior sections of the nasal turbinates. Only slight epithelial hyperplasia of nasal turbinates was noted at 10 ppm (Nitschke 1981 and EPA 2004).

- Reznik et al. (1980) also examined the respiratory system in both the rat and mouse exposed subchronically to EDB in a 13-wk inhalation study. Male and female F344 rats (5 animals/sex/exposure group) and B6C3F1 mice (10 animals/sex/exposure group) were exposed via inhalation to 0, 3, 15, or 75 ppm EDB for 6 h/d, 5 d/wk for 13 wk. Histomorphological changes were observed in the respiratory tract (nasal cavity, trachea, and lung) of mice and rats exposed to 75 ppm EDB with a higher incidence in mice. Concentration-dependent changes included cytomegaly, focal hyperplasia, squamous metaplasia, and loss of cilia. Rats and mice exposed to 75 ppm showed severe necrosis and atrophy of the olfactory epithelium. No lesions were noted in any other tissues. No histomorphological alterations were observed in the nasal cavity at 3 ppm in both species. LOAELs were 15 ppm in rats and 75 ppm in mice (EPA 2004).

4.1.1.3 Reproductive and Developmental Studies

As discussed in Section 3.1.2.3, some studies provide evidence that EDB may cause both reproductive and developmental effects in humans although the significant limitations of the studies (i.e., poor exposure measurements, lack of appropriate control groups, and concomitant exposure to other chemicals) prevent their use in the development of ReVs. Animal studies provide evidence for EDB-induced developmental and reproductive toxicity and are reviewed extensively in USEPA (1994), ATSDR (1996), and NRC (2008).

- Ratcliff et al. (1987) investigated potential mutagenicity and spermatotoxicity of EDB exposure amongst papaya workers in Hawaii through a cross-sectional study. Six fumigation plants were investigated where fruit is sorted and packed in rooms that often share the door to the fumigation chambers. Forklift drivers and fumigators enter the chamber frequently with no personal protective clothing. According to the authors, there was minimal dermal exposure; however, dermal exposure was not quantified. Two industrial hygiene surveys were conducted a year prior and during the study timeframe. Air samples were collected at all plants on two separate occasions and workers were sampled using personal monitors for the full 8-h shift. Full-shift exposures for papaya packers/sorters ranged from 36 to 148 ppb and those for forklift operators ranged from 16-175 ppb (0.1-1.4 mg/m^3). Average duration of exposure was 5 years with a geometric mean air concentration of 88 ppb (8-h time weighted average). Semen analysis of 46 men employed in the papaya factories were compared to the control group that consisted of 43 unexposed men from a nearby sugar processing plant. After adjusting for confounding factors of: smoking, caffeine, and alcohol consumption; subject's age; abstinence of sex; age of sample; and history of urogenital illness, statistically significant decreases in sperm count per ejaculate, the percentage of viable and motile sperm, and increases in the proportion of sperm with specific morphological abnormalities (tapered heads, absent heads, and abnormal tails) were observed among exposed men (Ratcliffe et al. 1987). Semen pH was significantly more alkaline than that of unexposed workers. Measurement of male fertility was not conducted. OEHHA (2001) used the Ratcliff et al. (1987) study to derive the chronic Reference Exposure Level (REL) of 0.1 ppb. However, due to the high variation in inhalation exposure data, small sample size, short-exposure duration, and the lack of dermal quantification, the TCEQ did not use this study for the development of the ReV.
- Wong et al. (1979), as cited in EPA (2004), conducted a retrospective evaluation of the reproductive performance of 297 male workers in four chemical plants (Plants A-D) in Arkansas and Texas that produced EDB during the 1958-1977 time period. EDB exposures ranged from <0.5 to 5 ppm. In addition to EDB, Plant A produced dibromochloropropane (a known male reproductive toxicant). Plant B produced EDB exclusively. Plant C produced EDB along with other brominated compounds, and workers in Plant D were exposed to EDB and ethylene dichloride (EDC). EDB exposure was monitored through industrial hygiene studies only at Plants A, B, and C. A surrogate measure of male fertility was derived from the reproductive performance of wives based on the numbers of live births and were compared to the expected numbers of live births derived from national fertility tables published by the National Center for Health Statistics. Maternal age, parity, race, and calendar year were standardized to adjust for confounding factors. Ratios of observed births to expected births were computed as index fertility and a ratio larger than one

indicated higher fertility of the study group as compared to the US cohorts. Workers were classified as being exposed to either < 0.5 ppm or 0.5–5.0 ppm. There was no difference between observed and expected births in wives of workers for three of the plants A-C. There was, however, a significant difference ($p < 0.05$) pertaining to Plant D producing EDB (0.1 to 4 ppm) and also using EDC. Fertility was 20% below expected for the four plants combined; however, this decrease was largely due to Plant D, which was 49% below the expected level. Considering the limited exposure data and co-exposure to other chemicals, no conclusions can be drawn concerning the potential effect of EDB on fertility from this study.

4.1.2 MOA and Dose Metric

With respect to long-term toxicity, as cited by EPA 2004,

> "…the mechanism of 1,2-dibromoethane-mediated cytotoxicity has been studied in isolated rat hepatocytes (Khan et al., 1993). Microsomal cytochrome P 450-dependent oxidative metabolism of 1,2-dibromoethane produces the metabolite 2-bromoacetaldehyde. The results suggest that the cytotoxic mechanisms for 1,2-dibromoethane may possibly be attributed to lipid peroxidation and/or protein binding induced by 2-bromoacetaldehyde. In addition, the study authors considered that the conjugation of 1,2-dibromoethane with GSH may also contribute to cytotoxicity. Botti et al. (1982, 1986, 1989a, 1989b) and Masini et al. (1986) provided evidence that 1,2-dibromoethane-induced depletion of hepatic mitochondrial GSH correlated with hepatotoxicity and perturbations in mitochondrial Ca2+ homeostasis. The results of *in vitro* and *in vivo* experiments suggest that the renal toxicity of 1,2-dibromoethane may be due to its biotransformation by GSH conjugation followed by further conversion in the kidney to highly reactive metabolites (Novotna and Duverger-van Bogaert 1994). Repeated administration of 1,2-dibromoethane to rats has been shown to enhance the content of GSH in the liver and kidney (Mann and Darby 1985 & EPA 2004)."

With respect to reproductive effects, as cited by ATSDR 1992,

> "The mechanism of action for the antispermatogenic effects of 1,2-dibromoethane may be related to covalent binding of metabolites of 1,2-dibromoethane with thiol groups of nucleoproteins in nuclei of spermatozoa. Such adduct formation interferes with DNA, causing improper packing of the chromatin (Amir and Lavon 1976; Amir et al. 1977). Antispermatogenic effects in exposed workers and this preferential binding of 1,2-dibromoethane in the testis of rodents and ruminants suggest that similar effects on spermatozoa could occur in men exposed to low levels of 1,2-dibromoethane."

4.1.3 POD for Key Study and Dosimetric Adjustments

The NTP (1982) inhalation study is used as the key study. This study most clearly demonstrated dose-response for multiple, sensitive adverse effects at relatively low exposure levels. The most sensitive endpoints (those with responses that may have begun at 10 ppm in Table 6 and Table 7) were considered in identifying the critical effect.

4.1.3.1 Benchmark Concentration (BMC) Modeling

The TCEQ performed Benchmark Concentration (BMC) modeling using USEPA Benchmark Dose (BMD) software (version 2.6) for the data in Table 6 (rats) and Table 7 (mice), which were taken from the NTP (1982) study. Data were used to predict 95% lower confidence limits on the BMCs using dichotomous models. A default benchmark response (BMR) of 10% was selected for extra risk (BMC_{10}) and $BMCL_{10}$. For each of the identified endpoints, all of the available dichotomous models were run (Appendices 1.1 and 1.2), and the best fit models (global goodness of fit (p) > 0.1, scaled residuals < |2|, lowest AIC/BMDL) are listed in Table 8.

Table 8. BMC Modeling Results for the Nonneoplastic Endpoints from NTP (1982)

Endpoint	Model	p-value	AIC	BMC	BMCL
Male Rats					
Suppurative inflammation in the nasal cavity	LogLogistic	0.962	113.34	6.36	4.37
Epithelial hyperplasia in the lung/bronchus	LogLogistic	0.487	101.14	10.3	6.80
Congestion in the lung	Gamma [a]	1.000	89.173	12.8	8.87
Congestion in the liver	LogLogistic	0.768	77.511	17.7	11.0
Hepatic necrosis	Quantal-Linear	0.732	124.01	9.92	6.88
Mineralization in the kidney	LogLogistic	0.238	64.837	27.1	15.7
Toxic nephropathy	Multistage 2°	1.000	100.47	11.7	6.27
Testicular degeneration	LogLogistic	0.327	129.21	6.93	4.56
Testicular atrophy	Quantal-Linear	0.972	62.895	48.4	22.9
Female Rats					
Suppurative inflammation in the nasal cavity	Multistage 2°	0.996	72.900	21.8	13.9
Epithelial hyperplasia in the nasal cavity	No Viable Model	--	--	--	--
Congestion in the lung	Quantal-Linear	0.742	55.296	25.6	15.5
Hepatic Necrosis	Logistic	0.903	99.453	24.5	19.4
Degeneration of the adrenal cortex	LogLogistic	0.943	127.51	16.3	8.66
Thyroid C-cell hyperplasia	Quantal-Linear	0.996	38.726	46.2	24.0
Vaginal suppurative inflammation	LogLogistic	0.894	51.512	36.0	19.7
Female Mice					
Suppurative inflammation of the nasal cavity	Quantal-Linear	0.734	97.839	8.99	6.52
Epithelial hyperplasia in the lung/bronchus	LogLogistic	0.423	118.57	6.31	4.33
Epithelial hyperplasia in the lung/bronchiole	Multistage 2°	1.000	97.389	3.99	2.29
Alveolar epithelial hyperplasia	Multistage 2°	1.000	92.881	5.05	2.81
Hematopoiesis in the spleen	LogLogistic	0.623	108.42	7.75	5.24
Hepatic necrosis	LogLogistic	0.821	65.561	24.1	14.3

[a] Gamma, Weibull, Multistage 2°, and Quantal-Linear Models gave the same results.

4.1.3.2 Exposure Duration Adjustments

The POD/$BMCL_{10}$ values from Table 8 based on the NTP (1982) study were adjusted to continuous exposure concentrations:

POD_{ADJ} = POD x (D/24 h) x (F/7 d)

where:

D = Exposure duration, hours per day

F = Exposure frequency, days per week

POD_{ADJ} = POD x (6/24 h) x (5/7 d) = POD x 0.1786

The resulting POD_{ADJ} for each of the endpoints considered in identifying the critical effect can be found in Table 9.

4.1.3.3 Default Dosimetry Adjustments from Animal-to-Human Exposure

As discussed in the Section 3, EDB is considered a Category 2 gas (EPA 2004). Because the critical adverse effects caused by EDB are both point of entry (POE) and systemic in nature, each endpoint will be treated as either a Category 1 (POE effects) or a Category 3 (systemic effects) gas (TCEQ 2015a). A dosimetric adjustment from an animal concentration to a human equivalent concentration (POD_{HEC}) for each of the identified endpoints was performed for EDB according to the subsections below. The resulting POD_{HEC} values for each of the endpoints can be found in Table 9, which is provided and discussed in Section 4.1.4.4.

4.2.3.3.1 POE effects – Category 1 gas

For Category 1 gases, the DAF is dependent upon the respiratory tract site, which the POE effects occur. When the critical effect is in the extrathoracic (ET) region, including the nasal cavity, a default DAF of 1 is applied (TCEQ 2015a, USEPA 2012). When the critical effects is in the tracheobronchial (TB) or pulmonary (PU) region, the DAF is the ratio of the regional gas dose ratio in the respiratory region of interest (e.g., $RGDR_r$) (USEPA 2012):

$$POD_{HEC} = POD_{ADJ} \times RGDR_r$$

$$RGDR_r = (V_E/SA_r)_A \,/\, (V_E/SA_r)_H$$

where: V_E (ml/min) = minute volume

SA_r = surface area of the exposed respiratory tract region

A = animal

H = human

4.2.3.3.1.1 Male Rat Dosimetric Adjustments

For epithelial hyperplasia in the bronchus in male rats, the minute volume, calculated using the default chronic body weight of 0.380 grams, is 0.2535 L/min and the default tracheobronchial surface area is 22.5 m^2 (USEPA 1994). For humans, the default minute volume is 13.8 L/min and the default tracheobronchial surface area is 3200 m^2 (USEPA 1994).

$$RGDR_{TB} = ((0.2535\ L/min)/(22.5\ m^2)) / ((13.8\ L/min)/(3200\ m^2))$$

$$RGDR_{TB} = 2.6126$$

$$POD_{HEC} = 1.2145\ ppm\ (POD_{ADJ}) \times 2.6126 = 3.1730\ ppm$$

For congestion in the lung in male rats, the minute volume, calculated using the default chronic body weight of 0.380 grams, is 0.2535 L/min and the default pulmonary surface area is 0.34 m^2 (USEPA 1994). For humans, the default minute volume is 13.8 L/min and the default pulmonary surface area is 54 m^2 (USEPA 1994).

$$RGDR_{PU} = ((0.2535\ L/min)/(0.34\ m^2)) / ((13.8\ L/min)/(54\ m^2))$$

$$RGDR_{PU} = 2.9175$$

$$POD_{HEC} = 1.5842\ (POD_{ADJ}) \times 2.9175 \times = 4.6220\ ppm$$

4.2.3.3.1.2 Female Rat Dosimetric Adjustments

For congestion in the lung in female rats, the minute volume, calculated using the default chronic body weight of 0.229 grams, is 0.1673 L/min and the default pulmonary surface area is 0.34 m^2 (USEPA 1994). For humans, the default minute volume is 13.8 L/min and the default pulmonary surface area is 54 m^2 (USEPA 1994).

$$RGDR_{PU} = ((0.1673\ L/min)/(0.34\ m^2)) / ((13.8\ L/min)/(54\ m^2))$$

$$RGDR_{PU} = 1.9250$$

$$POD_{HEC} = 2.7683\ (POD_{ADJ}) \times 1.9250 = 5.3291\ ppm$$

4.2.3.3.1.3 Female Mice Dosimetric Adjustments

For epithelial hyperplasia in the bronchus in female mice, the minute volume, calculated using the default chronic body weight of 0.0353 grams, is 0.0414 L/min and the default tracheobronchial surface area is 3.5 m^2 (USEPA 1994). For humans, the default minute volume is 13.8 L/min and the default tracheobronchial surface area is 3200 m^2 (USEPA 1994).

$RGDR_{TB} = ((0.0414\ L/min)/(3.5\ m^2)) / ((13.8\ L/min)/(3200\ m^2))$

$RGDR_{TB} = 2.7429$

$POD_{HEC} = 0.7733\ (POD_{ADJ}) \times 2.7429 = 2.1211\ ppm$

For epithelial hyperplasia in the bronchiole in female mice, the minute volume, calculated using the default chronic body weight of 0.0353 grams, is 0.0414 L/min and the default tracheobronchial surface area is 3.5 m^2 (USEPA 1994). For humans, the default minute volume is 13.8 L/min and the default tracheobronchial surface area is 3200 m^2 (USEPA 1994).

$RGDR_{TB} = ((0.0414\ L/min)/(3.5\ m^2)) / ((13.8\ L/min)/(3200\ m^2))$

$RGDR_{TB} = 2.7429$

$POD_{HEC} = 0.4090\ (POD_{ADJ}) \times 2.7429 = 1.1218\ ppm$

For alveolar epithelial hyperplasia in female mice, the minute volume, calculated using the default chronic body weight of 0.0353 grams, is 0.0414 L/min and the default pulmonary surface area is 0.05 m^2 (USEPA 1994). For humans, the default minute volume is 13.8 L/min and the default pulmonary surface area is 54 m^2 (USEPA 1994).

$RGDR_{PU} = ((0.0414\ L/min)/(0.05 m^2)) / ((13.8\ L/min)/(54\ m^2))$

$RGDR_{PU} = 3.24$

$POD_{HEC} = 0.5019\ (POD_{ADJ}) \times 3.24 = 1.6262\ ppm$

4.2.3.3.2 Systemic effects – Category 3 gas

For Category 3 gases, when available, animal and human blood:gas partition coefficients are used to dosimetrically adjust for species differences in toxicokinetics (TCEQ 2015a).

$POD_{HEC} = POD_{ADJ} \times ((H_{b/g})_A / (H_{b/g})_H)$

where: $H_{b/g}$ = blood:gas partition coefficient
A = animal
H = human

Gargas et al. (1989) reported rat blood:gas partition coefficients of 119 for rats, which is greater than the estimated human blood:gas partition coefficient of 24.8. According to TCEQ guidelines, if the animal/human ratio of the blood:gas partition coefficients is greater than 1, a default value of 1 is used (TCEQ 2015a). A rat blood:gas partition coefficient is not available for the

mouse, and according to TCEQ guidelines a default value of 1 is used (TCEQ 2015a). Therefore, the POD_{HEC} for each of the systemic endpoints is equal to the POD_{ADJ} (Table 9).

4.1.3.4 Selection of the Critical Effect and POD

Based on the key study presented above (NTP 1982), increased incidences of adverse effects with increasing exposure levels were observed at several sites in male and female rats and female mice. These dose-dependent endpoints were considered in identifying the critical effect (Table 9). Suppurative inflammation in the nasal cavity in male rats was chosen as the critical effect since it has the lowest POD_{HEC} (0.7805 ppm). Testicular degeneration in male rats has a very similar POD_{HEC} (0.8144 ppm), with six other POD_{HEC} values being within a factor of 2.

Table 9. Endpoints and POD_{HEC} for the Nonneoplastic Endpoints from NTP (1982)

Endpoint	$POD/BMCL_{10}$ (ppm)	POD_{ADJ} (ppm)	Dosimstric Adjustment	DAF	POD_{HEC} (ppm)
Male Rats					
Suppurative inflammation in the nasal cavity	4.37	0.7805	POE, ET	1	0.7805
Epithelial hyperplasia in the lung/bronchus	6.80	1.2145	POE, TB	2.6126	3.1730
Congestion in the lung	8.87	1.5842	POE, PU	2.9175	4.6220
Congestion in the liver	11.0	1.9646	Systemic	1	1.9646
Hepatic necrosis	6.88	1.2288	Systemic	1	1.2288
Mineralization in the kidney	15.7	2.8040	Systemic	1	2.8041
Toxic nephropathy	6.27	1.1198	Systemic	1	1.1198
Testicular degeneration	4.56	0.8144	Systemic	1	0.8144
Testicular atrophy	22.9	4.0899	Systemic	1	4.0899
Female Rats					
Suppurative inflammation in the nasal cavity	13.9	2.4825	POE, ET	1	2.4825
Congestion in the lung	15.5	2.7683	POE, PU	1.9250	5.3291
Hepatic Necrosis	19.4	3.4648	Systemic	1	3.4648
Degeneration of the adrenal cortex	8.66	1.5467	Systemic	1	1.5467
Thyroid C-cell hyperplasia	24.0	4.2864	Systemic	1	4.2864
Vaginal suppurative inflammation	19.7	3.5184	Systemic	1	3.5184
Female Mice					
Suppurative inflammation of the nasal cavity	6.52	1.1645	POE, ET	1	1.1645
Epithelial hyperplasia in the lung/bronchus	4.33	0.7733	POE, TB	2.7429	2.1211
Epithelial hyperplasia in the lung/bronchiole	2.29	0.4090	POE, TB	2.7429	1.1218
Alveolar epithelial hyperplasia	2.81	0.5019	POE, PU	3.24	1.6261
Hematopoiesis in the spleen	5.24	0.9359	Systemic	1	0.9359
Hepatic necrosis	14.3	2.5540	Systemic	1	2.5540

4.1.4 Adjustments of the POD_{HEC}

The critical effect identified in NTP (1982) is suppurative inflammation in the nasal cavity in male rats since it has the lowest POD_{HEC}. Noncarcinogenic effects are assumed to have a threshold (TCEQ 2015a); therefore, UFs were applied to the POD_{HEC} to derive the chronic ReV (i.e., assume a threshold/nonlinear MOA).

- A UF_H of 10 was applied to account for human variability and sensitive subpopulations (e.g., children, individuals with pre-existing conditions).
- A UF_A of 3 was used to account for potential interspecies toxicodynamic variability because interspecies dosimetric adjustments have been conducted.
- A UF_D of 3 was used to account for deficiencies in the database. According to EPA (2004), the NTP (1982) inhalation study was well designed and is considered to be of high quality, but the database is considered limited because of excessive mortality in the NTP (1982) study. In addition, EDB shows a very steep dose-response curve, with multiple nonneoplastic lesions observed in mice and rats following chronic exposure to 10 ppm (NTP 1982) and death in some mice following multiple exposures to 38 ppm (Short et al. 1978). This steep dose-response curve and lack of studies examining sensitive effects at lower exposure concentrations requisites due consideration when selecting the UF_D given the studies available. The database for EDB was considered moderate and of medium quality.

A total UF of 90 was applied to the POD_{HEC} of 0.7805 ppm to derive the chronic ReV of 0.99 ppb (rounded to two significant figures):

$$\text{Chronic ReV} = POD_{HEC}/(UF_H \times UF_A \times UF_D)$$

$$= 0.7805 \text{ ppm} / (10 \times 3 \times 3)$$
$$= 0.7805 \text{ ppm} / 90$$
$$= 0.0087 \text{ ppm}$$
$$= 8.7 \text{ ppb (rounded to two significant figures)}$$

4.1.5 Health-Based Chronic ReV and $^{chronic}ESL_{threshold(nc)}$

The chronic ReV value was rounded to the least number of significant figures for a measured value at the end of all calculations. Rounding to two significant figures, the chronic ReV is 8.7 ppb (67 µg/m^3). The rounded chronic ReV was then used to calculate the $^{chronic}ESL_{threshold(nc).}$ At the target hazard quotient of 0.3, the $^{chronic}ESL_{threshold(nc)}$ is 2.61 ppb (20 µg/m^3) (Table 10).

Table 10. Derivation of the Chronic ReV and chronicESL

Parameter	Values and Descriptions
Study	NTP (1982)
Study Population	50 rats and 50 mice of both sexes
Study Quality	Medium
Exposure Method	Inhalation
Critical Effects	Suppurative inflammation in the nasal cavity in male rats
Exposure Duration	6 h/d, 5 d per wk for 89-104 wk
Extrapolation to continuous exposure (POD_{ADJ})	0.7805 ppm
POD_{HEC}	0.7805 ppm
Total UFs	90
Interspecies UF	3
Intraspecies UF	10
Incomplete Database UF *Database Quality*	3 Medium
Chronic ReV (HQ = 1)	**8.7 ppb (67 µg/m^3)**
$^{chronic}ESL_{threshold(nc)}$ (HQ = 0.3)	**2.6 ppb (20 µg/m^3)**

4.1.6 Comparison of TCEQ's Chronic ReV to other Long-Term, Health Protective Comparison Levels from Other Agencies

Table 11 presents a comparison of the TCEQ chronic ReV to long-term, health protective comparison levels of other regulatory agencies.

Table 11. Long-Term, Health Protective Comparison Levels Developed by TCEQ and Other Agencies

Agency	Long-Term Comparison Value Name	Long-Term Comparison Value (ppb)	PODHEC	Total Uncertainty Factor	Key Study and Critical Effect
TCEQ (2016)	Reference Value (ReV)	8.7 ppb	0.7805 ppm	90	NTP (1982) – Suppurative inflammation in the nasal cavity
USEPA (1995)	Reference Concentration (RfC)	1	2.8 mg/m3 (0.36 ppm)	300	NTP (1982) – Nasal inflammation in female mice.
OEHHA (2001)	Reference Exposure Level (REL)	0.1	31 ppb	300	Ratcliff et al. (1987); Reproductive toxicity; decreased sperm count/ejaculate, decreased percentage of viable and motile sperm, increased semen pH, and increased proportion of sperm with specific morphological abnormalities (tapered heads, absent heads, and abnormal tails) in human males

4.2 Carcinogenic Potential

EDB is a suspected human carcinogen although there are no correlations of workers exposed to EDB and cancer; however, rats and mice that were repeatedly exposed to EDB via inhalation developed cancer in multiple organs and direct points of contact (e.g., nasal cavity and lung tumors following inhalation) (EPA 2004 and NTP 1982).

4.2.1 Carcinogenic Weight of Evidence (WOE)

EDB has been evaluated for carcinogenic potential by the International Agency for Research on Cancer (IARC), the National Toxicology Program (NTP), USEPA, and the European Union (Table 12). Generally, the TCEQ only performs carcinogenic dose-response assessments for chemicals considered by the TCEQ either to be “Carcinogenic to Humans” or “Likely to Be Carcinogenic to Humans” and for which available data adequately characterize the dose-response curve.

Table 12. Carcinogenic Weight of Evidence

Group	Classification
IARC 1999	Probably carcinogenic to humans
NTP 2011	Reasonably anticipated to be a human carcinogen
USEPA 2004	Probable Human Carcinogen

4.2.2 Relevant Data

4.2.2.1 Epidemiological Studies

Studies have examined the correlation between excess cancer risk in humans and EDB exposure. However, these studies looked at industrial workers exposed to various chemicals including EDB and/or lack information on individual exposures, therefore, causality cannot be determined based on human data. Several of these studies are detailed in EPA (2004) and ATSDR (1992) and a few are summarized here. There are no definitive reports of cancer in humans associated with exposure to EDB.

- Ott, Scharnweber and Langner (1979) examined mortality of employees exposed to EDB in two production facilities located in Michigan and Texas. The Texas plant was operated from 1942 to 1969 and the process consisted of reactor and distillation operations. Quantitative data to calculate an 8-h, time-weighted-average (TWA) exposure concentration were not available from this facility. The Michigan facility was operated from the mid-1920's to 1976. Sampling data from 1950 (1 – 10.6 ppm), 1952 (19 - 31 ppm), and 1971–72 (0 - 110 ppm) and personal air monitoring in 1975 (1.8 - 96 ppm) allowed for estimation of EDB exposure in the second facility. An estimated TWA of 3.5 ppm was calculated for 1971 - 1972 and 5 ppm for 1975. Past reports indicated that industrial hygienists experienced strong odor and respiratory irritation at 75 ppm. Vomiting and gastrointestinal discomfort were also reported at 75 ppm. No statistically significant increase in deaths was observed when data were examined in terms of duration of exposure or interval since first exposure. Although there was an increase in cancer mortality among employees with more than 6 years of exposure to EDB in both plants, this increase was not statistically significant and specific target sites were not identified. In addition, study limitations included not controlling for confounding factors such as smoking, lack of exposure information to other chemicals, lack of a matched control group, small sample sizes and lack of completeness of report and sampling data (Ott et al. 1979 and ATSDR 2001).
- Sweeney et al. (1986) investigated mortality workers employed at an east Texas chemical plant. The authors examined the cause-specific mortality of 2,510 males

working with EDB or other specified chemicals from 1952-1977 and compared the values to the US population. There were no significant increases in mortalities from malignancies or non-cancer causes. For the non-cancer-related causes of death, cardiovascular diseases and nonmalignant respiratory diseases, the observed number of deaths was slightly lower than the expected number (Sweeney et al. 1986). The authors cited the low number of total deaths, low power for detecting excess risk for rare causes of death, and incomplete exposure data as potential deficiencies of the study.

4.2.2.2 Animal Studies

Multiple studies have reported cancer risk in animals due to EDB exposure. Stinson et al. (1981) reported benign neoplasms and carcinomas of the nasal cavity in male and female $B6C3F_1$ mice. Although the study was well designed and an adequate number of test animals were used, this study is limited for the development of an inhalation unit risk factor (URF) because only the nasal cavities of the animals were examined. NTP (1982) demonstrated that the nasal cavity is not necessarily the most sensitive site of tumor formation in mice. Therefore, the Stinson et al. (1981) study was not used because similarly sensitive sites (lung, circulatory system) were not examined. The study by Wong et al. (1982) is also not suitable for the development of an inhalation URF because only one dose group was examined. The NTP (1982) study was well-conducted, used an adequate number of test animals and dose levels, and examined appropriate tumorigenic endpoints. Therefore, the study by NTP (1982) was used for development of an inhalation URF.

4.2.2.2.1 Key Study - NTP 1982

NTP (1982) provided evidence of EDB-induced nasal cavity tumors and other benign and malignant tumors in male and female Fischer 344 rats and in female $B6C3F_1$ mice in a 2-year inhalation cancer bioassay. NTP (1982) exposed 50 male and 50 female $B6C3F_1$ mice at five wk of age and 50 male and 50 female Fischer 344 rats at six wk of age to EDB by whole-body inhalation at concentrations of 0, 10, and 40 ppm for 78-106 wk (mice) and 88-106 wk (rats) (50/sex/exposure group) for 6 h/d, 5 d/wk. Untreated controls consisted of 50 rats and 50 mice of each sex exposed in chambers to ambient air. Mean body weights of high-dose rats and high-dose mice of both sexes were lower than untreated controls. Survival of high-dose rats (male and female) and of the low- and high-dose female mice were significantly lower than controls. Ascending, suppurative urinary tract infection that resulted in necrotic, ulcerative lesions was the principal cause of early death in control and dosed mice (unrelated to exposure of EDB).

Sacrifices were conducted at 106 wk in control animals and at 104 wk in low-dose animals. Survival in low-dose and control rats was similar for both sexes. Terminal sacrifices were conducted at 79 wk in the male mice, 89 wk in the high-dose male rats and 91 wk in the high-dose female rats and mice. Although the treated male mice demonstrated histopathology

similar to that seen in the female mice, high mortality in all groups that was not related to EDB exposure made these data unsuitable for quantitative assessment.

- Rats: Statistically significant incidences of carcinomas and adenocarcinomas of the nasal cavity were observed in low-dose (10 ppm) and high-dose (40 ppm) rats of either sex when compared to controls. Adenomatous polyps of the nasal cavity showed a statistically significant increase in low-dose male rats and the combined incidence of alveolar/bronchiolar adenomas and carcinomas were statistically significant in high-dose female rats. Hemangiosarcomas of the circulatory system and mesotheliomas of the tunica vaginalis were statistically increased in high-dose and both low- and high-dose male rats, respectively. Fibroadenomas of the mammary gland were significantly elevated in dosed female rats.
- Mice: Alveolar/bronchiolar carcinoma and adenoma were significantly increased in high-dose mice of both sexes relative to controls. Hemangiosarcomas were significantly greater than controls in low- and high-dose female mice. High-dose female mice also had increased incidences of subcutaneous fibrosarcomas and nasal cavity carcinomas. Mammary gland adenocarcinomas were also significantly increased in low-dose females.

These data are summarized in Table 13 and Table 14.

Table 13. Statistically Significant Tumor Incidence in Rats Exposed to EDB via Inhalation

Tumor Type/Incidence	Control	10 ppm	40 ppm
Males			
Nasal cavity carcinoma [a]	0/50	0/50	21/50*
Nasal cavity adenoma	0/50	11/50*	0/50
Nasal cavity adenocarcinoma [a]	0/50	20/50*	28/50*
Nasal cavity adenomatous polyp	0/50	18/50*	5/50*
Nasal cavity tumors [a,b]	0/50	39/50*	41/50*
Hemangiosarcoma of circulatory system [a]	0/50	1/50	15/50*
Pituitary adenoma	0/45	7/48*	2/47
Testis interstitial-cell tumor	35/50	45/50*	10/49*
Tunica vaginalis mesothelioma, not otherwise specified (NOS) [a]	0/50	7/50*	25/50*
Tunica vaginalis mesothelioma, NOS or malignant [a]	1/50	8/50*	25/50*
Females (#)			
Nasal cavity carcinoma [a]	0/50	0/50	25/50*
Nasal cavity adenoma	0/50	11/50*	3/50
Nasal cavity adenocarcinoma [a]	0/50	20/50*	29/50*
Nasal cavity adenomatous polyp	0/50	5/50*	5/50*
Nasal cavity tumors [a,c]	1/50	34/50*	43/50*
Lung alveolar/bronchiolar carcinoma or adenoma [a]	0/50	0/48	5/47*
Hemangiosarcoma of circulatory system [a]	0/50	0/50	5/50*
Pituitary adenoma	1/50	18/49*	4/45
Mammary gland fibroadenoma [a]	4/50	29/50*	24/50*

Highlighted endpoints were further analyzed by the TCEQ for use as a POD

* Significant difference from control ($p < 0.05$), Fisher exact test

[a] Significant increasing trend ($p < 0.05$), Cochran-Armitage test

[b] Adenoma, carcinoma, adenocarcinoma, adenomatous polyp, papillary adenoma, squamous cell carcinoma, or squamous cell papilloma.

[c] Adenoma, carcinoma, adenocarcinoma, adenomatous polyp, papillary adenoma, papillary polyp, or squamous cell carcinoma.

Table 14. Statistically Significant Incidence of Tumors in Mice

Tumor Type/Incidence	Control	10 ppm	40 ppm
Males (#)			
Lung/Bronchus adenomatous polyp [a]	0/41	0/48	5/46*
Lung alveolar/bronchiolar adenoma [a]	0/41	0/48	11/46*
Lung alveolar/bronchiolar carcinoma [a]	0/41	3/48	19/46*
Lung alveolar/bronchiolar adenoma or carcinoma [a]	0/41	3/48	23/46*
Respiratory tumors [a,b]	0/41	3/48	25/46*
Females (#)			
Nasal cavity carcinoma [a]	0/50	0/50	6/50*
Nasal cavity carcinoma or adenoma [a]	0/50	0/50	8/50*
Nasal cavity adenomatous polyp or adenoma [a]	0/50	0/50	5/50*
Nasal cavity tumors [a,c]	0/50	0/50	12/50*
Lung/bronchus adenoma [a]	0/49	0/49	5/50*
Lung/bronchus adenoma or adenomatous polyp [a]	0/49	0/49	6/50*
Lung alveolar/bronchiolar adenoma [a]	3/49	7/49	13/50*
Lung alveolar/bronchiolar carcinoma [a]	1/49	5/49	37/50*
Respiratory tumors [a,d]	4/49	11/49*	42/50*
Hemangiosarcoma of circulatory system [a]	0/50	11/50*	23/50*
Subcutaneous tissue or rib fibrosarcoma [a]	0/50	5/50*	11/50*
Hematopoietic system lymphoma and leukemia	8/50	7/50	1/50*
Pituitary adenoma	8/48	1/46*	0/40*
Mammary gland adenocarcinoma	2/50	14/50*	8/50*

Highlighted endpoints were further analyzed by the TCEQ for use as a POD

* Significant difference from control ($p < 0.05$), Fisher exact test

[a] Significant increasing trend ($p < 0.05$), Cochran-Armitage test

[b] Adenoma, adenomatous polyp, alveolar/bronchiolar adenoma, or alveolar/bronchiolar carcinoma.

[c] Adenoma, carcinoma, adenomatous polyp, or hemangiosarcoma.

[d] Adenoma, carcinoma, adenomatous polyp, alveolar/bronchiolar adenoma, or alveolar/bronchiolar carcinoma.

4.2.2.2.2 Supporting Studies

Two additional studies indicated that EDB induces tumors following inhalation.

- Stinson et al. (1981) examined groups of 50 male and female B6C3F$_1$ mice exposed to 10 or 40 ppm via inhalation for 6 h/d, 5 d/wk for 103 (10 ppm) or 90 (40 ppm) wk. Squamous, adeno-, or mixed carcinomas of the nasal cavity were present in 7 females at 40 ppm. Two hemangiosarcomas were also observed in females at 10 and 40 ppm. This study supports the endpoints identified in the NTP (1982) study at similar concentrations.
- Wong et al. (1982) conducted a chronic inhalation study to evaluate the carcinogenic potential of exposure to 20 ppm EDB when inhaled by Sprague-Dawley rats either alone or in combination with 0.05 % disulfiram in the diet. For 18 months (7 h/d, 5 d/wk), 4 groups of 48 male and 48 female rats received either control air, 0.05% disulfiram in the diet, 20 ppm EDB via inhalation, or 20 ppm EDB via inhalation and 0.05% disulfiram in the diet. Rats receiving 0.05% disulfiram in the diet showed a decrease in body weight gain than control rats. Rats receiving 20 ppm EDB alone and those receiving the combination of 20 ppm and 0.05% of disulfiram had high mortality when compared to control and disulfiram-treated rats. The rats that inhaled 20 ppm alone had a mortality of 90% for males and 77% for females at the end of the 18 months. Male rats exposed EDB alone had a statistically significant increase of splenic atrophy (6/48), hemangiosarcoma (10/48), hemosiderosis (5/48), adrenal tumors (11/50), and tumors of the subcutaneous mesenchymal tissue (11/50) when compared to control male rats. Female rats exposed to 20 ppm EDB alone had a statistically significant increase in splenic atrophy (6/48), adrenal tumors (6/48) and mammary tumors (25/48). Rats exposed to 20 ppm EDB and disulfiram exhibited a substantial increase in tumors of the liver, kidney, and thyroid compared to rats receiving EDB or disulfiram alone. Hemangiosarcoma was present in the liver, spleen, and mesentery, and males had a statistically significant increase in lung tumors when compared to animals receiving EDB alone. Based on the results of this study, disulfiram appears to increase the toxicity of EDB. However, this study was not suitable for the development of a ReV because only one dose group was examined (e.g., insufficient to define the dose-rersponse) in one species.

4.2.3 Carcinogenic MOA

As reported by ATDSR, metabolism can occur through two different pathways in various tissues:

- Microsomal monooxygenase system (cytochrome P-450 oxidation) to form 2-bromoacetaldehyde (Tamura et al. 1986; Van Duuren et al. 1985). This metabolite can produce histopathological changes such as liver damage, by binding to cellular proteins (Hill et al. 1978). 2-Bromoacetaldehyde can be metabolized further by

aldehyde dehydrogenase in the presence of nicotinamide adenine dinucleotide dehydrogenase to 2-bromoethanol which is highly toxic and causes genotoxicity. 2-Bromoacetaldehyde can also be metabolized by aldehyde dehydrogenase in the presence of nicotinamide adenine dinucleotide to bromoacetic acid which is excreted in the urine. In addition, 2-bromoacetaldehyde can also be conjugated with glutathione. The conjugated metabolite is reduced to S-carboxymethylglutathione. This compound can form S-carboxymethylcysteine which may be metabolized to thioglycolic acid and excreted in the urine or can be metabolized to S-(β-hydroxyethyl) cysteine. The latter is excreted in the urine following action by N-acetyl transferase in the presence of acetyl CoA enzyme and subsequent sulfoxidation to form mercapturic acids (Nachtomi et al. 1966; Van Bladeren 1983). Mercapturic acids are the primary urinary metabolites of 1,2-dibromoethane. Tomasi et al. (1983) demonstrated that 1,2-dibromoethane can form a free radical intermediate under a hypoxic condition suggesting a new metabolic pathway for 1,2-dibromoethane. The 2-bromoacetaldehyde is responsible for tissue damage caused by covalent binding to cellular macromolecules.

- Cytosolic activation system (glutathione conjugation) forms S-(2-bromoethyl) glutathione. Ethylene dibromide can be conjugated with glutathione through the action of glutathione transferases to form S-(2-bromoethyl) glutathione (Peterson et al. 1988). This reactive intermediate can react to form the detoxification products, ethylene and glutathione disulfide, through further action of glutathione transferases. The ethylene is exhaled, and the glutathione disulfide is eliminated in the feces via the bile. S-(2-bromoethyl) glutathione is considered to be the genotoxic, and probably the carcinogenic, intermediate of EDB metabolism (Van Bladeren et al. 1981). In laboratory animals, S-(2-bromoethyl) glutathione has been shown to cause various carcinogenic effects.

Although metabolites of EDB have shown to cause carcinogenic effects, no MOA studies have been conducted regarding tumorigenesis induced by the inhalation of EDB, and the MOA is unclear.

4.2.4 POD for Key Study and Critical Effect

The NTP (1982) study is used as the key study as it clearly demonstrated statistically significant tumor incidences with increasing exposure levels at several sites in multiple species. Since several tumor types in both rats and mice were observed, the tumor incidences that were statistically increased at the low dose (10 ppm) compared to control and that showed a statistically significant increasing trend (i.e., more sensitive endpoints with statistical increases beginning at the lowest dose and a better defined dose-response) were considered in identifying the critical effect (Table 13 and Table 14).

4.2.4.1 BMC Modeling

The TCEQ performed BMC modeling using USEPA BMD software (version 2.6) for the data in Table 13 (rat data) and Table 14 (mouse data) which was taken from the NTP (1982) study. Data were used to predict 95% lower confidence limits on the BMCs using dichotomous models. A default benchmark response (BMR) of 10% was selected for extra risk (BMC_{10}) and $BMCL_{10}$. For the selected rat and mouse data, all of the available dichotomous and multistage cancer models were run (Appendices 1.1 and 1.2), and the best fit models (global goodness of fit (p) > 0.1, scaled residuals < |2|, lowest AIC/BMDL) are listed in Table 15.

Table 15. BMD Modeling for the Neoplastic Endpoints from NTP (1982)

Endpoint	Model	p-value	AIC	BMC10	BMCL10
Male Rats					
Nasal cavity adenocarcinoma	Log logistic	0.186	141.14	2.43	1.71
Nasal cavity tumors	No Viable Models	--	--	--	--
Tunica vaginalis mesothelioma or malignant	Quantal-Linear	0.849	127.12	6.37	4.74
Female Rats					
Nasal cavity adenocarcinoma	LogLogistic	0.267	139.89	2.32	1.64
Nasal cavity tumors	No Viable Models	--	--	--	--
Mammary gland fibroadenoma	No Viable Models	--	--	--	--
Female Mice					
Respiratory tumors	Probit	0.888	127.88	7.46	6.02
Subcutaneous tissue or rib fibrosarcoma	LogLogistic	0.734	87.782	13.7	8.81
Circulatory system hemangiosarcoma	Multistage-Cancer 2°	0.432	125.26	5.98	4.55

Modeling of the rat and mouse data from the NTP (1982) study resulted in several BMCL10 values, and since they are relatively close (within a factor of 5), each of the identified endpoints were considered in the selection of the POD.

4.2.4.2 Default Exposure Duration Adjustments

In the NTP (1982) study, animals were exposed for 6 h/d, 5 d/wk. An adjustment from a discontinuous to a continuous exposure duration was conducted (TCEQ 2015a) as follows:

POD_{ADJ} = POD x (D/24 h) x (F/7 d)

where:

D = Exposure duration, hours per day

F = Exposure frequency, days per week

POD_{ADJ} = POD x (6/24 h) x (5/7 d) = POD x 0.1786

The resulting POD_{ADJ} for each of the endpoints examined can be found in Table 16, which is provided and discussed in Section 4.2.4.4.

4.2.4.3 Default Dosimetry Adjustments from Animal-to-Human Exposure

As discussed in the Section 3, EDB is considered a Category 2 gas (EPA 2004). Because the critical adverse effects caused by EDB are both POE and systemic in nature, each endpoint will be treated as either a Category 1 (POE effects) or a Category 3 (systemic effects) gas (TCEQ 2015a). A dosimetry adjustment from an animal concentration to a human equivalent concentration (POD_{HEC}) for each of the identified endpoints was performed for EDB according to the subsections below.

4.2.4.3.1 POE effects – Category 1 gas

For Category 1 gases, the DAF is dependent upon the site at which the POE effects occur. When the critical effect is in the extrathoracic (ET) region, including the nasal cavity, a default DAF of 1 is applied (TCEQ 2015a). When the critical effect is in the pulmonary (PU) region, such as the observed respiratory tumors, the DAF is the ratio of the regional gas dose ratio in the pulmonary region ($RGDR_{PU}$).

$POD_{HEC} = POD_{ADJ} \times RGDR_{PU}$

$RGDR_{PU} = (V_E/SA_{PU})_A / (V_E/SA_{PU})_H$

where: V_E (ml/min) = minute volume

SA_{PU} = pulmonary surface area

A = animal

H = human

For respiratory tumors in female mice, the minute volume, calculated using an average body weight of 35 grams, is 0.041 L/min and the default pulmonary surface area is 0.05 m^2 (USEPA 1994). For humans, the default minute volume is 13.8 L/min and the default pulmonary surface area is 54 m^2 (USEPA 1994).

$RGDR_{PU}$ = ((0.041 L/min)/(0.05 m^2)) / ((13.8 L/min)/(54 m^2))

$RGDR_{PU}$ = 3.21

POD_{HEC} = 6.02 ppm x 3.21 = 19.32 ppm

4.2.4.3.2 Systemic effects – Category 3 gas

For Category 3 gases, when available, animal and human blood:gas partition coefficients are used to dosimetrically adjust for species differences in toxicokinetics (TCEQ 2015a).

$$POD_{HEC} = POD_{ADJ} \times ((H_{b/g})_A / (H_{b/g})_H)$$

where: $H_{b/g}$ = blood:gas partition coefficient
A = animal
H = human

Gargas et al. (1989) reported rat blood:gas partition coefficients of 119 for rats, which is greater than the estimated human blood:gas partition coefficient of 24.8. According to TCEQ guidelines, if the animal/human ratio of the blood:gas partition coefficients is greater than 1, a default value of 1 is used (TCEQ 2015a). A blood:gas partition coefficient is not available for the mouse, and according to TCEQ guidelines a default value of 1 is used (TCEQ 2015a). Therefore, the POD_{HEC} for each of the systemic endpoints is equal to the POD_{ADJ} (Table 16).

4.2.4.4 Selection of the Critical Effect and POD

The lowest POD_{HEC} identified from the NTP (1982) study was 0.2928 ppm for nasal cavity adenocarcinomas in female rats (Table 16) and was used in the derivation of the URF. An almost identical POD_{HEC} (0.3053 ppm) was calculated for nasal cavity adenocarcinomas in male rats, and two other endpoints were within a factor of 3.

Table 16. Endpoints and POD_{HEC} for the Neoplastic Endpoints from NTP (1982)

Endpoint	POD/BMCL10 (ppm)	PODADJ (ppm)	Dosimstric Adjustment	DAF	PODHEC (ppm)
Male Rats					
Nasal cavity adenocarcinoma	1.71	0.3053	POE, ET	1	0.3053
Tunica vaginalis mesothelioma or malignant	4.74	0.8464	Systemic	1	0.8464
Female Rats					
Nasal cavity adenocarcinoma	1.64	0.2928	POE, ET	1	0.2928
Female Mice					
Respiratory tumors	6.02	1.075	POE, PU	3.21	19.32
Subcutaneous tissue or rib fibrosarcoma	8.81	1.5732	Systemic	1	1.5732
Circulatory system hemangiosarcoma	4.55	0.8125	Systemic	1	0.8125

4.2.5 Calculation of a Unit Risk Factor

From this data, an inhalation URF can be derived using the following equation (TCEQ 2015a):

$URF = 0.1 / POD_{HEC}$
$URF = 0.1 / 0.2928 \text{ ppm} = 0.3415 (\text{ppm})^{-1}$ or $0.0444 (\text{mg/m}^3)^{-1}$
$URF = 3.4E\text{-}04 (\text{ppb})^{-1}$ or $4.4E\text{-}05 (\mu\text{g/m}^3)^{-1}$ (rounded to two significant figures)

4.2.6 Calculation of an Air Concentration at 1 x 10^{-5} Excess Cancer Risk

The calculated URF based on increased incidence of nasal cavity adenocarcinomas in female rats from the NTP (1982) study is $1.4E\text{-}05 (\text{ppb})^{-1}$ or $3.4E\text{-}06 (\mu\text{g/m}^3)^{-1}$. The no significant risk level of 1E-05 is calculated as follows (TCEQ 2015a):

$^{chronic}ESL_{nonthreshold(c)} = 1E\text{-}05 / URF$

$= 1E\text{-}05 / 3.4E\text{-}04 (\text{ppb})^{-1}$
$= 0.029 \text{ ppb} (0.22 \mu\text{g/m}^3)$

4.2.7 Comparison of Cancer Potency Factors

Table 17 lists the inhalation URF and toxicity values calculated at a cancer risk level of 1E-05 that are available.

Table 17. Available Inhalation URFs and Chronic Toxicity Values

Agency	Inhalation URF	Chronic Toxicity Value
TCEQ $^{chronic}ESL_{nonthreshold(c)}$	4.4E-06 $(\mu g/m^3)^{-1}$	0.22 $\mu g/m^3$
USEPA (2004)	6E-04 $(\mu g/m^3)^{-1}$	0.02 $\mu g/m^3$
OEHHA	7.1E-05 $(\mu g/m^3)^{-1}$	0.14 $\mu g/m^3$

4.2.8 Evaluating Susceptibility from Early-Life Exposures

TCEQ (2015a) states that carcinogens acting through a mutagenic MOA need to be evaluated for the potential increase in cancer due to early-life exposures compared with adult and whole-life exposure. USEPA (2005) provides default age-dependent adjustment factors (ADAFs) to account for potential increased susceptibility in children due to early-life exposure when a chemical has been identified as acting through a mutagenic MOA for carcinogenesis.

Although there is evidence to suggest the potential for genotoxic and/or mutagenic effects under certain conditions, once a carcinogen has been determined to have mutagenic potential, there are several important considerations in assessing evidence for a mutagenic MOA for cancer. For example: (1) whether the chemical-induced mutation occurs prior to the initiation of the carcinogenic process (i.e., early in relation to the key events that lead to cancer) in the target tissue (i.e., site and temporal concordance between mutagenicity and carcinogenicity), and if so (2) whether the chemical-induced mutation is the key event that initiates the carcinogenic process in the target tissue. See Section 5.7.5.1.2 of TCEQ (2015a) for additional information, including a hierarchy for types of relevant evidence. Most importantly, for a chemical to act by a mutagenic MOA, either the chemical or its direct metabolite must be the agent inducing the mutations that initiate cancer in the target tissue. As there is no default carcinogenic MOA, the scientific burden of proof is a reasonably robust demonstration through direct evidence that the specific mutation(s) caused by the chemical or its metabolite is in fact the first step in target tissue which initiates a cascade of other key events that are critical to the carcinogenic process in the specific tumors. Mere plausibility (whether or not information on other possible MOAs is available) is not tantamount to an adequately robust demonstration that mutagenicity is in fact the initiating event in target tissues. Thus, if the weight of evidence supports a chemical's genotoxic and/or mutagenic potential, for evaluation of the MOA emphasis should then be placed on evidence of the chemical's mutagenicity being the critical, initiating carcinogenic event in target cells (at relevant doses if possible). In the event scientifically convincing data on the carcinogenic MOA are lacking, the carcinogenic MOA may ultimately be judged simply to be unknown or not sufficiently elucidated or established (TCEQ 2015a). This is the case for EDB, for which the carcinogenic MOA is certainly unclear. As the MOA for EDB has not been demonstrated to be mutagenic, consistent with TCEQ guidance

(TCEQ 2015a), ADAFs will not be applied to the URF at this time. This issue will be reevaluated periodically as new scientific information on EDB's carcinogenic MOA becomes available.

4.3 Welfare-Based Chronic ESL

No studies were found regarding chronic effects of EDB on vegetation.

4.4 Long-Term ESL and Values for Air Monitoring Evaluation

The chronic evaluation resulted in the derivation of the following values:

- Chronic ReV = 67 µg/m^3 (8.7 ppb)
- $^{chronic}ESL_{threshold(nc)}$ = 20 µg/m^3 (2.6 ppb)
- $^{chronic}ESL_{nonthreshold(c)}$ = 0.22 µg/m^3 (0.029 ppb)

The long-term ESL for air permit reviews is the $^{chronic}ESL_{nonthreshold(c)}$ of 0.22 µg/m^3 (0.029 ppb). For evaluation of long-term ambient air monitoring data, the $^{chronic}ESL_{nonthreshold(c)}$ of 0.22 µg/m^3 (0.029 ppb) is lower than the chronic ReV of 67 µg/m^3 (8.7 ppb) (Table 2). However, the ReV value may be used for the evaluation of air data as well as the $^{chronic}ESL_{nonthreshold(c)}$ and URF. The $^{chronic}ESL_{threshold(nc)}$ (HQ = 0.3) would not be used to evaluate ambient air monitoring data (Table 2).

4.5 Chronic IOAELs

IOAELs are described in more detail in Section 3.4 and in TCEQ (2015a).

4.5.1 Noncarcinogenic Chronic IOAEL

The chronic POD ($BMCL_{10}$) of 4.37 ppm determined from the NTP (1982) study was based on supperative inflammation in the nasal cavity of male rats following exposure to EDB for 6 h/d, 5 d/wk for up to 103 wk. The concentration of 6.36 ppm associated with a 10% response rate (BMC_{10}) represents a concentration at which similar effects could possibly occur in some individuals exposed over the same duration (i.e., a lifetime). Based on the TCEQ guidelines (2015a), no duration adjustment is conducted; however an animal-to-human dosimetric adjustment is used to calculate the $BMC_{10\text{-}HEC}$. Since the RGDR is 1, based on updated guidelines from the USEPA (2015a), the chronic IOAEL is equal to the $BMC_{10\text{-}HEC}$ of 6.4 ppm (rounded to 2 significant digits). Effects are not a certainty as there may be inter- and intra-species differences in sensitivity. The chronic IOAEL of 6.4 ppm (49 mg/m^3) is provided for informational purposes only (TCEQ 2015a). As the basis for development of inhalation observed adverse effect levels is limited to available data, future studies could possibly identify a lower POD for this purpose.

The margin of exposure between the chronic noncarcinogenic IOAEL (6.4 ppm) and the chronic ReV (0.0087 ppm) is a factor of approximately 730.

4.5.2 Carcinogenic Chronic IOAEL

The carcinogenic POD ($BMCL_{10}$) of 1.64 ppm determined from the NTP (1982) study was based on increased incidence of nasal cavity adenocarcinomas in female rats following exposure to EDB for 6 h/d, 5 d/wk for up to 103 wk. The concentration of 2.32 ppm associated with a 10% response rate (BMC_{10}) represents a concentration at which similar effects could possibly occur in some individuals exposed over the same duration (i.e., a lifetime). Based on the TCEQ guidelines (2015a), no duration adjustment is conducted; however an animal-to-human dosimetric adjustment is used to calculate the $BMC_{10\text{-}HEC}$. Since the RGDR is 1, based on updated guidelines from the USEPA (2015a), the $BMC_{10\text{-}HEC}$ is equal to the BMC_{10} of 2.3 ppm (rounded to 2 significant digits). Effects are not a certainty as there may be inter- and intra-species differences in sensitivity. The carcinogenic chronic IOAEL of 2.3 ppm is provided for informational purposes only (TCEQ 2015a). As the basis for development of IOAELs is limited to available data, future studies could possibly identify a lower POD for this purpose.

The margin of exposure between the chronic carcinogenic IOAEL (2.32 ppm) and the $^{chronic}ESL_{nonthreshold(c)}$ (0.000029 ppm) is a factor of 80,000.

Chapter 5 References

Acute Exposure Guideline Levels (AEGLs). 2008. 1,2-Dibromoethane. Available from: http://www2.epa.gov/sites/production/files/2014-08/documents/1_2_dibromoethane_tsd_interim_5_2008_v1.pdf

Agency for Toxic Substances Diseases (ATSDR). 1992. Toxicological Profile for 1,2 Dibromoethane. Available From: http://www.atsdr.cdc.gov/toxprofiles/tp.asp?id=726&tid=131#bookmark12

American Conference of Governmental Industrial Hygienists (ACGIH). 1991. Threshold limit values for chemical substances and physical agents and biological exposure indices.

ChemSpider. 2015. http://www.chemspider.com

Environmental Protection Agency (EPA). 2007. Ethylene Dibromide. Available From: http://www.epa.gov/ttnatw01/hlthef/ethyl-di.html

Hazardous Substance Data Bank (HSDB). 2009. 1,2-Dibromoethane. TOXNET - Databases on toxicology, hazardous chemicals, environmental health, and toxic releases.

Letz GA, Pond SM, Osterloh JD, Wade, RL and Becker, CE. 1984. Two fatalities after acute occupational exposure to ethylene dibromide. J. Am. Med. Assoc. 252:2428-2431.

National Toxicology Program (NTP). 1982. Carcinogenesis bioassay of 1,2-dibromoethane (CAS No. 106-93-4) in F344 rats and B6C3F1 mice (inhalation study). NTP Technical Report Series No. 210. NTP-80-28. NIH Publication No. 82-1766. NTP, Bethesda, MD.

Office of Environmental Health Hazard Assessment (OEHHA). 2001. Chronic Toxicity Summary: Ethylene Dibromide. Available from: http://www.oehha.ca.gov/air/chronic_rels/pdf/ethylenedibromide.pdf

Ott MG, Scharnweber HC, and Langner RR. 1980. Mortality experience of 161 employees exposed to ethylene dibromide in two production units. Br. J. Ind. Med. 37:163-168.

Ratcliffe JM, Schrader SM, Steenland K, Clapp DE, Turner T, Hornung RW. 1987. Semen Quality in papaya workers with long term exposure to ethylene dibromide. Br. J. Ind. Med. 44:317-326.

Rowe VK, Spencer HC, McCollister DD, et al. 1952. Toxicity of ethylene dibromide determined on experimental animals. AMA Arch Ind Hyg Occup Med 6:158-173.

Ruth, JH. 1986. Odor Threshold and Irritation Levels of Several ChemicalSubstances: Review. Am. Ind. Hyg. Assoc. 47:A142-151.

Schrader SM, Turner TW, Ratcliffe JM. 1988. The effects of ethylene dibromide on semen quality: a comparison of short-term and chronic exposure. Reprod. Toxicol. 2:191-198.

Short RD, Minor JL, Winston JM, et al. 1978. Inhalation of ethylene dibromide during gestation by rats and mice. Toxicol Appl Pharmacol 46:173-182.

Short RD, Winston JM, Hong C, et al. 1979. Effects of ethylene dibromide on reproduction in male and female rats. Toxicol Appl Pharmacol 49:97-105.

Stinson SF, Reznik G, Ward JM. 1981. Characteristics of proliferative lesions in the nasal epithelium of mice following chronic inhalation of 1,2-dibromoethane. Cancer Lett 12:121-129.

Texas Commission on Environmental Quality (TCEQ). 2015a. TCEQ Guidelines to Develop Toxicity Factors. Office of the Executive Director. RG-442, revised.

Texas Commission on Environmental Quality (TCEQ). 2015b. Approaches to derive odor-based values. Texas Commission on Environmental Quality. Chief Engineer's Office.

United States Environmental Protection Agency (USEPA). 2004. 1,2-Dibromoethane. Integrated Risk Information System (IRIS) on-line database.

United States Environmental Protection Agency (USEPA). 2012. Advances in Inhalation Gas Dosimetry for Derivation of a Reference Concentration (RfC) and Use in Risk Assessment.

Wong LC, Winston JM, Hong CB, Plotnick H. 1981. Carcinogenicity and toxicity of 1,2-Dibromoethane in the rat. Toxicol Appl Pharmacol 63 (2): 155-165.

Appendix 1 Benchmark Concentrations (BMC) Modeling

1.1 Noncarcinogenic Endpoint Modeling

The TCEQ performed Benchmark Concentration (BMC) modeling using USEPA Benchmark Dose (BMD) software (version 2.6) for the data presented in Table 6 and Table 7 which were taken from the NTP (1982) study. Data were used to predict 95% lower confidence limits on the BMCs using dichotomous models. A default BMR of 10% was selected for extra risk (BMC_{10}) and $BMCL_{10}$. All of the available dichotomous models were run for all of the rat (Appendix 1.1.1) and mouse (Appendix 1.1.2) data. All of the models are presented below, with the best fit model based in the lowest $BMCL_{10}$ and the best fit to the curve shown in bold and graphically below its respective table.

1.1.1 Dichotomous models using rat nonneoplastic data from NTP (1982)

Table 18. Rat Nonneoplastic Data from NTP (1982)

Histological Endpoint in Rat	0 ppm	10 ppm	40 ppm
Males (#)	(50)	(50)	(50)
Hepatic necrosis	2	6	19
Toxic nephropathy	0	4	28
Testicular degeneration	1	10	18
Testicular atrophy	1	2	5
Spermatic granulomas	-	0	2
Degeneration of the adrenal cortex	0	1	1
Females (#)	(50)	(50)	(50)
Hepatic Necrosis	2	3	13
Toxic nephropathy	-	0	8
Degeneration of the adrenal cortex	4	7	13
Retinal atrophy	-	10	5
Hyperplasia of the nasal cavities	-	27	31

1.1.1.1 BMDS Summary for suppurative inflammation in the nasal cavity of male rats

Table 19. Summary of BMD Modeling Results for suppurative inflammation in the nasal cavity of male rats

Model[a]	Goodness of fit		$BMD_{10}Pct$	$BMDL_{10}Pct$	Basis for model selection
	***p*-value**	**AIC**			
Gamma[b] Weibull[c] Quantal-Linear[d]	0.760	113.79	7.61	5.64	Of the models that provided an adequate fit and a valid BMDL estimate, the LogLogistic Model was selected based on the lowest AIC and the lowest BMDL.
Dichotomous-Hill Multistage 4° [f] Multistage 3°	error	error	errorg	errorg	
Logistic	0.0198	122.79	17.9	14.4	
LogLogistic	**0.962**	**113.34**	**6.36**	**4.37**	
Probit	0.0240	122.18	16.5	13.3	
LogProbit	1.000	115.27	5.84	0.658	
Multistage 2° [h]	0.760	113.79	7.61	5.64	

[a] Selected model in bold; scaled residuals for selected model for doses 0, 10, and 40 were 0, 0.22, -0.16, respectively.
[b] For the Gamma and Weibull models, the power parameter estimates were 1 (boundary of parameter space).For the Gamma model, the power parameter estimate was 1. The model is equivalent to the Quantal-Linear model.
[c] For the Weibull and Gamma models, the power parameter estimates were 1 (boundary of parameter space).For the Weibull model, the power parameter estimate was 1. The models in this row reduced to the Quantal-Linear model.
[d] The Quantal-Linear model may appear equivalent to the Multistage 2° model, however differences exist in digits not displayed in the table.
[e] BMD or BMDL computation failed for this model.
[f] For the Multistage 4° model, the beta coefficient estimates were 0 (boundary of parameters space). The models in this row reduced to the Multistage 3° model.
[g] BMD or BMDL computation failed for this model
[h] The Multistage 2° model may appear equivalent to the Gamma model, however differences exist in digits not displayed in the table. This also applies to the Weibull model. This also applies to the Quantal-Linear model.

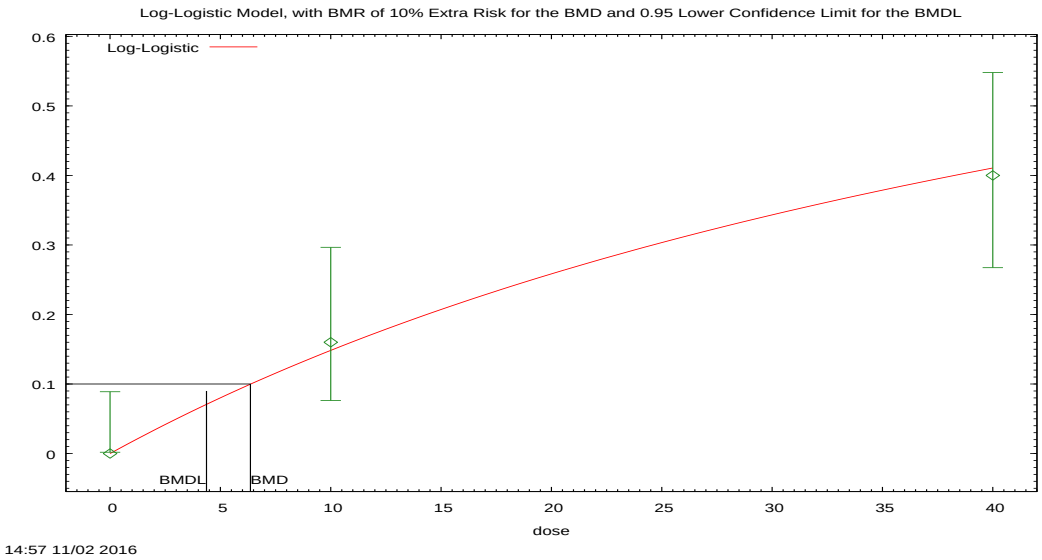

Figure 3. Plot of incidence rate by dose with fitted curve for LogLogistic model for suppurative inflammation in the nasal cavity of male rats; dose shown in ppm.
Logistic Model. (Version: 2.14; Date: 2/28/2013)

The form of the probability function is: P[response] = background+(1-background)/[1+EXP(-intercept-slope*Log(dose))]

Slope parameter is restricted as slope >= 1

Benchmark Dose Computation.

BMR = 10% Extra risk

BMD = 6.36128

BMDL at the 95% confidence level = 4.37074

Parameter Estimates

Variable	Estimate	Default Initial Parameter Values
background	0	0
intercept	-4.0475E+00	-4.0276E+00
slope	1	1

Analysis of Deviance Table

Model	Log(likelihood)	# Param's	Deviance	Test d.f.	p-value
Full model	-55.63	3			
Fitted model	-55.67	1	0.0759253	2	0.96
Reduced model	-72.2	1	33.1378	2	<.0001

AIC: = 113.344

Goodness of Fit Table

Dose	Est. Prob.	Expected	Observed	Size	Scaled Resid
0	0	0	0	50	0
10	0.1487	7.435	8	50	0.22
40	0.4113	20.565	20	50	-0.16

Chi^2 = 0.08 d.f = 2 P-value = 0.9623

1.1.1.2 BMDS Summary for epithelial hyperplasia in the lung/bronchus of male rats

Table 20. Summary of BMD Modeling Results for epithelial hyperplasia in the lung/bronchus of male rats

Model[a]	Goodness of fit		$BMD_{10}Pct$	$BMDL_{10}Pct$	Basis for model selection
	***p*-value**	**AIC**			
Gamma[b] Weibull[c] Multistage 2° Quantal-Linear	0.326	101.82	11.5	8.14	Of the models that provided an adequate fit and a valid BMDL estimate, the LogLogistic Model was selected based on the lowest AIC and the lowest BMDL.
Dichotomous-Hill Multistage 4°[e] Multistage 3°	error	error	error[f]	error[f]	
Logistic	0.0201	109.06	23.7	18.7	
LogLogistic	**0.487**	**101.14**	**10.3**	**6.80**	
Probit	0.0223	108.69	22.3	17.3	
LogProbit	1.000	101.80	5.28	error[d]	

[a] Selected model in bold; scaled residuals for selected model for doses 0, 10, and 40 were 0, 1.01, -0.65, respectively.
[b] For the Gamma and Weibull models, the power parameter estimates were 1 (boundary of parameter space).For the Gamma model, the power parameter estimate was 1. The model is equivalent to the Quantal-Linear model.
[c] For the Weibull and Gamma models, the power parameter estimates were 1 (boundary of parameter space).For the Weibull model, the power parameter estimate was 1. The models in this row reduced to the Quantal-Linear model.
[d] BMD or BMDL computation failed for this model.
[e] For the Multistage 4° model, the beta coefficient estimates were 0 (boundary of parameters space). The models in this row reduced to the Multistage 3° model.
[f] BMD or BMDL computation failed for this model

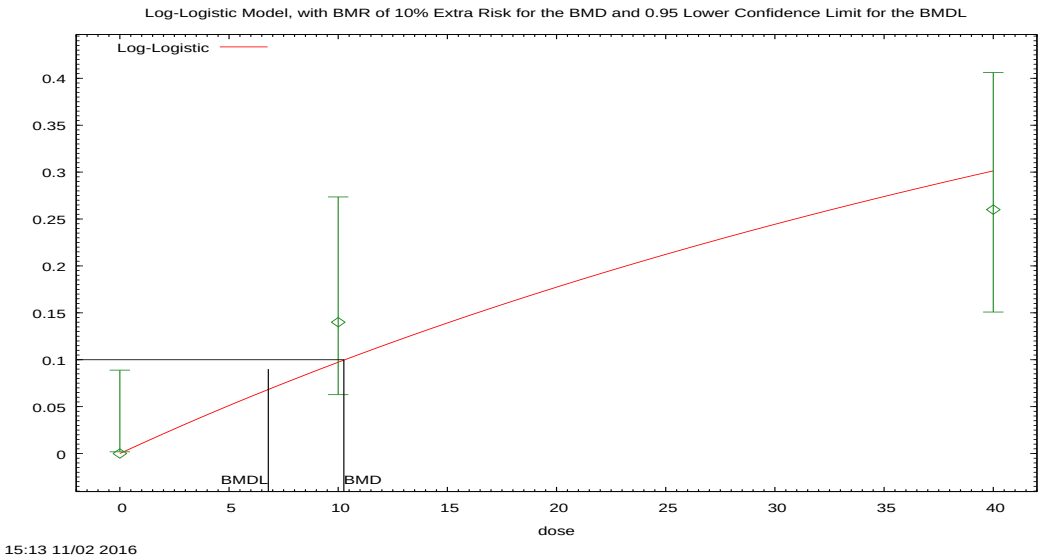

Figure 4. Plot of incidence rate by dose with fitted curve for LogLogistic model for epithelial hyperplasia in the lung/bronchus of male rats; dose shown in ppm.
Logistic Model. (Version: 2.14; Date: 2/28/2013)

The form of the probability function is: P[response] = background+(1-background)/[1+EXP(-intercept-slope*Log(dose))]

Slope parameter is restricted as slope >= 1

Benchmark Dose Computation.

BMR = 10% Extra risk

BMD = 10.2588

BMDL at the 95% confidence level = 6.79948

Parameter Estimates

Variable	Estimate	Default Initial Parameter Values
background	0	0
intercept	-4.5254E+00	-4.4264E+00
slope	1	1

Analysis of Deviance Table

Model	Log(likelihood)	# Param's	Deviance	Test d.f.	p-value
Full model	-48.9	3			
Fitted model	-49.57	1	1.34201	2	0.51
Reduced model	-58.9	1	20.0003	2	<.0001

AIC: = 101.144

Goodness of Fit Table

Dose	Est. Prob.	Expected	Observed	Size	Scaled Resid
0	0	0	0	50	0
10	0.0977	4.886	7	50	1.01
40	0.3023	15.114	13	50	-0.65

Chi^2 = 1.44 d.f = 2 P-value = 0.4874

1.1.1.3 BMDS Summary for congestion in the lung of male rats

Table 21. Summary of BMD Modeling Results for congestion in the lung of male rats

Model[a]	Goodness of fit		$BMD_{10}Pct$	$BMDL_{10}Pct$	Basis for model selection
	p-value	AIC			
Gamma[b] **Weibull[c]** **Multistage 2°** **Quantal-Linear**	**1.000**	**89.173**	**12.8**	**8.87**	**Of the models that provided an adequate fit and a valid BMDL estimate, the Gamma Model was selected based on the lowest AIC.**
Dichotomous-Hill Multistage 4°[e] Multistage 3°	error	error	errorf	error[f]	
Logistic	0.120	94.616	24.6	19.9	
LogLogistic	1.000	91.172	12.5	7.72	
Probit	0.138	94.252	23.0	18.4	
LogProbit	1.000	91.172	12.3	3.49	

[a] Selected model in bold; scaled residuals for selected model for doses 0, 10, and 40 were 0, 0.02, -0.01, respectively.
[b] For the Gamma and Weibull models, the power parameter estimates were 1 (boundary of parameter space).For the Gamma model, the power parameter estimate was 1. The model is equivalent to the Quantal-Linear model.
[c] For the Weibull and Gamma models, the power parameter estimates were 1 (boundary of parameter space).For the Weibull model, the power parameter estimate was 1. The models in this row reduced to the Quantal-Linear model.
[d] BMD or BMDL computation failed for this model.
[e] For the Multistage 4° model, the beta coefficient estimates were 0 (boundary of parameters space). The models in this row reduced to the Multistage 3° model.
[f] BMD or BMDL computation failed for this model

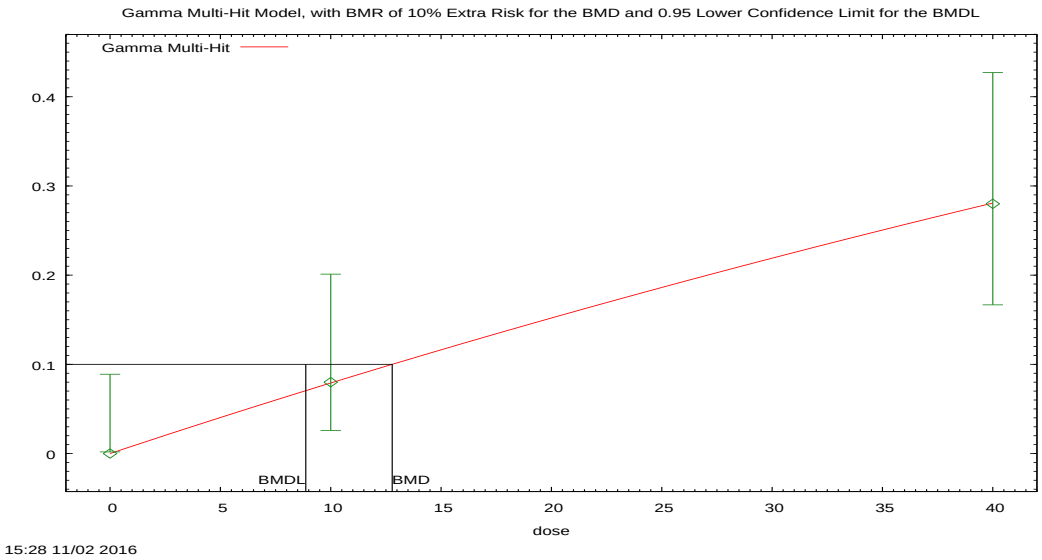

Figure 5. Plot of incidence rate by dose with fitted curve for Gamma model for congestion in the lung of male rats; dose shown in ppm.
Gamma Model. (Version: 2.16; Date: 2/28/2013)

The form of the probability function is: P[response]= background+(1-background)*CumGamma[slope*dose,power], where CumGamma(.) is the cumulative Gamma distribution function

Power parameter is restricted as power >=1

Benchmark Dose Computation.

BMR = 10% Extra risk

BMD = 12.7859

BMDL at the 95% confidence level = 8.86922

Parameter Estimates

Variable	Estimate	Default Initial Parameter Values
Background	0	0.0192308
Slope	0.00824036	0.00887375
Power	1	1.0542

Analysis of Deviance Table

Model	Log(likelihood)	# Param's	Deviance	Test d.f.	p-value
Full model	-43.59	3			
Fitted model	-43.59	1	0.000712478	2	1
Reduced model	-55.04	1	22.9052	2	<.0001

AIC: = 89.173

Goodness of Fit Table

Dose	Est. Prob.	Expected	Observed	Size	Scaled Resid
0	0	0	0	50	0
10	0.0791	3.955	4	50	0.02
40	0.2808	14.04	14	50	-0.01

Chi^2 = 0 d.f = 2 P-value = 0.9996

1.1.1.4 BMDS Summary for congestion in the liver of male rats

Table 22. Summary of BMD Modeling Results for congestion in the liver of male rats

Model[a]	Goodness of fit		BMD_{10}Pct	$BMDL_{10}$Pct	Basis for model selection
	p-value	AIC			
Gamma[b] Weibull[c] Multistage 2° Quantal-Linear	0.685	77.709	18.6	12.2	Of the models that provided an adequate fit and a valid BMDL estimate, the LogLogistic Model was selected based on the lowest AIC and the lowest BMDL.
Dichotomous-Hill Multistage 4°[e] Multistage 3°	error	error	error[f]	error[f]	
Logistic	0.0906	82.939	30.7	24.0	
LogLogistic	**0.768**	**77.511**	**17.7**	**11.0**	
Probit	0.0980	82.701	29.4	22.5	
LogProbit	1.000	79.016	14.2	error[d]	

[a] Selected model in bold; scaled residuals for selected model for doses 0, 10, and 40 were 0, 0.63, -0.37, respectively.
[b] For the Gamma and Weibull models, the power parameter estimates were 1 (boundary of parameter space).For the Gamma model, the power parameter estimate was 1. The model is equivalent to the Quantal-Linear model.
[c] For the Weibull and Gamma models, the power parameter estimates were 1 (boundary of parameter space).For the Weibull model, the power parameter estimate was 1. The models in this row reduced to the Quantal-Linear model.
[d] BMD or BMDL computation failed for this model.
[e] For the Multistage 4° model, the beta coefficient estimates were 0 (boundary of parameters space). The models in this row reduced to the Multistage 3° model.
[f] BMD or BMDL computation failed for this model

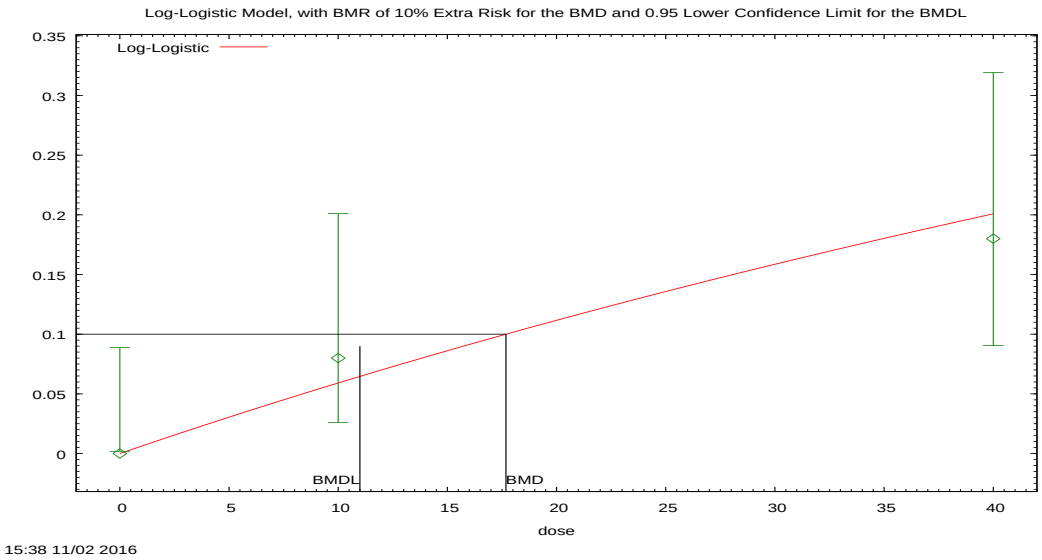

Figure 6. Plot of incidence rate by dose with fitted curve for LogLogistic model for congestion in the liver of male rats; dose shown in ppm.
Logistic Model. (Version: 2.14; Date: 2/28/2013)

The form of the probability function is: P[response] = background+(1-background)/[1+EXP(-intercept-slope*Log(dose))]

Slope parameter is restricted as slope >= 1

Benchmark Dose Computation.

BMR = 10% Extra risk

BMD = 17.6811

BMDL at the 95% confidence level = 10.9952

Parameter Estimates

Variable	Estimate	Default Initial Parameter Values
background	0	0
intercept	-5.0697E+00	-4.9751E+00
slope	1	1

Analysis of Deviance Table

Model	Log(likelihood)	# Param's	Deviance	Test d.f.	p-value
Full model	-37.51	3			
Fitted model	-37.76	1	0.494219	2	0.78
Reduced model	-44.21	1	13.4108	2	0

AIC: = 77.5105

Goodness of Fit Table

Dose	Est. Prob.	Expected	Observed	Size	Scaled Resid
0	0	0	0	50	0
10	0.0591	2.956	4	50	0.63
40	0.2009	10.044	9	50	-0.37

Chi^2 = 0.53 d.f = 2 P-value = 0.7682

1.1.1.5 BMDS Summary of hepatic necrosis in male rats

Table 23. Summary of BMD Modeling Results for hepatic necrosis in male rats

Model[a]	Goodness of fit		$BMD_{10}Pct$	$BMDL_{10}Pct$	Basis for model selection
	***p*-value**	**AIC**			
Gamma[b]	N/A[c]	125.89	11.8	6.93	Of the models that provided an adequate fit and a valid BMDL estimate, the Quantal-Linear model was selected based on lowest AIC and lowest BMDL.
Dichotomous-Hill Multistage 4°[e] Multistage 3°	error	error	error[f]	error[f]	
Logistic	0.457	124.46	18.5	14.8	
LogLogistic	N/A[c]	125.89	11.7	5.82	
Probit	0.523	124.31	17.2	13.7	
LogProbit	N/A[c]	125.89	11.5	3.62	
Weibullg	N/A[c]	125.89	11.8	6.93	
Multistage 2°	N/A[c]	125.89	11.9	6.93	
Quantal-Linear	**0.732**	**124.01**	**9.92**	**6.88**	

[a] Selected model in bold; scaled residuals for selected model for doses 0, 10, and 40 were 0.11, -0.29, 0.14, respectively.

[b] The Gamma model may appear equivalent to the Weibull model, however differences exist in digits not displayed in the table.

[c] No available degrees of freedom to calculate a goodness of fit value.

[d] BMD or BMDL computation failed for this model.

[e] For the Multistage 4° model, the beta coefficient estimates were 0 (boundary of parameters space). The models in this row reduced to the Multistage 3° model.

[f] BMD or BMDL computation failed for this model

[g] The Weibull model may appear equivalent to the Gamma model, however differences exist in digits not displayed in the table.

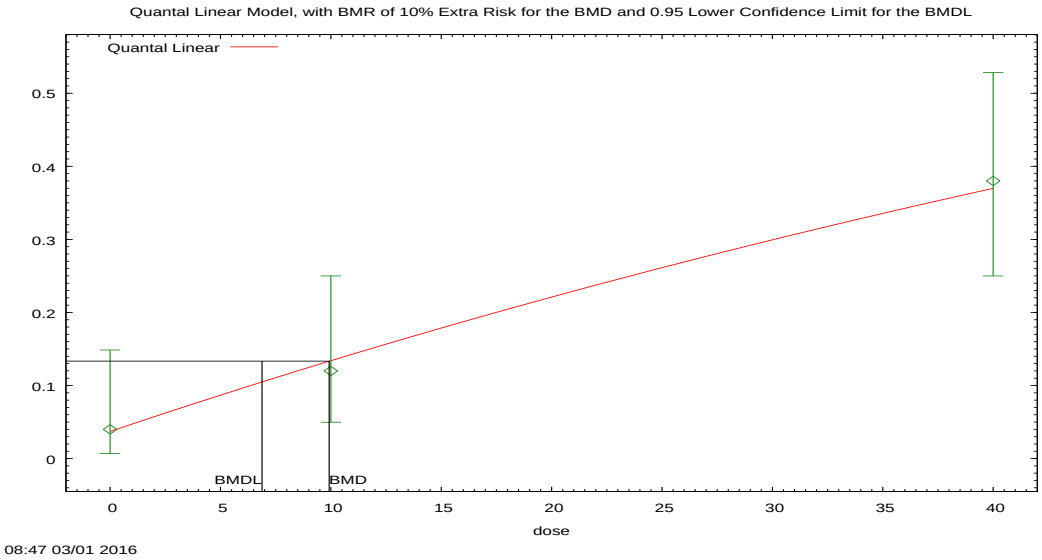

Figure 7. Plot of incidence rate by dose with fitted curve for Quantal-Linear model for hepatic necrosis in male rats; dose shown in ppm.
Quantal Linear Model using Weibull Model (Version: 2.16; Date: 2/28/2013)

The form of the probability function is: P[response] = background + (1-background)*[1-EXP(-slope*dose)]

Benchmark Dose Computation.

BMR = 10% Extra risk

BMD = 9.92337

BMDL at the 95% confidence level = 6.88129

Parameter Estimates

Variable	Estimate	Default Initial Parameter Values
Background	0.0370801	0.0576923
Slope	0.0106174	0.0106521
Power	n/a	1

Analysis of Deviance Table

Model	Log(likelihood)	# Param's	Deviance	Test d.f.	p-value
Full model	-59.95	3			
Fitted model	-60.01	2	0.119842	1	0.73
Reduced model	-70.71	1	21.5247	2	<.0001

AIC: = 124.013

Goodness of Fit Table

Dose	Est. Prob.	Expected	Observed	Size	Scaled Resid
0	0.0371	1.854	2	50	0.11
10	0.1341	6.704	6	50	-0.29
40	0.3703	18.514	19	50	0.14

Chi^2 = 0.12 d.f = 1 P-value = 0.7317

1.1.1.6 BMDS Summary for mineralization in the kidney of male rats

Table 24. Summary of BMD Modeling Results for mineralization in the kidney of male rats

Model[a]	Goodness of fit		$BMD_{10}Pct$	$BMDL_{10}Pct$	Basis for model selection
	p-value	AIC			
Gamma[b] Weibull[c] Multistage 2° Quantal-Linear	0.197	65.078	27.8	16.8	Of the models that provided an adequate fit and a valid BMDL estimate, the LogLogistic model was selected based on lowest AIC and lowest BMDL.
Dichotomous-Hill Multistage 4°[e] Multistage 3°	error	error	error[f]	error[f]	
Logistic	0.0621	68.923	44.5	30.1	
LogLogistic	**0.238**	**64.837**	**27.1**	**15.7**	
Probit	0.0634	68.811	43.9	28.7	
LogProbit	1.000	64.385	40	errord	

[a] Selected model in bold; scaled residuals for selected model for doses 0, 10, and 40 were 0, 1.48, -0.83, respectively.
[b] For the Gamma and Weibull models, the power parameter estimates were 1 (boundary of parameter space).For the Gamma model, the power parameter estimate was 1. The model is equivalent to the Quantal-Linear model.
[c] For the Weibull and Gamma models, the power parameter estimates were 1 (boundary of parameter space).For the Weibull model, the power parameter estimate was 1. The models in this row reduced to the Quantal-Linear model.
[d] BMD or BMDL computation failed for this model.
[e] For the Multistage 4° model, the beta coefficient estimates were 0 (boundary of parameters space). The models in this row reduced to the Multistage 3° model.
[f] BMD or BMDL computation failed for this model

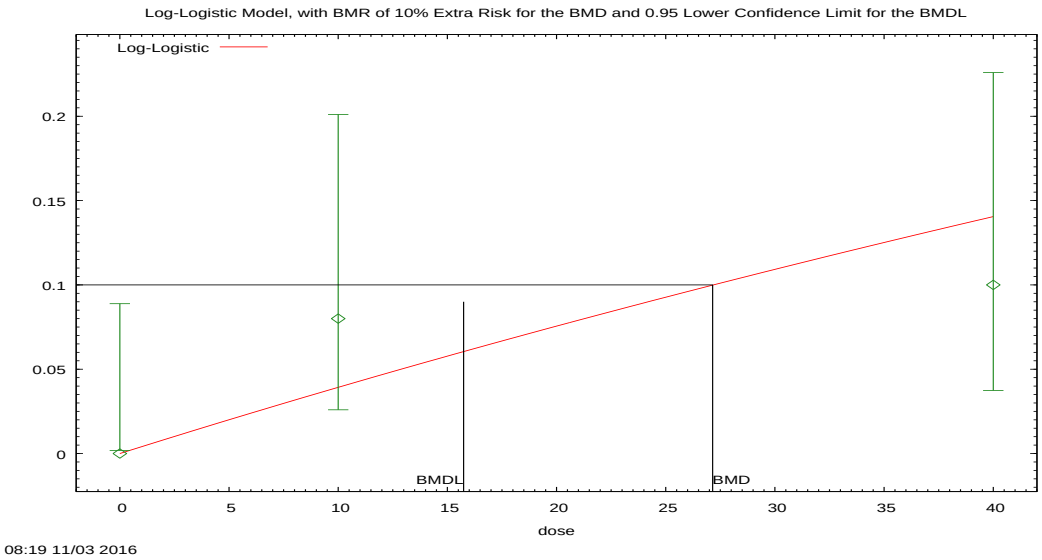

Figure 8. Plot of incidence rate by dose with fitted curve for LogLogistic model for mineralization in the kidney of male rats; dose shown in ppm.
Logistic Model. (Version: 2.14; Date: 2/28/2013)

The form of the probability function is: P[response] = background+(1-background)/[1+EXP(-intercept-slope*Log(dose))]

Slope parameter is restricted as slope >= 1

Benchmark Dose Computation.

BMR = 10% Extra risk

BMD = 27.1479

BMDL at the 95% confidence level = 15.7427

Parameter Estimates

Variable	Estimate	Default Initial Parameter Values
background	0	0
intercept	-5.4985E+00	-5.3155E+00
slope	1	1

Analysis of Deviance Table

Model	Log(likelihood)	# Param's	Deviance	Test d.f.	p-value
Full model	-30.19	3			
Fitted model	-31.42	1	2.45151	2	0.29
Reduced model	-34.05	1	7.70502	2	0.02

AIC: = 64.8367

Goodness of Fit Table

Dose	Est. Prob.	Expected	Observed	Size	Scaled Resid
0	0	0	0	50	0
10	0.0393	1.966	4	50	1.48
40	0.1407	7.034	5	50	-0.83

Chi^2 = 2.88 d.f = 2 P-value = 0.2375

1.1.1.7 BMDS Summary of toxic nephropathy in male rats

Table 25. Summary of BMD Modeling Results for toxic nephropathy in male rats

Model[a]	Goodness of fit		$BMD_{10}Pct$	$BMDL_{10}Pct$	Basis for model selection
	p-value	AIC			
Gamma	1.000	100.47	11.4	6.49	Of the models that provided an adequate fit and a valid BMDL estimate, the Multistage 2° model was selected based on lowest AIC. Since multiple models had the lowest AIC, the model with the lowest BMDL was chosen from those models.
Dichotomous-Hill Multistage 4°[c] Multistage 3°	error	error	error[d]	error[d]	
Logistic	0.195	103.05	18.2	14.3	
LogLogistic	1.000	100.47	11.4	6.80	
Probit	0.254	102.46	16.5	13.0	
LogProbit	1.000	100.47	11.2	7.11	
Weibull	1.000	100.47	11.5	6.44	
Multistage 2°	**1.000**	**100.47**	**11.7**	**6.27**	
Quantal-Linear	0.216	101.96	6.11	4.60	

[a] Selected model in bold; scaled residuals for selected model for doses 0, 10, and 40 were 0, 0, 0, respectively.
[b] BMD or BMDL computation failed for this model.
[c] For the Multistage 4° model, the beta coefficient estimates were 0 (boundary of parameters space). The models in this row reduced to the Multistage 3° model.
[d] BMD or BMDL computation failed for this model

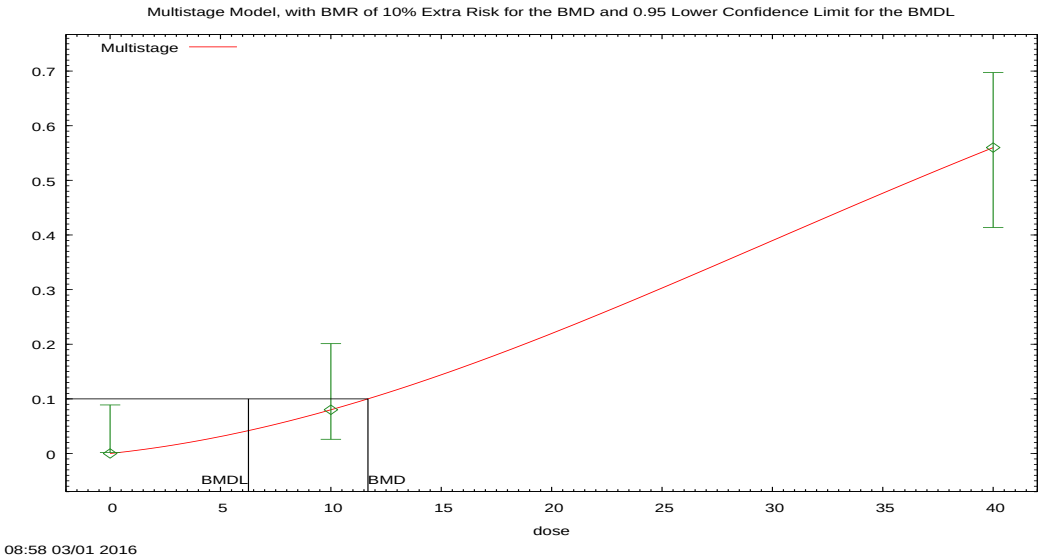

Figure 9. Plot of incidence rate by dose with fitted curve for Multistage 2° model for toxic nephropathy in male rats; dose shown in ppm.
Multistage Model. (Version: 3.4; Date: 05/02/2014)

The form of the probability function is: P[response] = background + (1-background)*[1-EXP(-beta1*dose^1-beta2*dose^2...)]

Benchmark Dose Computation.

BMR = 10% Extra risk

BMD = 11.68

BMDL at the 95% confidence level = 6.26808

Parameter Estimates

Variable	Estimate	Default Initial Parameter Values
Background	0	0
Beta(1)	0.00427604	0.00427604
Beta(2)	0.000406212	0.000406212

Analysis of Deviance Table

Model	Log(likelihood)	# Param's	Deviance	Test d.f.	p-value
Full model	-48.24	3			
Fitted model	-48.24	2	1.42109E-14	1	1
Reduced model	-77.75	1	59.032	2	<.0001

AIC: = 100.47

Goodness of Fit Table

Dose	Est. Prob.	Expected	Observed	Size	Scaled Resid
0	0	0	0	50	0
10	0.08	4	4	50	0
40	0.56	28	28	50	0

Chi^2 = 0 d.f = 1 P-value = 1

1.1.1.8 BMDS Summary of testicular degeneration in male rats

Table 26. Summary of BMD Modeling Results of testicular degeneration in male rats

Model[a]	Goodness of fit		BMD_{10Pct}	$BMDL_{10Pct}$	Basis for model selection
	p-value	AIC			
Gamma[b] Weibull[c] Quantal-Linear[d]	0.173	130.03	8.46	5.99	Of the models that provided an adequate fit and a valid BMDL estimate, the LogLogistic model was selected based on lowest AIC and lowest BMDL.
Dichotomous-Hill Multistage 4°[f] Multistage 3°	error	error	error[g]	error[g]	
Logistic	0.0226	134.01	17.6	14.0	
LogLogistic	**0.327**	**129.21**	**6.93**	**4.56**	
Probit	0.0265	133.62	16.4	13.0	
LogProbit	N/A[h]	130.28	3.69	3.90E-06	
Multistage 2°[i]	0.173	130.03	8.46	5.99	

[a] Selected model in bold; scaled residuals for selected model for doses 0, 10, and 40 were -0.19, 0.8, -0.54, respectively.
[b] For the Gamma and Weibull models, the power parameter estimates were 1 (boundary of parameter space). For the Gamma model, the power parameter estimate was 1. The model is equivalent to the Quantal-Linear model.
[c] For the Weibull and Gamma models, the power parameter estimates were 1 (boundary of parameter space). For the Weibull model, the power parameter estimate was 1. The models in this row reduced to the Quantal-Linear model.
[d] The Quantal-Linear model may appear equivalent to the Multistage 2° model, however differences exist in digits not displayed in the table.
[e] BMD or BMDL computation failed for this model.
[f] For the Multistage 4° model, the beta coefficient estimates were 0 (boundary of parameters space). The models in this row reduced to the Multistage 3° model.
[g] BMD or BMDL computation failed for this model
[h] No available degrees of freedom to calculate a goodness of fit value.
[i] The Multistage 2° model may appear equivalent to the Gamma model, however differences exist in digits not displayed in the table. This also applies to the Weibull model. This also applies to the Quantal-Linear model.

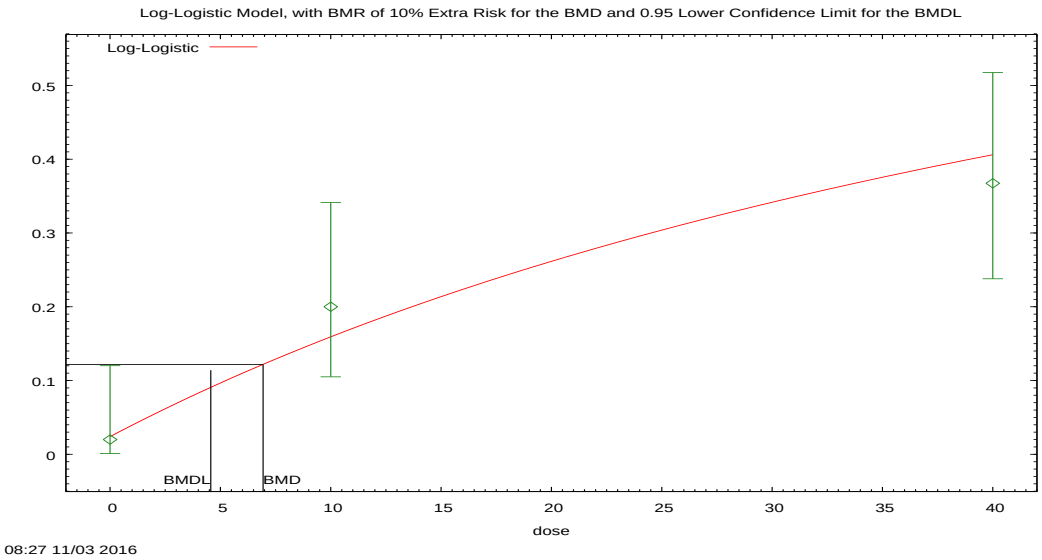

Figure 10. Plot of incidence rate by dose with fitted curve for LogLogistic model of testicular degeneration in male rats; dose shown in ppm.
Logistic Model. (Version: 2.14; Date: 2/28/2013)

The form of the probability function is: P[response] = background+(1-background)/[1+EXP(-intercept-slope*Log(dose))]

Slope parameter is restricted as slope >= 1

Benchmark Dose Computation.

BMR = 10% Extra risk

BMD = 6.93368

BMDL at the 95% confidence level = 4.56499

Parameter Estimates

Variable	Estimate	Default Initial Parameter Values
background	0.0240265	0.02
intercept	-4.1336E+00	-4.0414E+00
slope	1	1

Analysis of Deviance Table

Model	Log(likelihood)	# Param's	Deviance	Test d.f.	p-value
Full model	-62.14	3			
Fitted model	-62.6	2	0.927306	1	0.34
Reduced model	-73.44	1	22.5929	2	<.0001

AIC: = 129.209

Goodness of Fit Table

Dose	Est. Prob.	Expected	Observed	Size	Scaled Resid
0	0.024	1.201	1	50	-0.19
10	0.1588	7.941	10	50	0.8
40	0.4053	19.857	18	49	-0.54

Chi^2 = 0.96 d.f = 1 P-value = 0.3269

1.1.1.9 BMDS Summary of testicular atropy in male rats

Table 27. Summary of BMD Modeling Results of testicular atropy in male rats

Model[a]	Goodness of fit		$BMD_{10}Pct$	$BMDL_{10}Pct$	Basis for model selection
	p-value	AIC			
Gamma	N/Ab	64.894	47.9	22.9	Of the models that provided an adequate fit and a valid BMDL estimate, the Quantal-Linear model was selected based on lowest AIC and lowest BMDL.
Dichotomous-Hill Multistage 4°[d] Multistage 3°	error	error	error[e]	error[e]	
Logistic	0.786	62.967	44.7	30.8	
LogLogistic	N/Ab	64.894	48.1	22.3	
Probit	0.811	62.951	45.1	29.7	
LogProbit	N/Ab	64.894	49.2	19.1	
Weibull	N/Ab	64.894	47.8	22.9	
Multistage 2°	N/Ab	64.894	47.5	22.9	
Quantal-Linear	**0.972**	**62.895**	**48.4**	**22.9**	

[a] Selected model in bold; scaled residuals for selected model for doses 0, 10, and 40 were 0.02, -0.03, 0.01, respectively.
[b] No available degrees of freedom to calculate a goodness of fit value.
[c] BMD or BMDL computation failed for this model.
[d] For the Multistage 4° model, the beta coefficient estimates were 0 (boundary of parameters space). The models in this row reduced to the Multistage 3° model.
[e] BMD or BMDL computation failed for this model

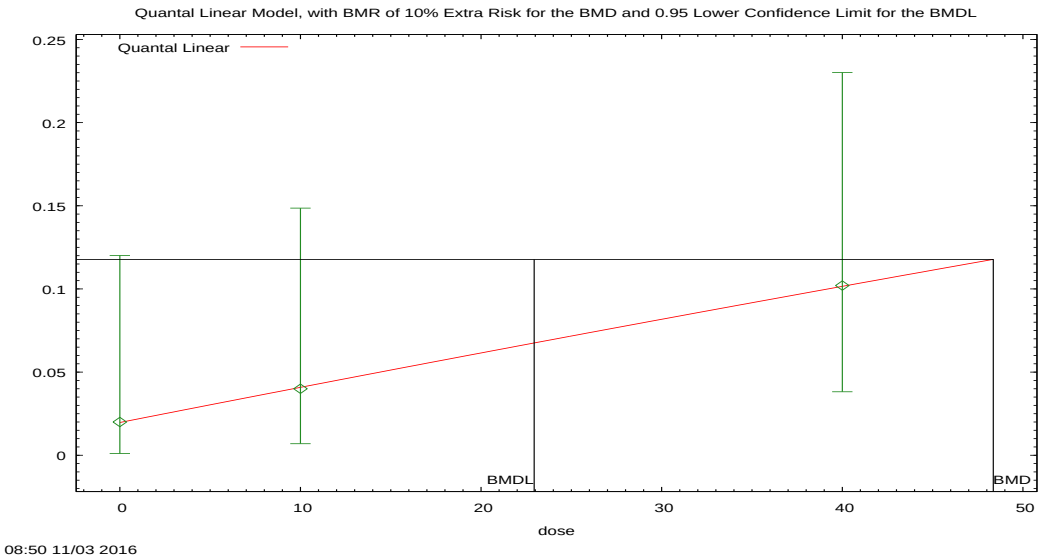

Figure 11. Plot of incidence rate by dose with fitted curve for Quantal-Linear model of testicular atrophy in male rats; dose shown in ppm.
Quantal Linear Model using Weibull Model (Version: 2.16; Date: 2/28/2013)

The form of the probability function is: P[response] = background + (1-background)*[1-EXP(-slope*dose)]

Benchmark Dose Computation.

BMR = 10% Extra risk

BMD = 48.3587

BMDL at the 95% confidence level = 22.9402

Parameter Estimates

Variable	Estimate	Default Initial Parameter Values
Background	0.0197006	0.0384615
Slope	0.00217873	0.00214856
Power	n/a	1

Analysis of Deviance Table

Model	Log(likelihood)	# Param's	Deviance	Test d.f.	p-value
Full model	-29.45	3			
Fitted model	-29.45	2	0.00125905	1	0.97
Reduced model	-31.18	1	3.461	2	0.18

AIC: = 62.8949

Goodness of Fit Table

Dose	Est. Prob.	Expected	Observed	Size	Scaled Resid
0	0.0197	0.985	1	50	0.02
10	0.0408	2.041	2	50	-0.03
40	0.1015	4.974	5	49	0.01

Chi^2 = 0 d.f = 1 P-value = 0.9717

1.1.1.10 BMDS Summary for suppurative inflammation in the nasal cavity of female rats

Table 28. Summary of BMD Modeling Results for suppurative inflammation in the nasal cavity of female rats

Model[a]	Goodness of fit		$BMD_{10}Pct$	$BMDL_{10}Pct$	Basis for model selection
	p-value	AIC			
Gamma	1.000	74.890	21.4	13.6	Of the models that provided an adequate fit and a valid BMDL estimate, the Multistage 2° model was selected based on lowest AIC.
Dichotomous-Hill Multistage 4°[c] Multistage 3°	error	error	error[d]	error[d]	
Logistic	0.549	75.460	28.5	23.1	
LogLogistic	1.000	74.890	21.6	13.4	
Probit	0.616	75.294	26.5	21.2	
LogProbit	1.000	74.890	20.1	13.1	
Weibull	1.000	74.890	22.2	13.6	
Multistage 2°	**0.996**	**72.900**	**21.8**	**13.9**	
Quantal-Linear	0.285	76.104	14.4	9.76	

[a] Selected model in bold; scaled residuals for selected model for doses 0, 10, and 40 were 0, -0.09, 0.02, respectively.
[b] BMD or BMDL computation failed for this model.
[c] For the Multistage 4° model, the beta coefficient estimates were 0 (boundary of parameters space). The models in this row reduced to the Multistage 3° model.
[d] BMD or BMDL computation failed for this model

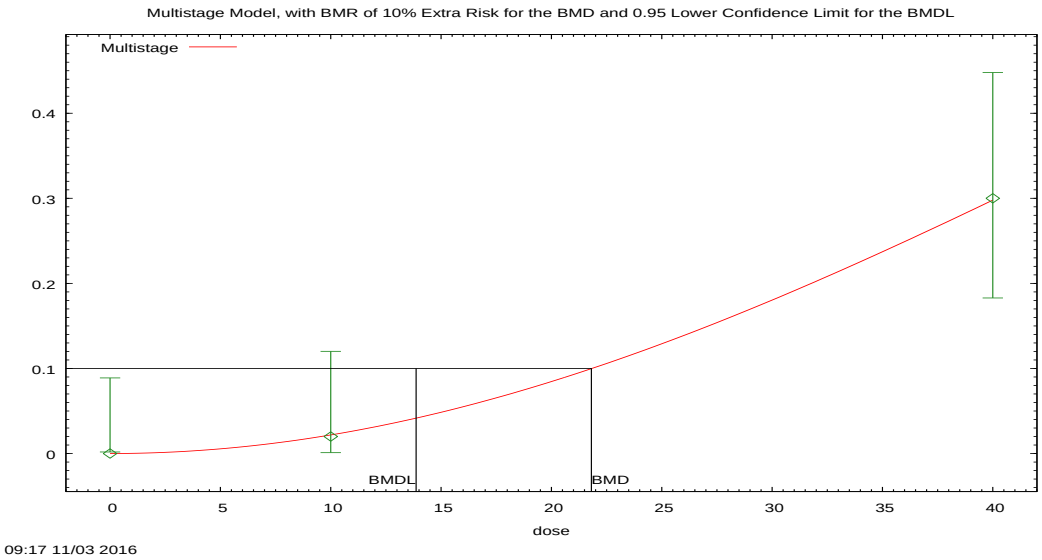

Figure 12. Plot of incidence rate by dose with fitted curve for Multistage 2° model for suppurative inflammation in the nasal cavity of female rats; dose shown in ppm. Multistage Model. (Version: 3.4; Date: 05/02/2014)

The form of the probability function is: P[response] = background + (1-background)*[1-EXP(-beta1*dose^1-beta2*dose^2...)]

Benchmark Dose Computation.

BMR = 10% Extra risk

BMD = 21.811

BMDL at the 95% confidence level = 13.8682

Parameter Estimates

Variable	Estimate	Default Initial Parameter Values
Background	0	0
Beta(1)	0	0
Beta(2)	0.000221476	0.000223529

Analysis of Deviance Table

Model	Log(likelihood)	# Param's	Deviance	Test d.f.	p-value
Full model	-35.45	3			
Fitted model	-35.45	1	0.00933957	2	1
Reduced model	-50.92	1	30.9563	2	<.0001

AIC: = 72.8997

Goodness of Fit Table

Dose	Est. Prob.	Expected	Observed	Size	Scaled Resid
0	0	0	0	50	0
10	0.0219	1.095	1	50	-0.09
40	0.2984	14.919	15	50	0.02

Chi^2 = 0.01 d.f = 2 P-value = 0.9955

1.1.1.11 BMDS Summary for epithelial hyperplasia in the nasal cavity of female rats

Table 29. Summary of BMD Modeling Results for epithelial hyperplasia in the nasal cavity of female rats

Model[a]	Goodness of fit		$BMD_{10}Pct$	$BMDL_{10}Pct$	Basis for model selection
	p-value	AIC			
Gamma[b]	1.00E-04	154.64	2.89	2.32	No Viable Models
Dichotomous-Hill Multistage 4°[d] Multistage 3°	error	error	error[e]	error[e]	
Logistic	0	174.97	8.32	6.68	
LogLogistic	0.0312	143.97	1.55	1.08	
Probit	0	174.33	7.98	6.51	
LogProbit	1.000	139.40	8.75E-04	error[c]	
Weibull[f] Multistage 2°[g] Quantal-Linear[h]	1.00E-04	154.64	2.89	2.32	

[a] No model was selected as a best-fitting model.
[b] The Gamma model may appear equivalent to the Weibull model, however differences exist in digits not displayed in the table. This also applies to the Multistage 2° model. This also applies to the Quantal-Linear model.
[c] BMD or BMDL computation failed for this model.
[d] For the Multistage 4° model, the beta coefficient estimates were 0 (boundary of parameters space). The models in this row reduced to the Multistage 3° model.
[e] BMD or BMDL computation failed for this model
[f] For the Weibull model, the power parameter estimate was 1. The models in this row reduced to the Quantal-Linear model.
[g] The Multistage 2° model may appear equivalent to the Gamma model, however differences exist in digits not displayed in the table.
[h] The Quantal-Linear model may appear equivalent to the Gamma model, however differences exist in digits not displayed in the table.

1.1.1.12 BMDS Summary for congestion in the lung female rats

Table 30. Summary of BMD Modeling Results for congestion in the lung female rats

Model[a]	Goodness of fit		$BMD_{10}Pct$	$BMDL_{10}Pct$	Basis for model selection
	p-value	AIC			
Gamma	1.000	56.606	27.5	16.5	Of the models that provided an adequate fit and a valid BMDL estimate, the Quantal-Linear model was selected based on lowest AIC.
Dichotomous-Hill Multistage 4°[c] Multistage 3°	error	error	error[d]	error[d]	
Logistic	0.489	57.325	33.7	27.6	
LogLogistic	1.000	56.606	27.5	16.0	
Probit	0.531	57.197	32.5	26.0	
LogProbit	1.000	56.606	26.3	15.2	
Weibull	1.000	56.606	27.8	16.5	
Multistage 2°	1.000	56.606	28.6	16.5	
Quantal-Linear	**0.742**	**55.296**	**25.6**	**15.5**	

[a] Selected model in bold; scaled residuals for selected model for doses 0, 10, and 40 were 0, -0.68, 0.36, respectively.
[b] BMD or BMDL computation failed for this model.
[c] For the Multistage 4° model, the beta coefficient estimates were 0 (boundary of parameters space). The models in this row reduced to the Multistage 3° model.
[d] BMD or BMDL computation failed for this model

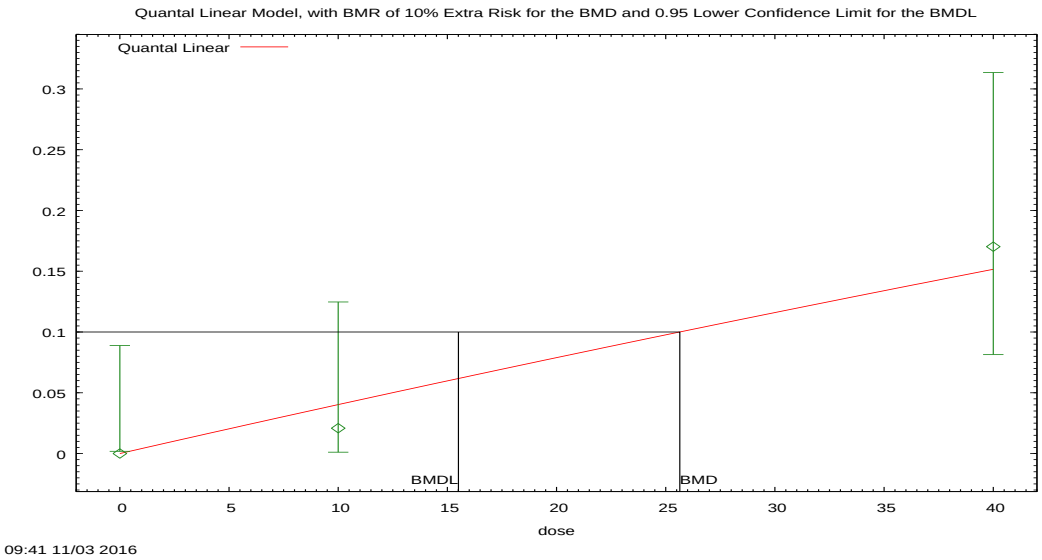

Figure 13. Plot of incidence rate by dose with fitted curve for Quantal-Linear model for congestion in the lung female rats; dose shown in ppm.
Quantal Linear Model using Weibull Model (Version: 2.16; Date: 2/28/2013)

The form of the probability function is: P[response] = background + (1-background)*[1-EXP(-slope*dose)]

Benchmark Dose Computation.

BMR = 10% Extra risk

BMD = 25.6446

BMDL at the 95% confidence level = 15.5061

Parameter Estimates

Variable	Estimate	Default Initial Parameter Values
Background	0	0.0192308
Slope	0.00410849	0.00458807
Power	n/a	1

Analysis of Deviance Table

Model	Log(likelihood)	# Param's	Deviance	Test d.f.	p-value
Full model	-26.3	3			
Fitted model	-26.65	1	0.689059	2	0.71
Reduced model	-33.73	1	14.8542	2	0

AIC: = 55.2955

Goodness of Fit Table

Dose	Est. Prob.	Expected	Observed	Size	Scaled Resid
0	0	0	0	50	0
10	0.0403	1.932	1	48	-0.68
40	0.1515	7.123	8	47	0.36

Chi^2 = 0.6 d.f = 2 P-value = 0.7423

1.1.1.13 BMDS Summary of hepatic necrosis in female rats

Table 31. Summary of BMD Modeling Results of hepatic necrosis in female rats

Model[a]	Goodness of fit		$BMD_{10}Pct$	$BMDL_{10}Pct$	Basis for model selection
	p-value	AIC			
Gamma	N/Ab	101.44	23.0	11.2	Of the models that provided an adequate fit and a valid BMDL estimate, the LogLogistic model was selected based on lowest AIC.
Dichotomous-Hill Multistage 4°[d] Multistage 3°	error	error	error[e]	error[e]	
Logistic	**0.903**	**99.453**	**24.5**	**19.4**	
LogLogistic	N/Ab	101.44	23.1	10.4	
Probit	0.833	99.483	23.1	18.0	
LogProbit	N/Ab	101.44	21.7	9.36	
Weibull	N/Ab	101.44	23.5	11.2	
Multistage 2°	N/Ab	101.44	24.0	11.2	
Quantal-Linear	0.382	100.26	16.6	10.5	

[a] Selected model in bold; scaled residuals for selected model for doses 0, 10, and 40 were 0.08, -0.09, 0.01, respectively.
[b] No available degrees of freedom to calculate a goodness of fit value.
[c] BMD or BMDL computation failed for this model.
[d] For the Multistage 4° model, the beta coefficient estimates were 0 (boundary of parameters space). The models in this row reduced to the Multistage 3° model.
[e] BMD or BMDL computation failed for this model

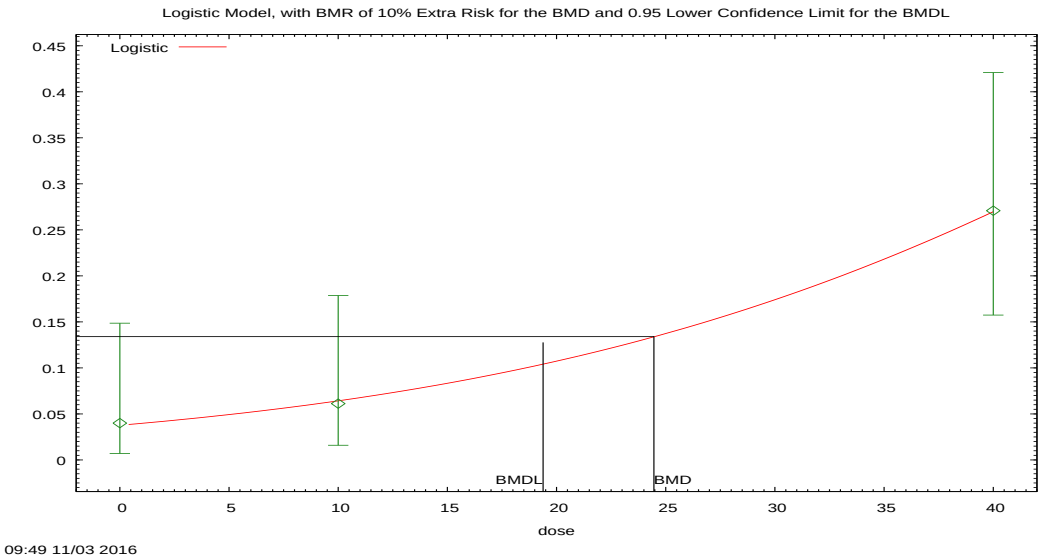

Figure 14. Plot of incidence rate by dose with fitted curve for Logistic model of hepatic necrosis in female rats; dose shown in ppm.
Logistic Model. (Version: 2.14; Date: 2/28/2013)

The form of the probability function is: P[response] = 1/[1+EXP(-intercept-slope*dose)]

Slope parameter is not restricted

Benchmark Dose Computation.

BMR = 10% Extra risk

BMD = 24.4587

BMDL at the 95% confidence level = 19.3844

Parameter Estimates

Variable	Estimate	Default Initial Parameter Values
background	n/a	0
intercept	-3.2387E+00	-3.0211E+00
slope	0.0561081	0.0508917

Analysis of Deviance Table

Model	Log(likelihood)	# Param's	Deviance	Test d.f.	p-value
Full model	-47.72	3			
Fitted model	-47.73	2	0.0149376	1	0.9
Reduced model	-54.65	1	13.8638	2	0

AIC: = 99.4533

Goodness of Fit Table

Dose	Est. Prob.	Expected	Observed	Size	Scaled Resid
0	0.0377	1.887	2	50	0.08
10	0.0643	3.151	3	49	-0.09
40	0.27	12.962	13	48	0.01

Chi^2 = 0.01 d.f = 1 P-value = 0.9027

1.1.1.14 BMDS Summary of degeneration of the adrenal cortex in female rats

Table 32. Summary of BMD Modeling Results of degeneration of the adrenal cortex in female rats

Model[a]	Goodness of fit		$BMD_{10}Pct$	$BMDL_{10}Pct$	Basis for model selection
	p-value	AIC			
Gamma[b] Weibull[c] Multistage 2° Quantal-Linear	0.877	127.53	17.4	10.0	Of the models that provided an adequate fit and a valid BMDL estimate, the LogLogistic Model was selected based on the lowest AIC and the lowest BMDL.
Dichotomous-Hill Multistage 4°[e] Multistage 3°	error	error	error[f]	error[f]	
Logistic	0.623	127.74	23.5	17.0	
LogLogistic	**0.943**	**127.51**	**16.3**	**8.66**	
Probit	0.651	127.70	22.6	16.0	
LogProbit	N/Ag	129.50	15.1	error[d]	

[a] Selected model in bold; scaled residuals for selected model for doses 0, 10, and 40 were -0.03, 0.06, -0.03, respectively.
[b] For the Gamma and Weibull models, the power parameter estimates were 1 (boundary of parameter space).For the Gamma model, the power parameter estimate was 1. The model is equivalent to the Quantal-Linear model.
[c] For the Weibull and Gamma models, the power parameter estimates were 1 (boundary of parameter space).For the Weibull model, the power parameter estimate was 1. The models in this row reduced to the Quantal-Linear model.
[d] BMD or BMDL computation failed for this model.
[e] For the Multistage 4° model, the beta coefficient estimates were 0 (boundary of parameters space). The models in this row reduced to the Multistage 3° model.
[f] BMD or BMDL computation failed for this model
[g] No available degrees of freedom to calculate a goodness of fit value.

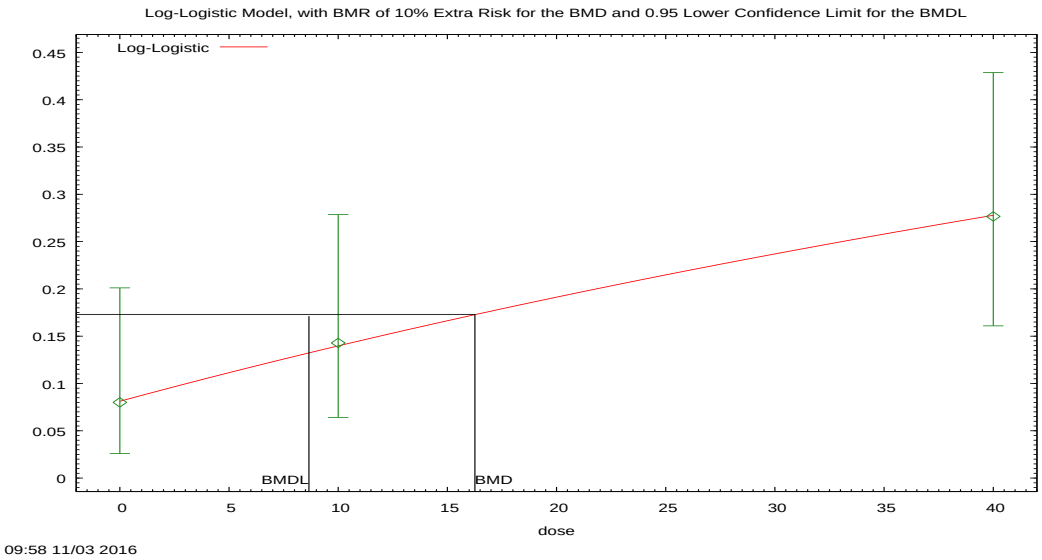

Figure 15. Plot of incidence rate by dose with fitted curve for LogLogistic model of degeneration of the adrenal cortex in female rats; dose shown in ppm.
Logistic Model. (Version: 2.14; Date: 2/28/2013)

The form of the probability function is: P[response] = background+(1-background)/[1+EXP(-intercept-slope*Log(dose))]

Slope parameter is restricted as slope >= 1

Benchmark Dose Computation.

BMR = 10% Extra risk

BMD = 16.2603

BMDL at the 95% confidence level = 8.65925

Parameter Estimates

Variable	Estimate	Default Initial Parameter Values
background	0.0811656	0.08
intercept	-4.9860E+00	-4.9535E+00
slope	1	1

Analysis of Deviance Table

Model	Log(likelihood)	# Param's	Deviance	Test d.f.	p-value
Full model	-61.75	3			
Fitted model	-61.75	2	0.00513209	1	0.94
Reduced model	-65.24	1	6.9844	2	0.03

AIC: = 127.506

Goodness of Fit Table

Dose	Est. Prob.	Expected	Observed	Size	Scaled Resid
0	0.0812	4.058	4	50	-0.03
10	0.1399	6.857	7	49	0.06
40	0.2784	13.085	13	47	-0.03

Chi^2 = 0.01 d.f = 1 P-value = 0.9428

1.1.1.15 BMDS Summary of thyroid C-cell hyperplasia in female rats

Table 33. Summary of BMD Modeling Results of thyroid C-cell hyperplasia in female rats

Model[a]	Goodness of fit		$BMD_{10}Pct$	$BMDL_{10}Pct$	Basis for model selection
	p-value	AIC			
Gamma[b]	1.000	40.718	44.9	24.0	Of the models that provided an adequate fit and a valid BMDL estimate, the Quantal-Linear model was selected based on lowest AIC.
Dichotomous-Hill Multistage 4°[d] Multistage 3°	error	error	error[e]	error[e]	
Logistic	0.442	41.566	42.4	33.0	
LogLogistic	1.000	40.718	45.0	23.6	
Probit	0.463	41.484	42.5	31.7	
LogProbit	1.000	40.718	45.7	22.5	
Weibull[f]	1.000	40.718	44.9	24.0	
Multistage 2°	1.000	40.718	44.6	24.0	
Quantal-Linear	0.996	38.726	46.2	24.0	

[a] Selected model in bold; scaled residuals for selected model for doses 0, 10, and 40 were 0, -0.08, 0.04, respectively.
[b] The Gamma model may appear equivalent to the Weibull model, however differences exist in digits not displayed in the table.
[c] BMD or BMDL computation failed for this model.
[d] For the Multistage 4° model, the beta coefficient estimates were 0 (boundary of parameters space). The models in this row reduced to the Multistage 3° model.
[e] BMD or BMDL computation failed for this model
[f] The Weibull model may appear equivalent to the Gamma model, however differences exist in digits not displayed in the table.

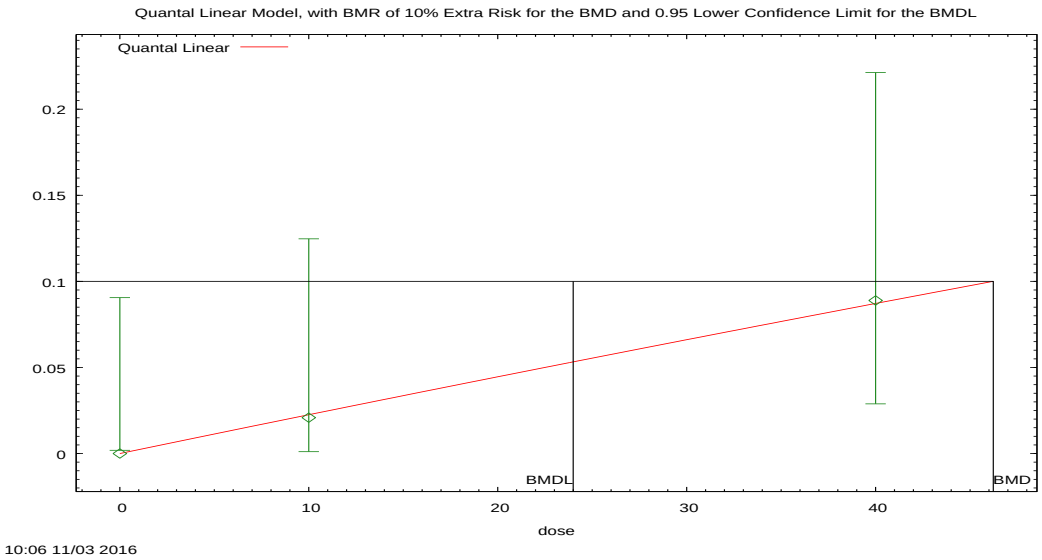

Figure 16. Plot of incidence rate by dose with fitted curve for Quantal-Linear model of thyroid C-cell hyperplasia in female rats; dose shown in ppm.
Quantal Linear Model using Weibull Model (Version: 2.16; Date: 2/28/2013)

The form of the probability function is: P[response] = background + (1-background)*[1-EXP(-slope*dose)]

Benchmark Dose Computation.

BMR = 10% Extra risk

BMD = 46.2273

BMDL at the 95% confidence level = 23.9954

Parameter Estimates

Variable	Estimate	Default Initial Parameter Values
Background	0	0.0196078
Slope	0.00227919	0.00231688
Power	n/a	1

Analysis of Deviance Table

Model	Log(likelihood)	# Param's	Deviance	Test d.f.	p-value
Full model	-18.36	3			
Fitted model	-18.36	1	0.00819409	2	1
Reduced model	-21.64	1	6.56795	2	0.04

AIC: = 38.726

Goodness of Fit Table

Dose	Est. Prob.	Expected	Observed	Size	Scaled Resid
0	0	0	0	49	0
10	0.0225	1.082	1	48	-0.08
40	0.0871	3.921	4	45	0.04

Chi^2 = 0.01 d.f = 2 P-value = 0.996

1.1.1.16 BMDS Summary of vaginal suppurative inflammation in female rats

Table 34. Summary of BMD Modeling Results of vaginal suppurative inflammation in female rats

Model[a]	Goodness of fit		$BMD_{10}Pct$	$BMDL_{10}Pct$	Basis for model selection
	p-value	AIC			
Gamma[b] Weibull[c] Multistage 2° Quantal-Linear	0.870	51.559	35.9	20.5	Of the models that provided an adequate fit and a valid BMDL estimate, the LogLogistic Model was selected based on the lowest AIC and the lowest BMDL
Dichotomous-Hill Multistage 4°[e] Multistage 3°	error	error	errorf	errorf	
Logistic	0.240	55.212	41.4	31.3	
LogLogistic	**0.894**	**51.512**	**36.0**	**19.7**	
Probit	0.251	55.097	41.2	30.0	
LogProbit	1.000	53.303	40	errord	

[a] Selected model in bold; scaled residuals for selected model for doses 0, 10, and 40 were 0, 0.42, -0.23, respectively.
[b] For the Gamma and Weibull models, the power parameter estimates were 1 (boundary of parameter space). For the Gamma model, the power parameter estimate was 1. The model is equivalent to the Quantal-Linear model.
[c] For the Weibull and Gamma models, the power parameter estimates were 1 (boundary of parameter space). For the Weibull model, the power parameter estimate was 1. The models in this row reduced to the Quantal-Linear model.
[d] BMD or BMDL computation failed for this model.
[e] For the Multistage 4° model, the beta coefficient estimates were 0 (boundary of parameters space). The models in this row reduced to the Multistage 3° model.
[f] BMD or BMDL computation failed for this model

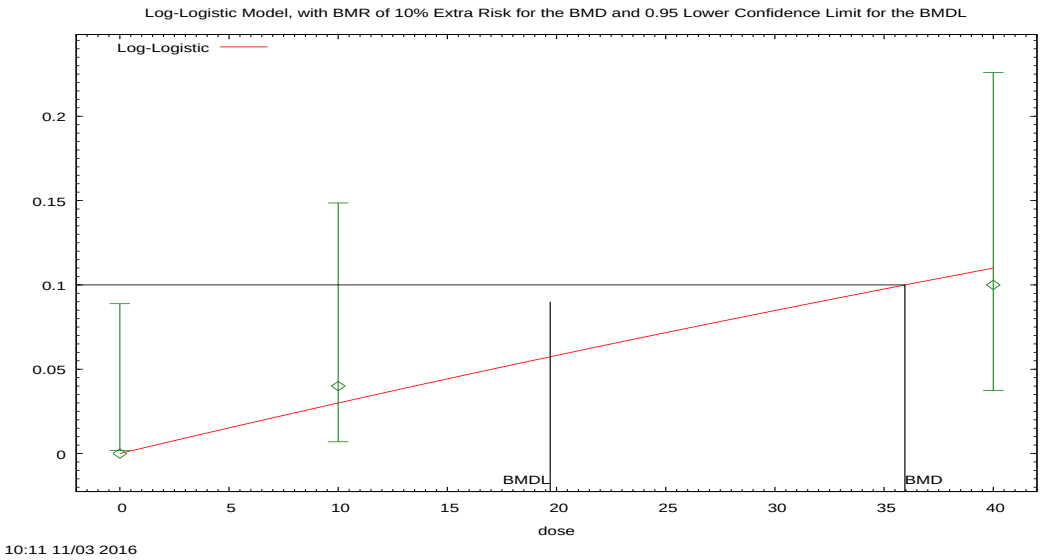

Figure 17. Plot of incidence rate by dose with fitted curve for LogLogistic model of vaginal suppurative inflammation in female rats; dose shown in ppm.
Logistic Model. (Version: 2.14; Date: 2/28/2013)

The form of the probability function is: P[response] = background+(1-background)/[1+EXP(-intercept-slope*Log(dose))]

Slope parameter is restricted as slope >= 1

Benchmark Dose Computation.

BMR = 10% Extra risk

BMD = 35.9519

BMDL at the 95% confidence level = 19.7071

Parameter Estimates

Variable	Estimate	Default Initial Parameter Values
background	0	0
intercept	-5.7794E+00	-5.6834E+00
slope	1	1

Analysis of Deviance Table

Model	Log(likelihood)	# Param's	Deviance	Test d.f.	p-value
Full model	-24.65	3			
Fitted model	-24.76	1	0.209334	2	0.9
Reduced model	-28.29	1	7.27157	2	0.03

AIC: = 51.512

Goodness of Fit Table

Dose	Est. Prob.	Expected	Observed	Size	Scaled Resid
0	0	0	0	50	0
10	0.03	1.499	2	50	0.42
40	0.11	5.501	5	50	-0.23

Chi^2 = 0.22 d.f = 2 P-value = 0.8941

1.1.2 Dichotomous models using mouse nonneoplastic data from NTP (1982)

Table 35. Mouse Nonneoplastic Data from NTP (1982)

Endpoint in Mouse	Model	p-value	AIC	BMC	BMCL
Females (#)					
Hyperplasia of the nasal cavities	Data not suitable	--	--	--	--
Suppurative inflammation of the nasal cavity	Quantal-Linear	0.734	97.839	8.99	6.52
Adenomatous hysperplasia of the lung	Data not suitable	--	--	--	--
Alveolar epithelium hyperplasia of the lung	Multistage 2°	1.000	93.383	5.18	2.89
Hematopoiesis in the spleen	LogLogistic	0.614	109.58	7.98	5.40
Hepatic necrosis	LogLogistic	0.894	51.512	36.0	19.7

1.1.2.1 BMDS Summary for suppurative inflammation in the nasal cavity of female mice

Table 36. Summary of BMD Modeling Results for suppurative inflammation in the nasal cavity of female mice

Model[a]	Goodness of fit		$BMD_{10}Pct$	$BMDL_{10}Pct$	Basis for model selection
	p-value	AIC			
Gamma	1.000	99.178	11.9	6.79	Of the models that provided an adequate fit and a valid BMDL estimate, the Quantal-Linear model was selected based on lowest AIC.
Dichotomous-Hill Multistage 4°[c] Multistage 3°	error	error	error[d]	error[d]	
Logistic	0.152	102.21	21.0	16.9	
LogLogistic	1.000	99.178	11.8	6.02	
Probit	0.186	101.73	19.3	15.5	
LogProbit	1.000	99.178	11.6	5.84	
Weibull	1.000	99.178	12.0	6.79	
Multistage 2°	1.000	99.178	12.2	6.79	
Quantal-Linear	**0.734**	**97.839**	**8.99**	**6.52**	

[a] Selected model in bold; scaled residuals for selected model for doses 0, 10, and 40 were 0, -0.69, 0.38, respectively.
[b] BMD or BMDL computation failed for this model.
[c] For the Multistage 4° model, the beta coefficient estimates were 0 (boundary of parameters space). The models in this row reduced to the Multistage 3° model.
[d] BMD or BMDL computation failed for this model

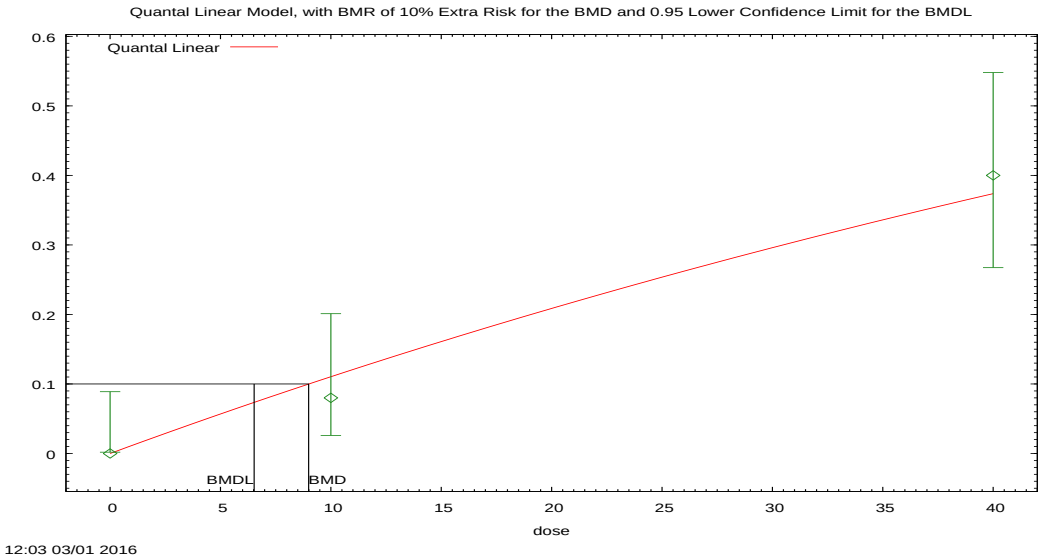

Figure 18. Plot of incidence rate by dose with fitted curve for Quantal-Linear model for inflammation in the nasal cavity of female mice; dose shown in ppm.
Quantal Linear Model using Weibull Model (Version: 2.16; Date: 2/28/2013)

The form of the probability function is: P[response] = background + (1-background)*[1-EXP(-slope*dose)]

Benchmark Dose Computation.

BMR = 10% Extra risk

BMD = 8.99287

BMDL at the 95% confidence level = 6.5245

Parameter Estimates

Variable	Estimate	Default Initial Parameter Values
Background	0	0.0192308
Slope	0.011716	0.012446
Power	n/a	1

Analysis of Deviance Table

Model	Log(likelihood)	# Param's	Deviance	Test d.f.	p-value
Full model	-47.59	3			
Fitted model	-47.92	1	0.661044	2	0.72
Reduced model	-65.95	1	36.7229	2	<.0001

AIC: = 97.8391

Goodness of Fit Table

Dose	Est. Prob.	Expected	Observed	Size	Scaled Resid
0	0	0	0	50	0
10	0.1106	5.528	4	50	-0.69
40	0.3741	18.707	20	50	0.38

Chi^2 = 0.62 d.f = 2 P-value = 0.7344

1.1.2.2 BMDS Summary of epithelial hyperplasia in the lung/bronchus of female mice

Table 37. Summary of BMD Modeling Results of epithelial hyperplasia in the lung/bronchus of female mice

Model[a]	Goodness of fit		$BMD_{10}Pct$	$BMDL_{10}Pct$	Basis for model selection
	p-value	AIC			
Gamma[b]	0.190	119.94	7.70	5.71	Of the models that provided an adequate fit and a valid BMDL estimate, the LogLogistic Model was selected based on the lowest AIC and the lowest BMDL
Dichotomous-Hill Multistage 4°[d] Multistage 3°	error	error	error[e]	error[e]	
Logistic	0.0049	129.52	18.1	14.4	
LogLogistic	**0.423**	**118.57**	**6.31**	**4.33**	
Probit	0.0056	128.98	16.8	13.4	
LogProbit	1.000	118.93	2.61	1.19E-17	
Weibull[f] Multistage 2°[g] Quantal-Linear[h]	0.190	119.94	7.70	5.71	

[a] Selected model in bold; scaled residuals for selected model for doses 0, 10, and 40 were 0, 1.07, -0.76, respectively.
[b] The Gamma model may appear equivalent to the Weibull model, however differences exist in digits not displayed in the table. This also applies to the Multistage 2° model. This also applies to the Quantal-Linear model.
[c] BMD or BMDL computation failed for this model.
[d] For the Multistage 4° model, the beta coefficient estimates were 0 (boundary of parameters space). The models in this row reduced to the Multistage 3° model.
[e] BMD or BMDL computation failed for this model
[f] For the Weibull model, the power parameter estimate was 1. The models in this row reduced to the Quantal-Linear model.
[g] The Multistage 2° model may appear equivalent to the Gamma model, however differences exist in digits not displayed in the table.
[h] The Quantal-Linear model may appear equivalent to the Gamma model, however differences exist in digits not displayed in the table.

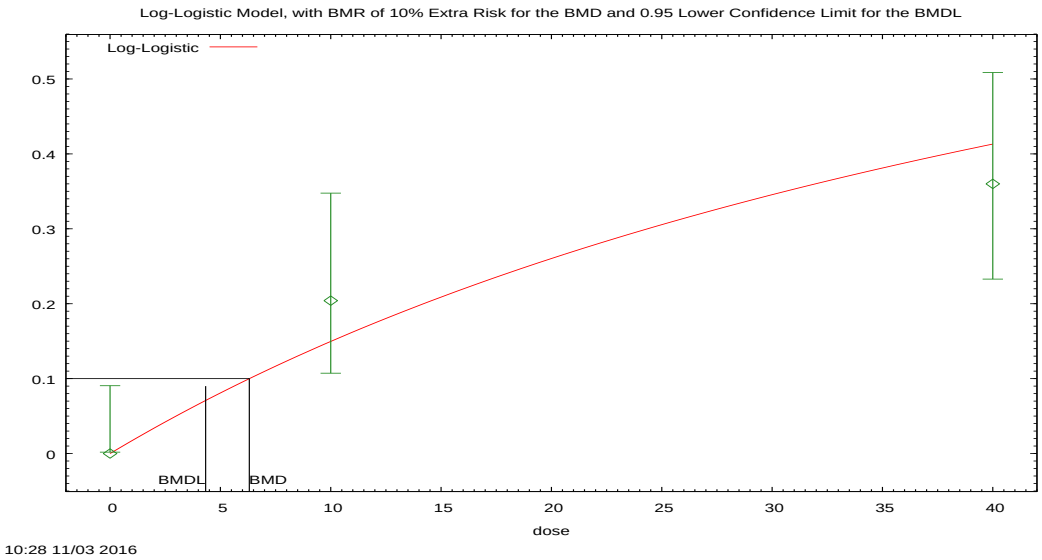

Figure 19. Plot of incidence rate by dose with fitted curve for LogLogistic model of epithelial hyperplasia in the lung/bronchus of female mice; dose shown in ppm.
Logistic Model. (Version: 2.14; Date: 2/28/2013)

The form of the probability function is: P[response] = background+(1-background)/[1+EXP(-intercept-slope*Log(dose))]

Slope parameter is restricted as slope >= 1

Benchmark Dose Computation.

BMR = 10% Extra risk

BMD = 6.3099

BMDL at the 95% confidence level = 4.33169

Parameter Estimates

Variable	Estimate	Default Initial Parameter Values
background	0	0
intercept	-4.0393E+00	-3.9639E+00
slope	1	1

Analysis of Deviance Table

Model	Log(likelihood)	# Param's	Deviance	Test d.f.	p-value
Full model	-57.47	3			
Fitted model	-58.28	1	1.63538	2	0.44
Reduced model	-71.79	1	28.6427	2	<.0001

AIC: = 118.566

Goodness of Fit Table

Dose	Est. Prob.	Expected	Observed	Size	Scaled Resid
0	0	0	0	49	0
10	0.1497	7.337	10	49	1.07
40	0.4133	20.663	18	50	-0.76

Chi^2 = 1.72 d.f = 2 P-value = 0.4227

1.1.2.3 BMDS Summary of epithelial hyperplasia in the lung/bronchiole of female mice

Table 38. Summary of BMD Modeling Results of epithelial hyperplasia in the lung/bronchiole of female mice

Model[a]	Goodness of fit		$BMD_{10}Pct$	$BMDL_{10}Pct$	Basis for model selection
	p-value	AIC			
Gamma	1.000	97.389	5.00	2.40	Of the models that provided an adequate fit and a valid BMDL estimate, the Multistage 2° model was selected based on lowest AIC. Since multiple models had the lowest AIC, the model with the lowest BMDL was chosen from those models.
Dichotomous-Hill Multistage 4°[c] Multistage 3°	error	error	error[d]	error[d]	
Logistic	0.0176	105.82	8.38	6.47	
LogLogistic	1.000	97.389	5.81	3.63	
Probit	0.0239	104.77	7.98	6.28	
LogProbit	1.000	97.389	6.04	3.85	
Weibull	1.000	97.389	4.62	2.38	
Multistage 2°	**1.000**	**97.389**	**3.99**	**2.29**	
Quantal-Linear	0.258	98.270	2.39	1.89	

[a] Selected model in bold; scaled residuals for selected model for doses 0, 10, and 40 were 0, 0, 0, respectively.
[b] BMD or BMDL computation failed for this model.
[c] For the Multistage 4° model, the beta coefficient estimates were 0 (boundary of parameters space). The models in this row reduced to the Multistage 3° model.
[d] BMD or BMDL computation failed for this model

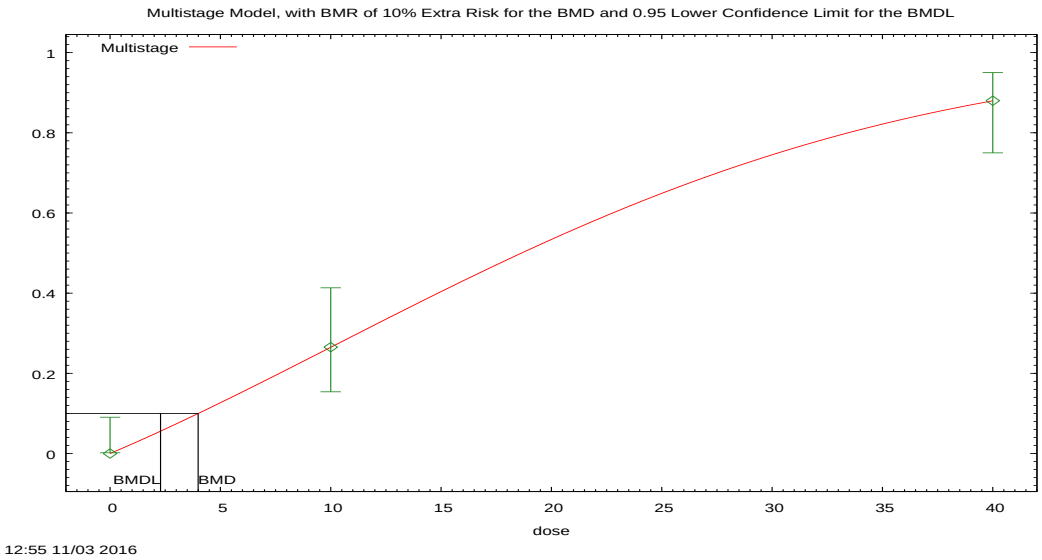

Figure 20. Plot of incidence rate by dose with fitted curve for Multistage 2° model of epithelial hyperplasia in the lung/bronchiole of female mice; dose shown in ppm.
Multistage Model. (Version: 3.4; Date: 05/02/2014)

The form of the probability function is: P[response] = background + (1-background)*[1-EXP(-beta1*dose^1-beta2*dose^2...)]

Benchmark Dose Computation.

BMR = 10% Extra risk

BMD = 3.99257

BMDL at the 95% confidence level = 2.28795

Parameter Estimates

Variable	Estimate	Default Initial Parameter Values
Background	0	0
Beta(1)	0.0234378	0.023438
Beta(2)	0.000739224	0.000739215

Analysis of Deviance Table

Model	Log(likelihood)	# Param's	Deviance	Test d.f.	p-value
Full model	-46.69	3			
Fitted model	-46.69	2	0.000000000460872	1	1
Reduced model	-98.65	1	103.902	2	<.0001

AIC: = 97.3888

Goodness of Fit Table

Dose	Est. Prob.	Expected	Observed	Size	Scaled Resid
0	0	0	0	49	0
10	0.2653	13	13	49	0
40	0.88	44	44	50	0

Chi^2 = 0 d.f = 1 P-value = 1

1.1.2.4 BMDS Summary of alveolar epithelial hyperplasia in female mice

Table 39. Summary of BMD Modeling Results of alveolar epithelial hyperplasia in female mice

Model[a]	Goodness of fit		$BMD_{10}Pct$	$BMDL_{10}Pct$	Basis for model selection
	p-value	AIC			
Gamma	1.000	92.881	6.04	3.33	Of the models that provided an adequate fit and a valid BMDL estimate, the Multistage 2° model was selected based on lowest AIC. Since multiple models had the lowest AIC, the model with the lowest BMDL was chosen from those models.
Dichotomous-Hill Multistage 4°[c] Multistage 3°	error	error	error[d]	error[d]	
Logistic	0.0374	99.493	9.19	7.06	
LogLogistic	1.000	92.881	6.63	4.41	
Probit	0.0527	98.435	8.69	6.79	
LogProbit	1.000	92.881	6.86	4.66	
Weibull	1.000	92.881	5.62	3.16	
Multistage 2°	**1.000**	**92.881**	**5.05**	**2.81**	
Quantal-Linear	0.106	95.773	2.52	1.99	

[a] Selected model in bold; scaled residuals for selected model for doses 0, 10, and 40 were 0, 0, 0, respectively.
[b] BMD or BMDL computation failed for this model.
[c] For the Multistage 4° model, the beta coefficient estimates were 0 (boundary of parameters space). The models in this row reduced to the Multistage 3° model.
[d] BMD or BMDL computation failed for this model

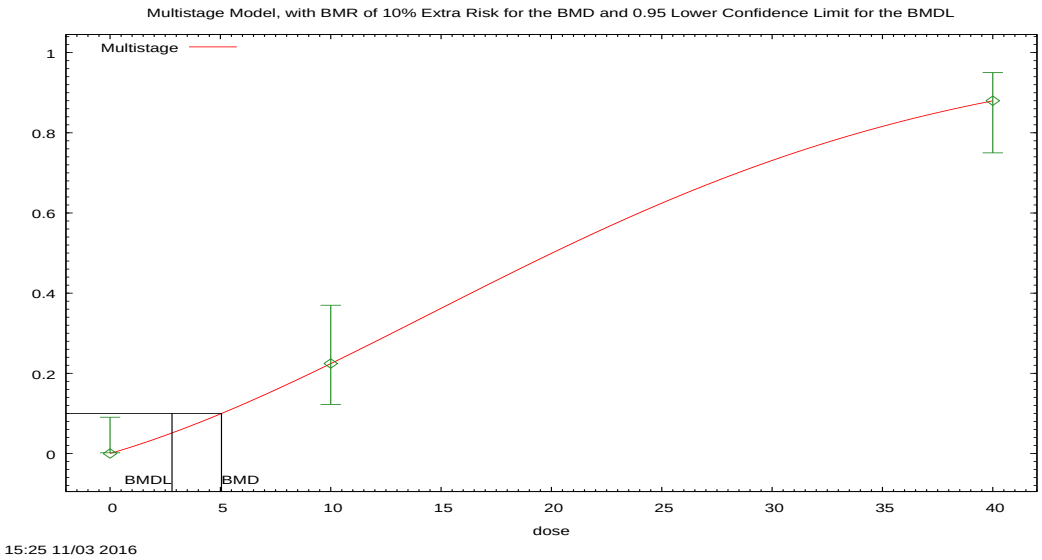

Figure 21. Plot of incidence rate by dose with fitted curve for Multistage 2° model of alveolar epithelial hyperplasia in female mice; dose shown in ppm.
Multistage Model. (Version: 3.4; Date: 05/02/2014)

The form of the probability function is: P[response] = background + (1-background)*[1-EXP(-beta1*dose^1-beta2*dose^2...)]

Benchmark Dose Computation.

BMR = 10% Extra risk

BMD = 5.04831

BMDL at the 95% confidence level = 2.80785

Parameter Estimates

Variable	Estimate	Default Initial Parameter Values
Background	0	0
Beta(1)	0.0162288	0.016229
Beta(2)	0.00091945	0.000919439

Analysis of Deviance Table

Model	Log(likelihood)	# Param's	Deviance	Test d.f.	p-value
Full model	-44.44	3			
Fitted model	-44.44	2	0.000000000659242	1	1
Reduced model	-97.65	1	106.424	2	<.0001

AIC: = 92.8806

Goodness of Fit Table

Dose	Est. Prob.	Expected	Observed	Size	Scaled Resid
0	0	0	0	49	0
10	0.2245	11	11	49	0
40	0.88	44	44	50	0

Chi^2 = 0 d.f = 1 P-value = 1

1.1.2.3 BMDS Summary of hematopoiesis in the spleen of female mice

Table 40. Summary of BMD Modeling Results of hematopoiesis in the spleen of female mice

Model[a]	Goodness of fit		$BMD_{10}Pct$	$BMDL_{10}Pct$	Basis for model selection
	p-value	AIC			
Gamma[b] Weibull[c] Multistage 2° Quantal-Linear	0.393	109.23	9.06	6.58	Of the models that provided an adequate fit and a valid BMDL estimate, the LogLogistic Model was selected based on the lowest AIC and the lowest BMDL
Dichotomous-Hill Multistage 4°[e] Multistage 3°	error	error	error[f]	error[f]	
Logistic	0.0135	117.75	20.1	16.1	
LogLogistic	**0.623**	**108.42**	**7.75**	**5.24**	
Probit	0.0155	117.26	18.7	14.9	
LogProbit	1.000	109.52	4.57	1.33E-04	

[a] Selected model in bold; scaled residuals for selected model for doses 0, 10, and 40 were 0, 0.8, -0.55, respectively.
[b] For the Gamma and Weibull models, the power parameter estimates were 1 (boundary of parameter space).For the Gamma model, the power parameter estimate was 1. The model is equivalent to the Quantal-Linear model.
[c] For the Weibull and Gamma models, the power parameter estimates were 1 (boundary of parameter space).For the Weibull model, the power parameter estimate was 1. The models in this row reduced to the Quantal-Linear model.
[d] BMD or BMDL computation failed for this model.
[e] For the Multistage 4° model, the beta coefficient estimates were 0 (boundary of parameters space). The models in this row reduced to the Multistage 3° model.
[f] BMD or BMDL computation failed for this model

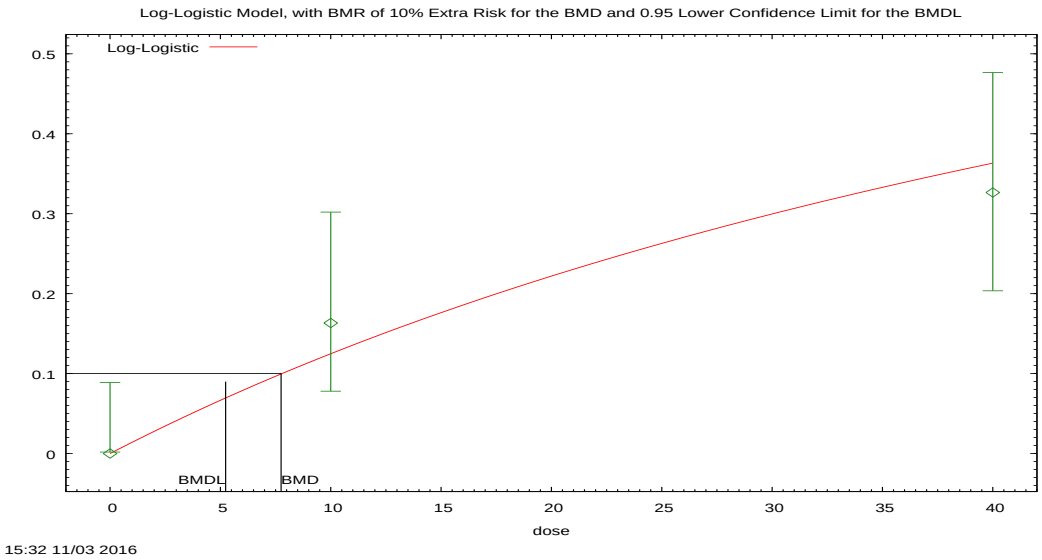

Figure 22. Plot of incidence rate by dose with fitted curve for LogLogistic model of hematopoiesis in the spleen of female mice; dose shown in ppm.
Logistic Model. (Version: 2.14; Date: 2/28/2013)

The form of the probability function is: P[response] = background+(1-background)/[1+EXP(-intercept-slope*Log(dose))]

Slope parameter is restricted as slope >= 1

Benchmark Dose Computation.

BMR = 10% Extra risk

BMD = 7.75138

BMDL at the 95% confidence level = 5.23786

Parameter Estimates

Variable	Estimate	Default Initial Parameter Values
background	0	0
intercept	-4.2451E+00	-4.1748E+00
slope	1	1

Analysis of Deviance Table

Model	Log(likelihood)	# Param's	Deviance	Test d.f.	p-value
Full model	-52.76	3			
Fitted model	-53.21	1	0.902227	2	0.64
Reduced model	-65.6	1	25.678	2	<.0001

AIC: = 108.423

Goodness of Fit Table

Dose	Est. Prob.	Expected	Observed	Size	Scaled Resid
0	0	0	0	50	0
10	0.1254	6.143	8	49	0.8
40	0.3644	17.857	16	49	-0.55

Chi^2 = 0.95 d.f = 2 P-value = 0.6233

1.1.2.4 BMDS Summary of hepatic necrosis in female mice

Table 41. Summary of BMD Modeling Results of hepatic necrosis in female mice

Model[a]	Goodness of fit		$BMD_{10}Pct$	$BMDL_{10}Pct$	Basis for model selection
	p-value	AIC			
Gamma[b] Weibull[c] Multistage 2° Quantal-Linear	0.770	65.672	24.7	15.3	Of the models that provided an adequate fit and a valid BMDL estimate, the LogLogistic Model was selected based on the lowest AIC and the lowest BMDL
Dichotomous-Hill Multistage 4°[e] Multistage 3°	error	error	error[f]	error[f]	
Logistic	0.145	70.107	35.3	27.2	
LogLogistic	**0.821**	**65.561**	**24.1**	**14.3**	
Probit	0.155	69.932	34.3	25.7	
LogProbit	1.000	67.193	22.2	error[d]	

[a] Selected model in bold; scaled residuals for selected model for doses 0, 10, and 40 were 0, 0.55, -0.31, respectively.
[b] For the Gamma and Weibull models, the power parameter estimates were 1 (boundary of parameter space).For the Gamma model, the power parameter estimate was 1. The model is equivalent to the Quantal-Linear model.
[c] For the Weibull and Gamma models, the power parameter estimates were 1 (boundary of parameter space).For the Weibull model, the power parameter estimate was 1. The models in this row reduced to the Quantal-Linear model.
[d] BMD or BMDL computation failed for this model.
[e] For the Multistage 4° model, the beta coefficient estimates were 0 (boundary of parameters space). The models in this row reduced to the Multistage 3° model.
[f] BMD or BMDL computation failed for this model

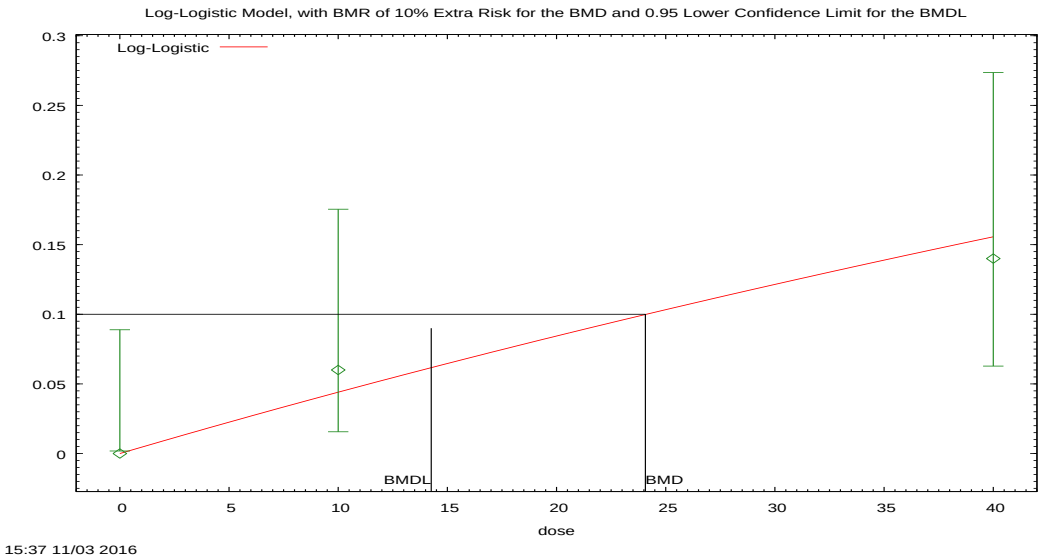

Figure 23. Plot of incidence rate by dose with fitted curve for LogLogistic model of hepatic necrosis in female mice; dose shown in ppm.
Logistic Model. (Version: 2.14; Date: 2/28/2013)

The form of the probability function is: P[response] = background+(1-background)/[1+EXP(-intercept-slope*Log(dose))]

Slope parameter is restricted as slope >= 1

Benchmark Dose Computation.

BMR = 10% Extra risk

BMD = 24.0688

BMDL at the 95% confidence level = 14.2606

Parameter Estimates

Variable	Estimate	Default Initial Parameter Values
background	0	0
intercept	-5.3781E+00	-5.2791E+00
slope	1	1

Analysis of Deviance Table

Model	Log(likelihood)	# Param's	Deviance	Test d.f.	p-value
Full model	-31.6	3			
Fitted model	-31.78	1	0.368136	2	0.83
Reduced model	-36.74	1	10.2859	2	0.01

AIC: = 65.5612

Goodness of Fit Table

Dose	Est. Prob.	Expected	Observed	Size	Scaled Resid
0	0	0	0	50	0
10	0.0441	2.206	3	50	0.55
40	0.1559	7.794	7	50	-0.31

Chi^2 = 0.39 d.f = 2 P-value = 0.821

1.2 Carcinogenic Endpoint Modeling

The TCEQ performed Benchmark Concentration (BMC) modeling using USEPA Benchmark Dose (BMD) software (version 2.6) for the data presented in Table 14 and Table 15 which were taken from the NTP (1982) study. Data were used to predict 95% lower confidence limits on the BMCs using dichotomous models. A default BMR of 10% was selected for extra risk (BMC_{10}) and $BMCL_{10}$. All of the available dichotomous and multistage cancer models were run for all of the rat (Appendix 1.2.1) and mouse (Appendix 1.2.2) data. All of the models are presented below, with the best fit model based in the lowest $BMCL_{10}$ and the best fit to the curve shown in bold and graphically below its respective table.

1.2.1 Dichotomous and multistage cancer models using rat neoplastic data from NTP (1982)

Table 42. Rat Neoplastic Data from NTP (1982)

Tumor Type/Incidence	Control	10 ppm	40 ppm
Males (#)			
Nasal cavity adenocarcinoma [a]	0/50	20/50*	28/50*
Nasal cavity tumors [a,b]	0/50	39/50*	41/50*
Tunica vaginalis mesothelioma or malignant [a]	1/50	8/50*	25/50*
Females (#)			
Nasal cavity adenocarcinoma [a]	0/50	20/50*	29/50*
Nasal cavity tumors [a,c]	1/50	34/50*	43/50*
Mammary gland fibroadenoma [a]	4/50	29/50*	24/50*

* Significant difference from control ($p < 0.05$), Fisher exact test

[a] Significant increasing trend ($p < 0.05$), Cochran-Armitage test

[b] Adenoma, carcinoma, adenocarcinoma, adenomatous polyp, papillary adenoma, squamous cell carcinoma, or squamous cell papilloma.

[c] Adenoma, carcinoma, adenocarcinoma, adenomatous polyp, papillary adenoma, papillary polyp, or squamous cell carcinoma.

1.2.1.1 BMDS Summary of Rat Male Nasal Cavity Adenocarcinoma

Table 43. Summary of BMD Modeling Results for male rat nasal cavity adenocarcinomas

Model[a]	**Goodness of fit**		**BMD_{10}Pct**	**$BMDL_{10}$Pct**	**Basis for model selection**
	p-value	**AIC**			
Gamma[b] Weibull[c] Multistage 2° Quantal-Linear	0.0085	146.58	3.81	3.01	Of the models that provided an adequate fit and a valid BMDL estimate, the log logistic model was selected based on the lowest BMDL, lowest AIC and the BMD was 3 times lower than the lowest non zero dose.
Dichotomous-Hill Multistage 4°[e] Multistage 3°	error	error	error[f]	error[f]	
Logistic	0	163.36	10.5	8.44	
LogLogistic	**0.186**	**141.14**	**2.43**	**1.71**	
Probit	0	162.59	9.84	8.02	
LogProbit	1.000	139.89	0.294	error[d]	

[a] Selected model in bold; scaled residuals for selected model for doses 0, 10, and 40 were 0, 1.32, -1.28, respectively.

[b] For the Gamma and Weibull models, the power parameter estimates were 1 (boundary of parameter space).For the Gamma model, the power parameter estimate was 1. The model is equivalent to the Quantal-Linear model.

[c] For the Weibull and Gamma models, the power parameter estimates were 1 (boundary of parameter space).For the Weibull model, the power parameter estimate was 1. The models in this row reduced to the Quantal-Linear model.

[d] BMD or BMDL computation failed for this model.

[e] For the Multistage 4° model, the beta coefficient estimates were 0 (boundary of parameters space). The models in this row reduced to the Multistage 3° model.

f BMD or BMDL computation failed for this model

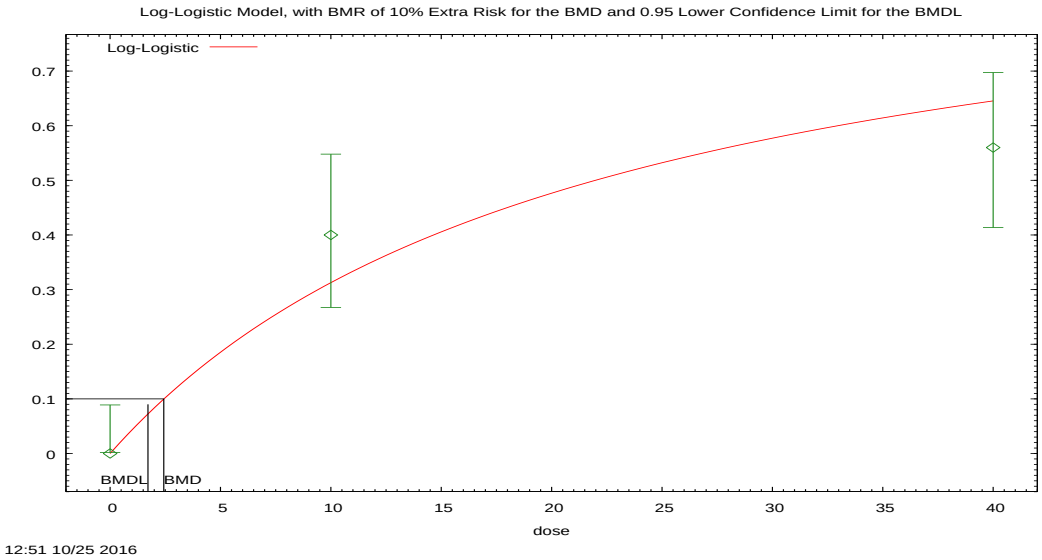

Figure 24. Plot of incidence rate by dose with fitted curve for LogLogistic model for male rat nasal cavity adenocarcinomas; dose shown in ppm.

Logistic Model. (Version: 2.14; Date: 2/28/2013)

The form of the probability function is: P[response] = background+(1-background)/[1+EXP(-intercept-slope*Log(dose))]

Slope parameter is restricted as slope >= 1

Benchmark Dose Computation.

BMR = 10% Extra risk

BMD = 2.4316

BMDL at the 95% confidence level = 1.71499

Parameter Estimates

Variable	Estimate	Default Initial Parameter Values
background	0	0
intercept	-3.0858E+00	-3.0779E+00
slope	1	1

Analysis of Deviance Table

Model	Log(likelihood)	# Param's	Deviance	Test d.f.	p-value
Full model	-67.95	3			
Fitted model	-69.57	1	3.2432	2	0.2
Reduced model	-94.03	1	52.1667	2	<.0001

AIC: = 141.137

Goodness of Fit Table

Dose	Est. Prob.	Expected	Observed	Size	Scaled Resid
0	0	0	0	50	0
10	0.3136	15.682	20	50	1.32
40	0.6464	32.318	28	50	-1.28

Chi^2 = 3.36 d.f = 2 P-value = 0.186

1.2.1.2 BMDS Summary of Rat Male Nasal cavity tumors

Table 44. Summary of BMD Modeling Results for Male Rat Nasal Cavity Tumors

Model[a]	**Goodness of fit**		**BMD_{10}Pct**	**$BMDL_{10}$Pct**	**Basis for model selection**
	***p*-value**	**AIC**			
Gamma[b] Weibull[c] Multistage 2° Quantal-Linear	0	126.44	1.47	1.19	No viable models found.
Dichotomous-Hill Multistage 4° [e] Multistage 3°	error	error	error[f]	error[f]	
Logistic	0	160.77	4.35	3.44	
LogLogistic	0.0658	106.69	0.481	0.309	
Probit	0	161.54	4.58	3.78	
LogProbit	1.000	103.83	2.31E-08	error[d]	

[a] Selected model in bold; scaled residuals for selected model for doses 0, 10, and 40 were 0, 1.27, -1.96, respectively.

[b] For the Gamma and Weibull models, the power parameter estimates were 1 (boundary of parameter space).For the Gamma model, the power parameter estimate was 1. The model is equivalent to the Quantal-Linear model.

[c] For the Weibull and Gamma models, the power parameter estimates were 1 (boundary of parameter space).For the Weibull model, the power parameter estimate was 1. The models in this row reduced to the Quantal-Linear model.

[d] BMD or BMDL computation failed for this model.

[e] For the Multistage 4° model, the beta coefficient estimates were 0 (boundary of parameters space). The models in this row reduced to the Multistage 3° model.

f BMD or BMDL computation failed for this model

1.2.1.3 BMDS Summary of rat male tunica vaginalis

Table 45. Summary of BMD Modeling Results for Male Rat Tunica Vaginalis Neoplasms

Model[a]	Goodness of fit		$BMD_{10}Pct$	$BMDL_{10}Pct$	Basis for model selection
	***p*-value**	**AIC**			
Gamma	N/A[b]	129.09	7.01	4.75	Of the models that provided an adequate fit and a valid BMDL estimate the log logistic model was selected based on the lowest BMDL and Lowest AIC.
Dichotomous-Hill Multistage 4°[d] Multistage 3°	error	error	error[e]	error[e]	
Logistic	0.108	129.94	15.1	12.2	
LogLogistic	N/A[b]	129.09	7.25	3.69	
Probit	0.139	129.46	13.9	11.2	
LogProbit	N/A[b]	129.09	7.52	2.67	
Weibull	N/A[b]	129.09	6.99	4.75	
Multistage 2°	N/A[b]	129.09	6.90	4.75	
Quantal-Linear	**0.849**	**127.12**	**6.37**	**4.74**	

[a] Selected model in bold; scaled residuals for selected model for doses 0, 10, and 40 were 0.04, -0.16, 0.09, respectively.

[b] No available degrees of freedom to calculate a goodness of fit value.

[c] BMD or BMDL computation failed for this model.

[d] For the Multistage 4° model, the beta coefficient estimates were 0 (boundary of parameters space). The models in this row reduced to the Multistage 3° model.

[e] BMD or BMDL computation failed for this model.

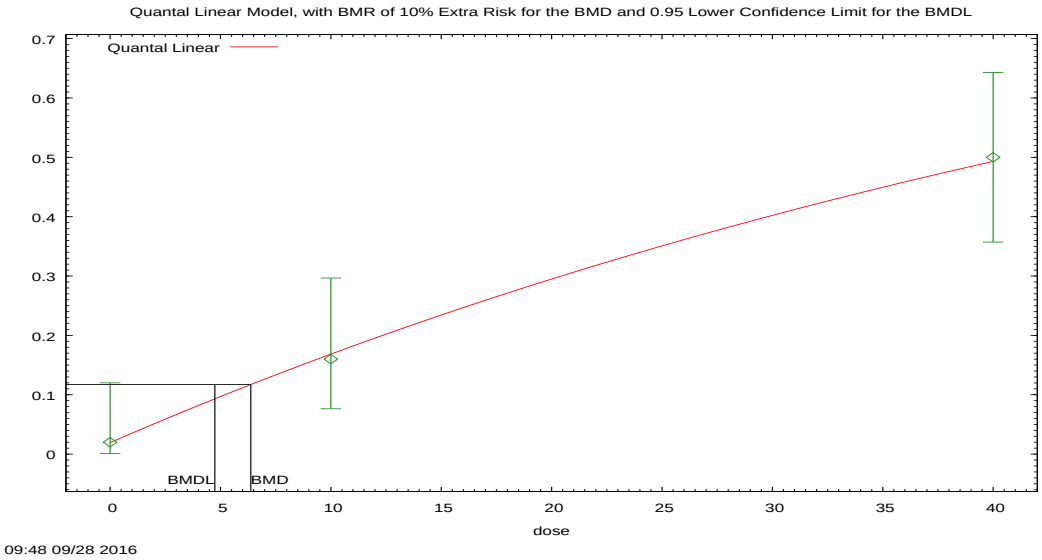

Figure 25. Plot of incidence rate by dose with fitted curve for Quantal-Linear model; dose shown in ppm.

Quantal Linear Model using Weibull Model (Version: 2.16; Date: 2/28/2013)

The form of the probability function is: P[response] = background + (1-background)*[1-EXP(-slope*dose)]

Benchmark Dose Computation.

BMR = 10% Extra risk

BMD = 6.37485

BMDL at the 95% confidence level = 4.74495

Parameter Estimates

Variable	Estimate	Default Initial Parameter Values
Background	0.019258	0.0384615
Slope	0.0165275	0.0163482
Power	n/a	1

Analysis of Deviance Table

Model	Log(likelihood)	# Param's	Deviance	Test d.f.	p-value
Full model	-61.54	3			
Fitted model	-61.56	2	0.0366217	1	0.85
Reduced model	-80.28	1	37.4795	2	<.0001

AIC: = 127.122

Goodness of Fit Table

Dose	Est. Prob.	Expected	Observed	Size	Scaled Resid
0	0.0193	0.963	1	50	0.04
10	0.1687	8.433	8	50	-0.16
40	0.4937	24.683	25	50	0.09

Chi^2 = 0.04 d.f = 1 P-value = 0.849

1.2.1.4 BMDS Summary of rats female nasal cavity adenocarcinoma ()

Table 46. Summary of BMD Modeling Results for female rat nasal cavity adenocarcinomas

Model[a]	**Goodness of fit**		**BMD_{10}Pct**	**$BMDL_{10}$Pct**	**Basis for model selection**
	***p*-value**	**AIC**			
Gamma[b] Multistage 2°[c]	0.0144	145.11	3.67	2.90	Of the models that provided an adequate fit and a valid BMDL estimate the log logistic model was selected based on the lowest BMDL, lowest AIC and BMD 3x lower than lowest non-zero dose.
Dichotomous-Hill Multistage 4°[e] Multistage 3°	error	error	error[f]	error[f]	
Logistic	0	162.43	10.1	8.18	
LogLogistic	**0.267**	**139.89**	**2.32**	**1.64**	
Probit	0	161.62	9.53	7.79	
LogProbit	1.000	139.33	0.437	3.34E-18	
Weibull[g] Quantal-Linear[h]	0.0144	145.11	3.67	2.90	

[a] Selected model in bold; scaled residuals for selected model for doses 0, 10, and 40 were 0, 1.16, -1.14, respectively.

[b] The Gamma model may appear equivalent to the Weibull model, however differences exist in digits not displayed in the table. This also applies to the Quantal-Linear model.

[c] The Multistage 2° model may appear equivalent to the Weibull model, however differences exist in digits not displayed in the table. This also applies to the Quantal-Linear model.

[d] BMD or BMDL computation failed for this model.

[e] For the Multistage 4° model, the beta coefficient estimates were 0 (boundary of parameters space). The models in this row reduced to the Multistage 3° model.

[f] BMD or BMDL computation failed for this model

[g] For the Weibull model, the power parameter estimate was 1. The models in this row reduced to the Quantal-Linear model.

[h] The Quantal-Linear model may appear equivalent to the Gamma model, however differences exist in digits not displayed in the table. This also applies to the Multistage 2° model.

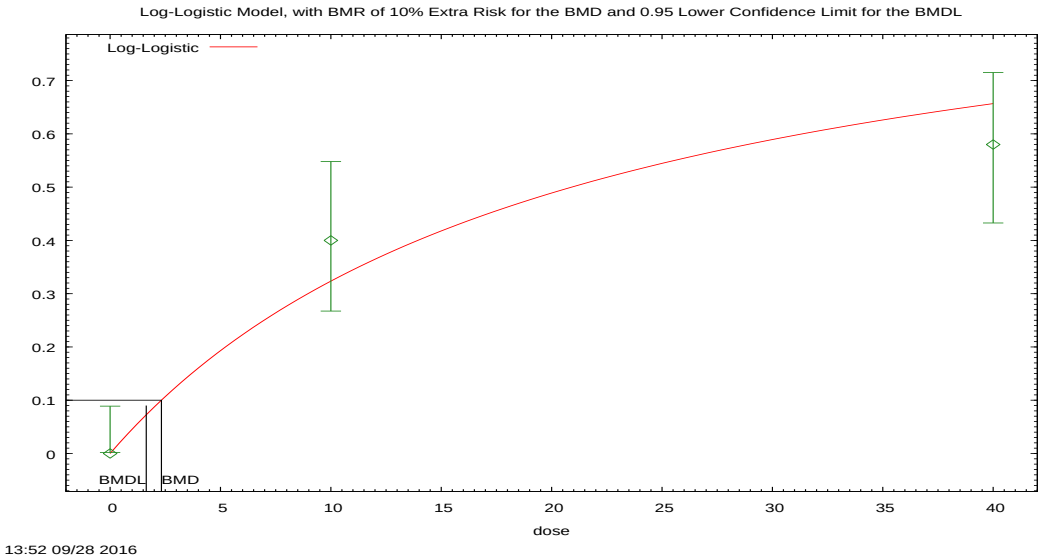

Figure 26. Plot of incidence rate by dose with fitted curve for LogLogistic model for female rat nasal cavity adenocarcinomas; dose shown in ppm.
Logistic Model. (Version: 2.14; Date: 2/28/2013)

The form of the probability function is: P[response] = background+(1-background)/[1+EXP(-intercept-slope*Log(dose))]

Slope parameter is restricted as slope >= 1

Benchmark Dose Computation.

BMR = 10% Extra risk

BMD = 2.32452

BMDL at the 95% confidence level = 1.63925

Parameter Estimates

Variable	Estimate	Default Initial Parameter Values
background	0	0
intercept	-3.0407E+00	-3.0371E+00
slope	1	1

Analysis of Deviance Table

Model	Log(likelihood)	# Param's	Deviance	Test d.f.	p-value
Full model	-67.67	3			
Fitted model	-68.94	1	2.55572	2	0.28
Reduced model	-94.77	1	54.2075	2	<.0001

AIC: = 139.886

Goodness of Fit Table

Dose	Est. Prob.	Expected	Observed	Size	Scaled Resid
0	0	0	0	50	0
10	0.3234	16.17	20	50	1.16
40	0.6566	32.83	29	50	-1.14

Chi^2 = 2.64 d.f = 2 P-value = 0.267

1.2.1.5 BMDS Summary of Rat Female Nasal Cavity Tumors

Table 47. Summary of BMD Modeling Results for female rat nasal cavity tumors

Model[a]	**Goodness of fit**		**BMD_{10}Pct**	**$BMDL_{10}$Pct**	**Basis for model selection**
	***p*-value**	**AIC**			
Gamma[b] Multistage 2°[c]	9.00E-04	126.88	1.53	1.23	No Viable Models
Dichotomous-Hill Multistage 4°[e] Multistage 3°	error	error	error[f]	error[f]	
Logistic	0	150.72	4.35	3.43	
LogLogistic	0.532	117.37	0.600	0.392	
Probit	0	151.40	4.55	3.74	
LogProbit	N/A[g]	118.99	0.206	1.03E-07	
Weibull[h] Quantal-Linear[i]	9.00E-04	126.88	1.53	1.23	

[a] No model was selected as a best-fitting model.

[b] The Gamma model may appear equivalent to the Weibull model, however differences exist in digits not displayed in the table. This also applies to the Quantal-Linear model.

[c] The Multistage 2° model may appear equivalent to the Weibull model, however differences exist in digits not displayed in the table. This also applies to the Quantal-Linear model.

[d] BMD or BMDL computation failed for this model.

[e] For the Multistage 4° model, the beta coefficient estimates were 0 (boundary of parameters space). The models in this row reduced to the Multistage 3° model.

[f] BMD or BMDL computation failed for this model

[g] No available degrees of freedom to calculate a goodness of fit value.

[h] For the Weibull model, the power parameter estimate was 1. The models in this row reduced to the Quantal-Linear model.

[i] The Quantal-Linear model may appear equivalent to the Gamma model, however differences exist in digits not displayed in the table. This also applies to the Multistage 2° model.

1.2.1.6 BMDS Summary of Rat Female Mammary Gland Fibroadenoma

Table 48. Summary of BMD Modeling Results for fmeal rat mammary gland fibroadenomas

Modela	Goodness of fit		$BMD_{10}Pct$	$BMDL_{10}Pct$	Basis for model selection
	p-value	AIC			
Gamma[b] Multistage 2°[c]	0	191.00	6.08	3.93	No usable model
Dichotomous-Hill Multistage 4°[e] Multistage 3°	error	error	error[f]	error[f]	
Logistic	0	194.45	11.8	8.47	
LogLogistic	0	185.82	2.82	1.75	
Probit	0	194.27	11.4	8.23	
LogProbit	0.316	170.15	error[d]	0	
Weibull[g] Quantal-Linear[h]	0	191.00	6.08	3.93	

[a] No model was selected as a best-fitting model.

[b] The Gamma model may appear equivalent to the Weibull model, however differences exist in digits not displayed in the table. This also applies to the Quantal-Linear model.

[c] The Multistage 2° model may appear equivalent to the Weibull model, however differences exist in digits not displayed in the table. This also applies to the Quantal-Linear model.

[d] BMD or BMDL computation failed for this model.

[e] For the Multistage 4° model, the beta coefficient estimates were 0 (boundary of parameters space). The models in this row reduced to the Multistage 3° model.

[f] BMD or BMDL computation failed for this model

[g] For the Weibull model, the power parameter estimate was 1. The models in this row reduced to the Quantal-Linear model.

[h] The Quantal-Linear model may appear equivalent to the Gamma model, however differences exist in digits not displayed in the table. This also applies to the Multistage 2° model.

1.2.2 Dichotomous and multistage cancer models using mouse neoplastic data from NTP (1982)

Table 49. Mouse Neoplastic Data from NTP 1982

Tumor Type/Incidence	Control	10 ppm	40 ppm
Females (#)			
Respiratory tumors [a,d]	4/49	11/49*	42/50*
Hemangiosarcoma of circulatory system [a]	0/50	11/50*	23/50*
Subcutaneous tissue or rib fibrosarcoma [a]	0/50	5/50*	11/50*

* Significant difference from control ($p < 0.05$), Fisher exact test

[a] Significant increasing trend ($p < 0.05$), Cochran-Armitage test

[d] Adenoma, carcinoma, adenomatous polyp, alveolar/bronchiolar adenoma, or alveolar/bronchiolar carcinoma.

1.2.2.1 BMDS Summary of Female Mice Respiratory Tumors

Table 50. Summary of BMD Modeling Results for female mice respiratory tumors

Model[a]	Goodness of fit		$BMD_{10}Pct$	$BMDL_{10}Pct$	Basis for model selection
	p-value	AIC			
Gamma	N/A[b]	129.86	7.82	4.01	Lowest BMDL Lowest AIC
Dichotomous-Hill Multistage 4°[d] Multistage 3°	error	error	error[e]	error[e]	
Logistic	0.761	127.96	8.03	6.32	
LogLogistic	N/A[b]	129.86	8.06	4.87	
Probit	**0.888**	**127.88**	**7.46**	**6.02**	
LogProbit	N/A[b]	129.86	8.26	5.19	
Weibull	N/A[b]	129.86	7.55	3.83	
Multistage 2°	N/A[b]	129.86	7.28	3.44	
Quantal-Linear	0.0322	132.77	2.97	2.30	

[a] Selected model in bold; scaled residuals for selected model for doses 0, 10, and 40 were -0.1, 0.1, -0.03, respectively.

[b] No available degrees of freedom to calculate a goodness of fit value.

[c] BMD or BMDL computation failed for this model.

[d] For the Multistage 4° model, the beta coefficient estimates were 0 (boundary of parameters space). The models in this row reduced to the Multistage 3° model.

[e] BMD or BMDL computation failed for this model

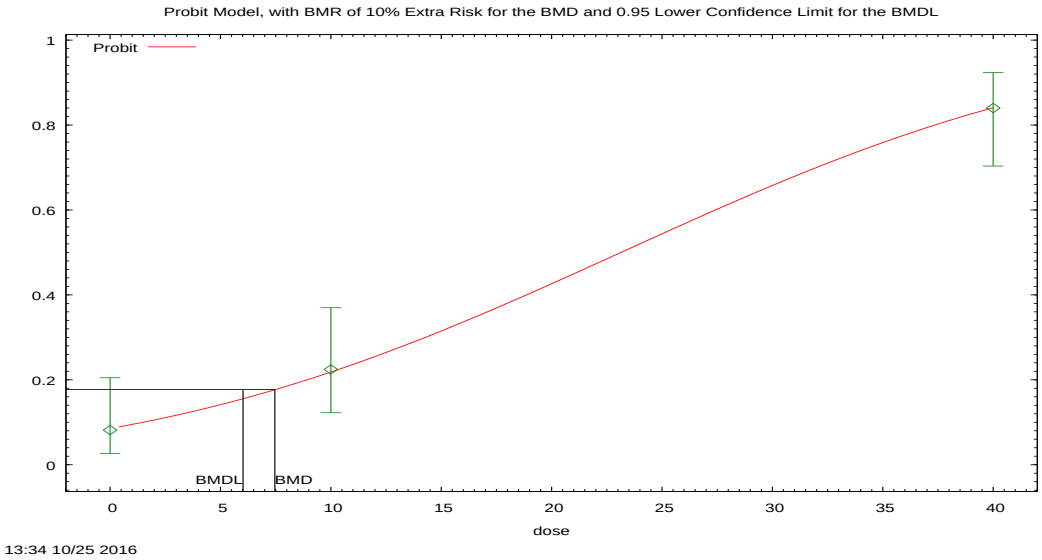

Figure 27. Plot of incidence rate by dose with fitted curve for Probit model for ; dose shown in ppm.

Probit Model. (Version: 3.3; Date: 2/28/2013)

The form of the probability function is: P[response] = CumNorm(Intercept+Slope*Dose), where CumNorm(.) is the cumulative normal distribution function

Slope parameter is not restricted

Benchmark Dose Computation.

BMR = 10% Extra risk

BMD = 7.46317

BMDL at the 95% confidence level = 6.02206

Parameter Estimates

Variable	Estimate	Default Initial Parameter Values
background	n/a	0
intercept	-1.3693E+00	-1.3630E+00
slope	0.0592358	0.0587478

Analysis of Deviance Table

Model	Log(likelihood)	# Param's	Deviance	Test d.f.	p-value
Full model	-61.93	3			
Fitted model	-61.94	2	0.0198843	1	0.89
Reduced model	-98.65	1	73.427	2	<.0001

AIC: = 127.883

Goodness of Fit Table

Dose	Est. Prob.	Expected	Observed	Size	Scaled Resid
0	0.0855	4.187	4	49	-0.1
10	0.2186	10.711	11	49	0.1
40	0.8414	42.069	42	50	-0.03

Chi^2 = 0.02 d.f = 1 P-value = 0.888

1.2.2.2 BMDS Summary of Mice Female circulatory system hemangiosarcoma

Table 51. Summary of BMD Modeling Results for female mice circulatory system hemangiosarcoma

Model[a]	**Goodness of fit**		**BMD_{10Pct}**	**$BMDL_{10Pct}$**	**Basis for model selection**
	p-value	**AIC**			
Gamma[b] Weibull[c] Quantal-Linear[d]	0.710	153.70	7.72	5.36	Of the models that provided an adequate fit and a valid BMDL estimate, the Log Logistic model was selected based on the lowest BMDL and lowest AIC.
Dichotomous-Hill Multistage 4°[f] Multistage 3°	error	error	error[g]	error[g]	
Logistic	0.241	154.95	14.0	11.2	
LogLogistic	0.974	153.56	6.29	3.98	
Probit	0.272	154.78	13.2	10.5	
LogProbit	N/A[h]	155.56	6.46	0.496	
Multistage 2°[i]	0.710	153.70	7.72	5.36	
Multistage Cancer Four Three	error	error	error[g]	error[g]	
Multistage Cancer **Two** **One**	**0.432**	**125.26**	**5.98**	**4.55**	

[a] Selected model in bold; scaled residuals for selected model for doses 0, 10, and 40 were 0, 1.12, -0.65, respectively..

[b] For the Gamma and Weibull models, the power parameter estimates were 1 (boundary of parameter space).For the Gamma model, the power parameter estimate was 1. The model is equivalent to the Quantal-Linear model.

[c] For the Weibull and Gamma models, the power parameter estimates were 1 (boundary of parameter space).For the Weibull model, the power parameter estimate was 1. The models in this row reduced to the Quantal-Linear model.

[d] The Quantal-Linear model may appear equivalent to the Multistage 2° model, however differences exist in digits not displayed in the table.
[e] BMD or BMDL computation failed for this model.
[f] For the Multistage 4° model, the beta coefficient estimates were 0 (boundary of parameters space). The models in this row reduced to the Multistage 3° model.
[g] BMD or BMDL computation failed for this model
[h] No available degrees of freedom to calculate a goodness of fit value.
[i] The Multistage 2° model may appear equivalent to the Gamma model, however differences exist in digits not displayed in the table. This also applies to the Weibull and Quantal-Linear models.

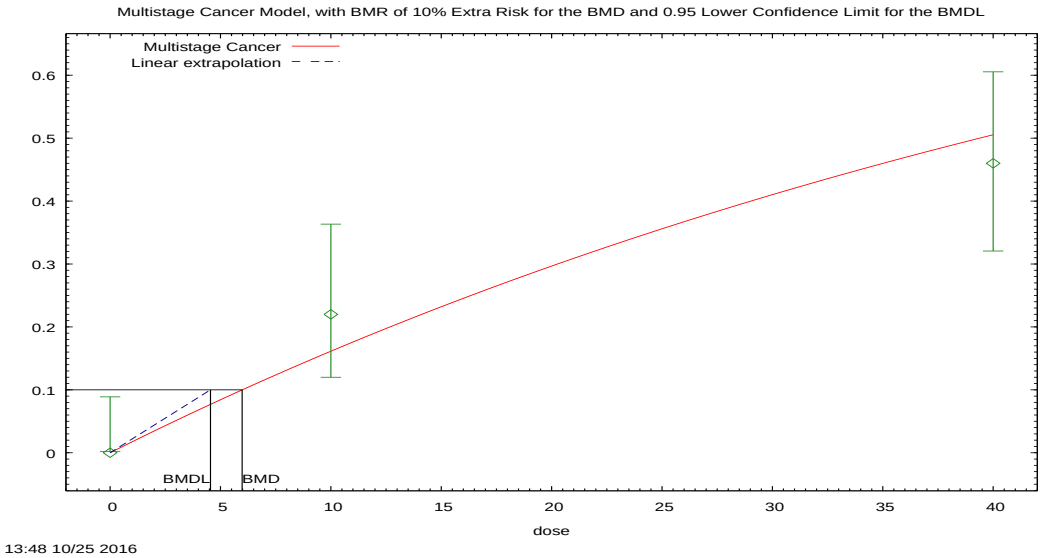

Figure 28. Plot of incidence rate by dose with fitted curve for Multistage-Cancer 2° model; dose shown in ppm.
Multistage Model. (Version: 3.4; Date: 05/02/2014)

The form of the probability function is: P[response] = background + (1-background)*[1-EXP(-beta1*dose^1-beta2*dose^2...)]

The parameter betas are restricted to be positive

Benchmark Dose Computation.

BMR = 10% Extra risk

BMD = 5.98013

BMDL at the 95% confidence level = 4.54743

BMDU at the 95% confidence level = 8.61867

Taken together, (4.54743, 8.61867) is a 90% two-sided confidence interval for the BMD

Multistage Cancer Slope Factor = 0.0219904

Parameter Estimates

Variable	Estimate	Default Initial Parameter Values
Background	0	0.0426403
Beta(1)	0.0176184	0.0146784
Beta(2)	0	0

Analysis of Deviance Table

Model	Log(likelihood)	# Param's	Deviance	Test d.f.	p-value
Full model	-60.84	3			
Fitted model	-61.63	1	1.57727	2	0.45
Reduced model	-80.28	1	38.88	2	<.0001

AIC: = 125.262

Goodness of Fit Table

Dose	Est. Prob.	Expected	Observed	Size	Scaled Resid
0	0	0	0	50	0
10	0.1615	8.077	11	50	1.12
40	0.5058	25.288	23	50	-0.65

Chi^2 = 1.68 d.f = 2 P-value = 0.4316

1.2.2.3 BMDS Summary of Female Mice Subcutaneous tissue or rib fibrosarcoma

Table 52. Summary of BMD Modeling Results for Female Mice Subcutaneous tissue or rib fibrosarcoma

Model[a]	Goodness of fit		$BMD_{10}Pct$	$BMDL_{10}Pct$	Basis for model selection
	p-value	AIC			
Gamma[b] Weibull[c] Multistage 2° Quantal-Linear	0.615	88.089	14.8	10.0	Lowest BMDL Lowest AIC
Dichotomous-Hill Multistage 4°[e] Multistage 3°	error	error	error[f]	error[f]	
Logistic	0.0574	94.132	27.1	21.4	
LogLogistic	**0.734**	**87.782**	**13.7**	**8.81**	
Probit	0.0633	93.829	25.6	19.9	
LogProbit	1.000	89.199	10	2.36E-63	
Multistage Cancer Four Three	error	error	errorf	error[f]	
Multistage Cancer Two One	0.615	88.089	14.8	10.0	

[a] Selected model in bold; scaled residuals for selected model for doses 0, 10, and 40 were 0, 0.67, -0.41, respectively.
[b] For the Gamma and Weibull models, the power parameter estimates were 1 (boundary of parameter space).For the Gamma model, the power parameter estimate was 1. The model is equivalent to the Quantal-Linear model.
[c] For the Weibull and Gamma models, the power parameter estimates were 1 (boundary of parameter space).For the Weibull model, the power parameter estimate was 1. The models in this row reduced to the Quantal-Linear model.
[d] BMD or BMDL computation failed for this model.

[e] For the Multistage 4° model, the beta coefficient estimates were 0 (boundary of parameters space). The models in this row reduced to the Multistage 3° model.
[f] BMD or BMDL computation failed for this model

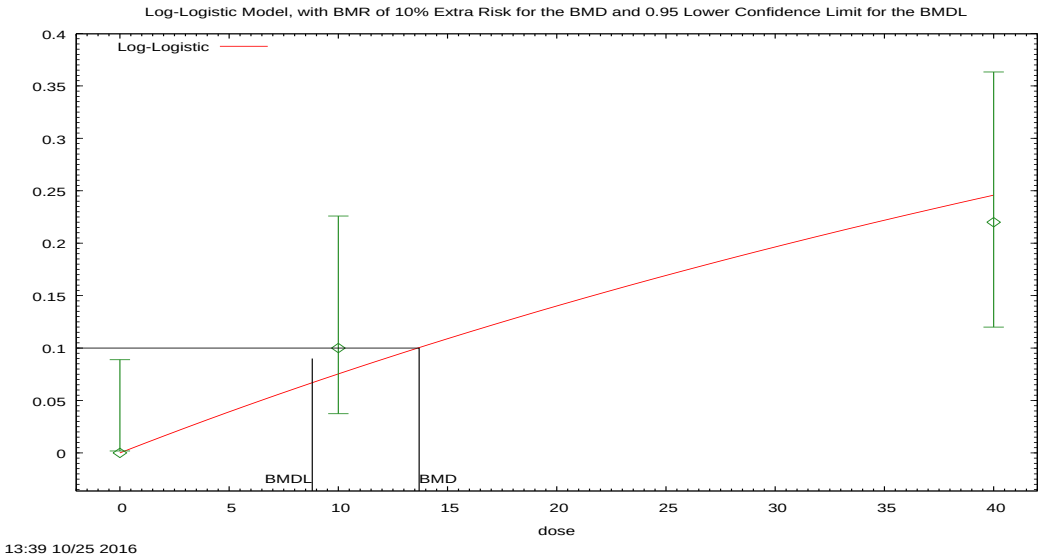

Figure 29. Plot of incidence rate by dose with fitted curve for LogLogistic model; dose shown in ppm.
Logistic Model.

The form of the probability function is: P[response] = background+(1-background)/[1+EXP(-intercept-slope*Log(dose))]

Slope parameter is restricted as slope >= 1

Benchmark Dose Computation.

BMR = 10% Extra risk
BMD = 13.6982
BMDL at the 95% confidence level = 8.80547

Parameter Estimates

Variable	Estimate	Default Initial Parameter Values
background	0	0
intercept	-4.8145E+00	-4.7272E+00
slope	1	1

Analysis of Deviance Table

Model	Log(likelihood)	# Param's	Deviance	Test d.f.	p-value
Full model	-42.6	3			
Fitted model	-42.89	1	0.582601	2	0.75
Reduced model	-50.92	1	16.6476	2	0

AIC: = 87.7817

Goodness of Fit Table

Dose	Est. Prob.	Expected	Observed	Size	Scaled Resid
0	0	0	0	50	0
10	0.075	3.751	5	50	0.67
40	0.245	12.249	11	50	-0.41

Chi^2 = 0.62 d.f = 2 P-value = 0.7342